Mechanistic Investigations into Catalytic Wittig Reactions

Filippo Ficarra

Thesis submitted to the University of Nottingham for the degree of Master of Research

Supervisor: Prof Ross M. Denton

September 2022

Dedication:

The work presented herein is dedicated to the memory of my grandfather Sante Carbon (1934-2022) and my uncle Santo Ficarra (1952-2022) who passed during the preparation of this thesis.

Acknowledgments

First and foremost, I have to thank my supervisor Professor Ross Denton, for giving me the opportunity to work in his group, and for his continues patience despite the difficult progress on this project. I must thank all my colleagues in the Denton group for making the past year all the more enjoyable. Specific thanks must go out to Nick Atkinson, Dr Ben Scrafield and Dr Tom Barber, for the continued help and mentorship. I must thank the analytical team at the University of Nottingham for their help in this project, specifically Dr Huw Williams and Dr Kevin Butler. Thank you as well the Dr. Chris O'Brien for the productive conversations. I must also thank the Ball group for lending equipment when necessary and letting me work in their lab occasionally. Finally, I must thank my partner for her continual support and encouragement and helping me some of my lowest moments this year.

Abstract

Catalytic Wittig reactions present a versatile organocatalytic approach to olefin synthesis reducing the problematic waste associated with the classic Wittig reaction. Although this chemistry has been known for over a decade it has not seen use beyond academic research. In this thesis we aim to address the limitations associated with this chemistry. We present a new less hazardous route to the phosphine oxides employed in catalytic Wittig reactions. We then present our initial results conducting the first kinetic study of this chemistry. Finally computational screening of phosphine oxides gives insight on the optimal catalyst structure to lower the energy barrier in the rate limiting reduction.

Abbreviations

Standard abbreviations and acronyms, as defined by the Journal of Organic Chemistry, are used throughout this thesis. All others are listed below.

CED – Cumulative energy demand

DIPEA – Diisopropylamine

GHG – Green house gas

HMG-CoA – hydroxy-3-methyl-glutaryl-coenzyme A reductase

HWE – Horner-Wadsworth-Emmons

NBO – Natural bond orbital

OPA – Oxaphosphetane

QM – Quantum Mechanical

RDS – Rate determining step

Contents

Acknowledgments 2
Abstract 3
Abbreviations 4
1. Introduction 6
1.1 Olefins 6
1.2 Methods for Olefin Synthesis 7
1.3 The Wittig Olefination 9
1.3.2 Phosphonium Ylides 10
1.3.3 The Mechanism of the Wittig Reaction 13
1.4 Modifications and related processes 15
1.4.1 Schlosser modification 15
1.4.2 Horner-Wadsworth-Emmons reaction 17
1.4.3 The Still-Genarri and Ando modifications 18
1.5 Industrial Relevance of the Wittig Olefination 19
1.6 Limitations and Disadvantages of the Wittig reaction 21
1.7 Wittig Reactions Catalytic in Phosphine 22
1.8 Project Aims 32
2. Results and Discussion 33
2.1 New route for the synthesis of phospholane oxide pre-catalysts 33
2.2 Investigation into Room Temperature Catalytic Wittig reaction 40
2.2.1 Reaction Monitoring and Kinetic Studies 42
2.2.2 Investigation on the Role of the Benzoic Acid Additive. 48
2.3 Computational Screening of Phosphine Oxide Catalysts 52
3. Conclusions and Future work 58
4. Supporting Information 60
4.1 General Procedures 60
4.2 General Procedures for Kinetic Studies 61
4.3 Computational Methods 63
4.4 Experimental procedures 66
4.5 Computational Data 85
5. References 148

1. Introduction

1.1 Olefins

Olefins constitute one of the most fundamental and important functional groups found in organic synthesis. The rich and diverse reactivity of olefins make them valuable intermediates in synthesis, as they can be derivatised into a variety of functionalities (**Figure 1**). The reactions of olefins can be generalised to go by one of four classes of mechanisms: 1) electrophilic additions, 2) nucleophilic additions, 3) radical additions and finally 4) pericyclic reactions.

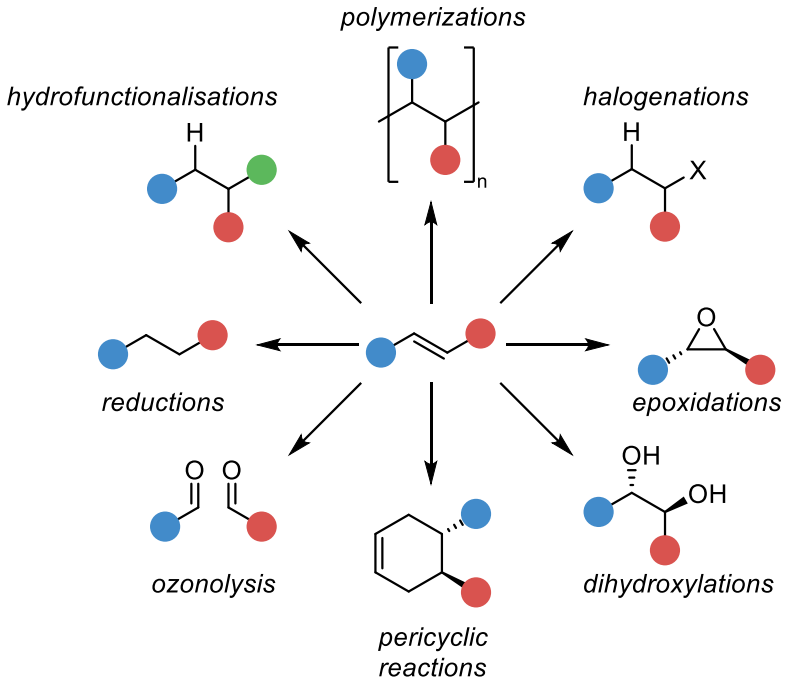
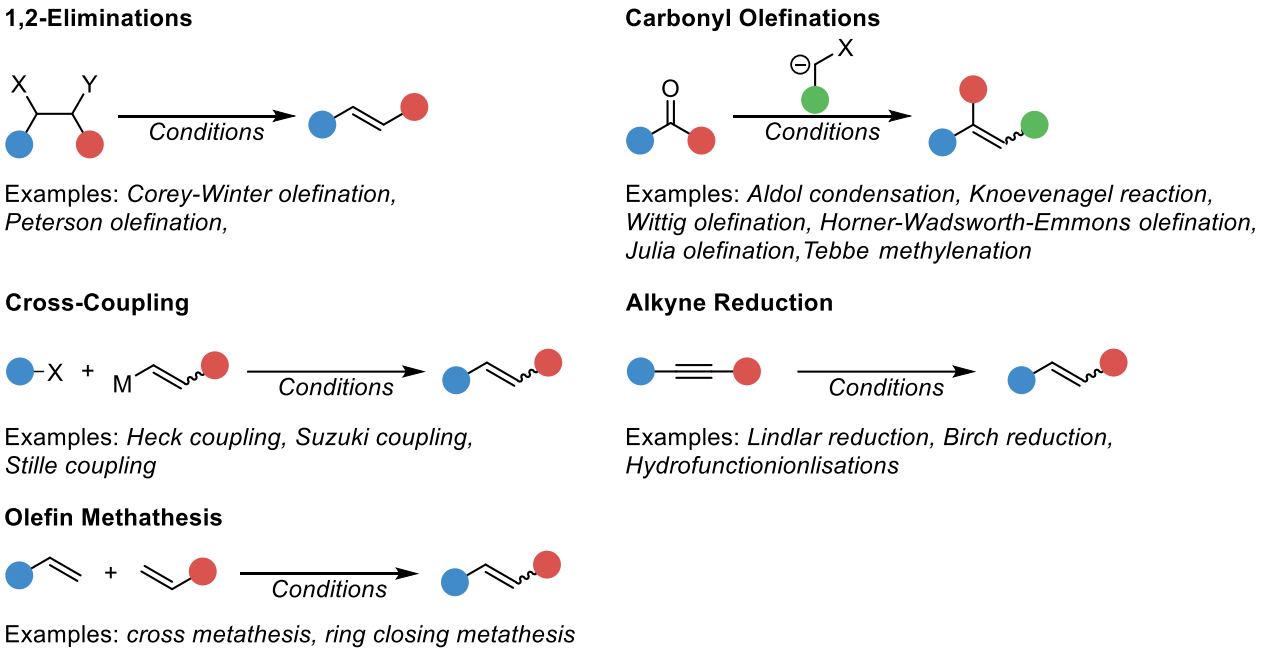


Figure 1. Synthetic utility of olefins.

Olefins are also featured in a range of natural products, pharmaceuticals and functional materials. A recent cheminformatic study of over 186,000 natural products found olefins were present in 40% of the compounds studied, the second most prevalent functional group after the hydroxyl group.[1]

1.2 Methods for Olefin Synthesis and Substitution

Efficient stereoselective olefin syntheses are of clear importance to synthetic chemists. Approaches to olefin synthesis be generalised as one of a few methods: 1) elimination reactions, 2) carbonyl olefinations, 3) cross-coupling reactions, 4) alkyne reduction and 5) olefin metathesis (**Scheme 1**).[2]



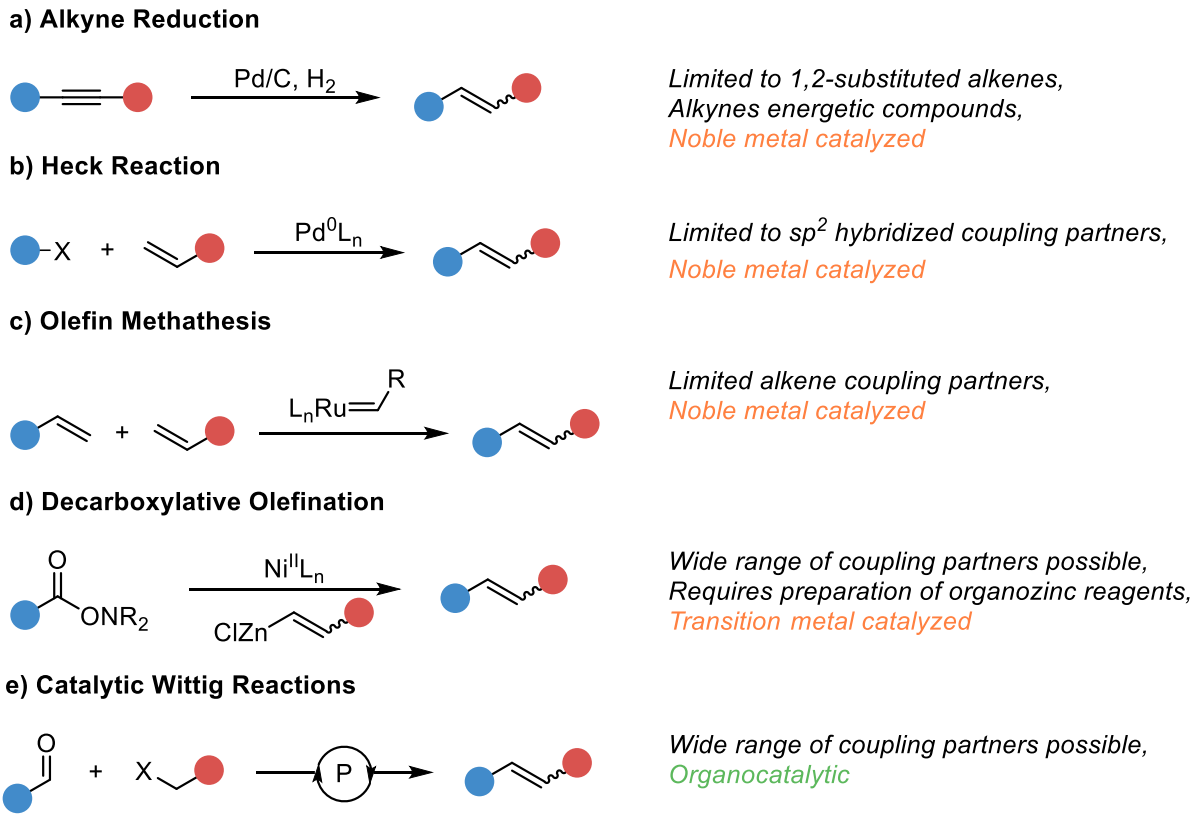
Scheme 1. General strategies for olefin synthesis

The olefination method chosen is highly dependent on the availability of the starting material, substitution and stereoselectivity desired. 1,2 eliminations such as the Corey-Winter olefination are therefore inherently limited, due to the lower commercial availability of diols, as well as the harsh reagents used. A variety of methodologies have been developed to convert carbonyls into olefins. In most of the carbonyl olefinations shown above stoichiometric by-products are generated, making them less atom economical. Among these distinct strategies, only cross-couplings, alkyne reductions, and olefin metathesis are catalytic (**Scheme 2**). Palladium-catalysed cross-couplings have been of great utility to

synthetic chemists. The most well-known, in the context of olefin synthesis, is the Heck reaction in which aryl halides and olefins can be coupled directly. Olefinations by Suzuki and Stille couplings are also possible with the use of the corresponding vinyl boron species or vinyl stanane. These methods are highly efficient, operate under mild conditions and are compatible with a wide range of functional groups.[3] However, palladium cross-couplings are largely limited to the coupling of arenes (or other sp^2 hybridised carbons) to alkenes. More recent work by Baran has demonstrated radical based nickel catalysed cross-couplings are able to perform alkyl-alkyl conjunctive olefinations (**Scheme 2d**).[4]

Olefin metathesis has also been an important addition to the synthetic chemist's toolkit.[5] Mild conditions and excellent functional group compatibility make metathesis a versatile method. Ring-closing metathesis is an especially important strategy in the synthesis of macrocyclic rings, which would be difficult to synthesise by other methods.

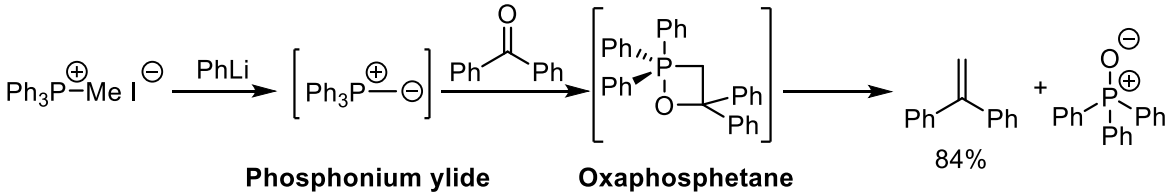
Despite these methods being highly successful, the continued use of toxic and expensive noble metal catalysts is problematic. Organocatalytic olefinations are therefore an attractive alternative. To date the most well-known example of which is arguably the catalytic Wittig olefination (**Scheme 2e**).[6] Due to the subject of this report the remainder of this introduction will involve a discussion the Wittig olefination and its derivatives.



Scheme 2. State of the art of catalytic olefinations

1.3 The Wittig Olefination

Since its discovery in 1953, the Wittig olefination[7] has been one of the most prevalent methods for the synthesis of alkenes. The Wittig olefination involves the reaction of a phosphonium ylide with an aldehyde or a ketone, forming an intermediate oxaphosphetane (OPA) which collapses to give an alkene and a phosphine oxide. This process is thermodynamically driven by the formation of the strong oxygen phosphorous bond (**Scheme 3**).



Scheme 3. The first Wittig olefination[7]

In the 70 years since its inception the Wittig reaction has become a staple of modern synthetic chemistry. There are several factors which have made the Wittig olefination a reaction of continued use and interest to synthetic chemists. Wittig reactions are high yielding, chemoselective, tolerant to many functional groups and can be stereoselective. The stereochemical outcome is a function of the ylide type but can be tuned depending on the reagents and conditions employed. In most cases mild conditions are used and, in the case of stabilised ylides, no special precautions need to be taken to exclude air or moisture. The starting materials required for a Wittig olefination are generally readily available.[2]

1.3.2 Phosphonium Ylides

Phosphonium ylides contain a short phosphorous-carbon bond which is strong and highly polar. For this reason, they are sometimes represented as phosphonium ylenes (**Figure 2a**), however this formalism is in contrast with the observation that the carbanion is pyramidalised and that the barrier to rotation of ylides is low.[8] A perhaps more coherent description of the bonding nature in phosphonium ylides is to describe the α-anion to be stabilized by negative-hyperconjugation involving the non-bonding pair of electrons on carbon and the P–C σ* orbital of the phosphine (**Figure 2b**).[8]

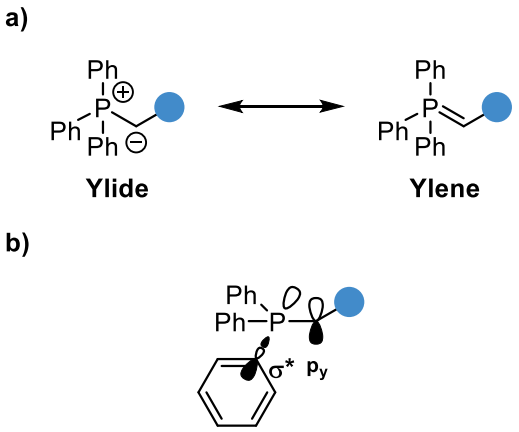


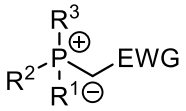
Figure 2. a) Representations of phosphonium ylides.
b) Negative hyperconjugation bonding description of ylides.

The structure and reactivity of the phosphonium ylides employed in a Wittig reaction has a significant effect on the stereochemistry of the alkene product. Phosphonium ylides are generally classified as being stabilised, semi-stabilised or non-stabilised depending on the nature of the substituent's vicinal to the carbanion (**Figure 3**). Electron-withdrawing substituents such as esters, nitriles and sulfones can stabilize the carbanion *via* resonance or negative inductive effects. The pK_as of the corresponding phosphonium salts are lower therefore mild bases are required for their formation, these ylides are also often isolatable. Stabilised ylides tolerate air and moisture and are even effective in reactions conducted in aqueous media.[9] Vinyl or aryl substituents can weakly stabilise the carbanion by resonance. Non-stabilised ylides bearing alkyl substituents are found to be unstable to air and moisture. Their formation requires strong bases, and ylides are typically formed *in-situ* before being employed in a Wittig reaction.[10]

In general, for ylides derived from triphenylphosphine, non-stabilised ylides favour forming *Z* alkenes, semi-stabilised tend to give mixtures of *E*/*Z* alkenes while stabilised ylides favour *E* products almost exclusively.[10] The substituents

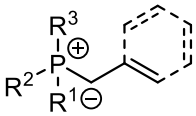
directly bound to phosphorous also play a role in the stereoselectivity of a Wittig reaction. Non-stabilised ylides derived from trialkylphosphines demonstrate *E*-selectivity contrasting the selectivity shown in those derived from triphenyl phosphine.[11] As demonstrated by Aggarwal, semi-stabilised ylides derived from trimethyl phosphite give very high *E*-selectivities, this is in contrast to the usual stereochemical outcome from triphenylphosphine derived semi-stabilized ylides.[12] Furthermore, Schlosser and co-workers discovered that stabilized ylides derived from tris(2-methoxymethoxyphenyl)phosphine gave moderate *Z*-selectivity, opposite to the high *E*-Selectivity expected from stabilized ylides.[13] In the case of semi-stabilized ylides these "methoxymethoxy-armed" ylides gave moderate *Z*-selectivity.[14]

Stabilized ylides



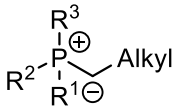
Substituents	*E:Z* Selectivity
R^1,R^2,R^3 = Ph	Very High *E*
R^1,R^2,R^3 = Alkyl	Very High *E*
R^1,R^2 = Ph, R^3 =Me	High *E*
R^1,R^2,R^3 = OMe	Moderate *E*
R^1,R^2,R^3 = 2-(MOM)C_6H_5	High *Z*

Semi-stabilized ylides



Substituents	*E:Z* Selectivity
R^1,R^2,R^3 = Ph	Mixture of *E*/*Z*
R^1,R^2,R^3 = Alkyl	Very High *E*
R^1,R^2 = Alkyl, R^3 =Aryl	Moderate *E*
R^1,R^2,R^3 = OMe	Very High *E*
R^1,R^2,R^3 = 2-(MOM)C_6H_5	Moderate *Z*

Unstabilized ylides

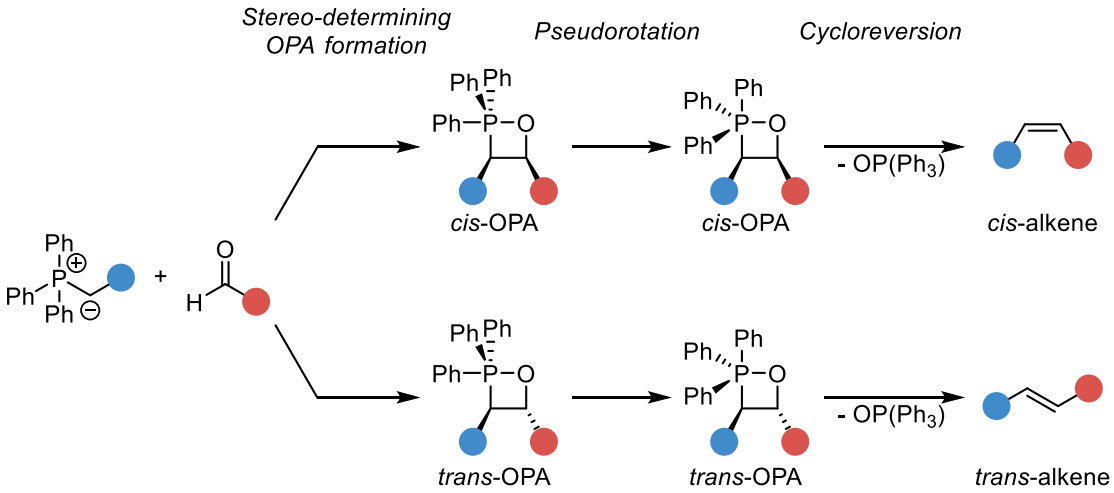


Substituents	*E:Z* Selectivity
R^1,R^2,R^3 = Ph	Very High *Z*
R^1,R^2 = Ph, R^3 = Alkyl	Moderate *Z*
R^1,R^2 = Ph, R^3 = ^{t}Bu	Very High *Z*
R^1,R^2,R^3 = Et	High *E*

Figure 3. General stereoselectivity trend of Wittig olefinations for different ylide structures.[10,12,14,15]

1.3.3 The Mechanism of the Wittig Reaction

The differences in stereoselectivity of Wittig reactions due to the presence of differing ylides, additives and solvents has made the elucidation of a unified mechanism for the Wittig reaction challenging. However, extensive studies conducted by Vedejs[16], Maryanoff[17] and Schlosser[11] (among many others) have led to a generally accepted mechanism consistent with most experimental observations (**Scheme 4**).[10] The Wittig reaction under lithium salt-free conditions proceeds *via* a concerted asynchronous [2+2] cycloaddition between the ylide and aldehyde to form an oxaphosphetane intermediate. In the case of ylides derived from triphenylphosphine this step is irreversible and therefore stereo determining.



Scheme 4. General mechanism of Wittig reaction.[2,8]

Computational modelling indicates that the formation of a *cis*- or *trans*-OPA is dependent on the steric and electronic properties of the phosphonium ylide and aldehyde involved (**Figure 4**).[18] Wittig reactions of non-stabilized ylides are under kinetic control. The asynchronous OPA formation allows for adoption of a highly puckered structure (the C-C bond being more developed than the P-O bond), minimising unfavourable 1,3- and 1,2- steric interactions. *Trans*-OPA

formation proceeds *via* a planar transition state in which 1,2-interactions are minimised, however there is the 1,3 steric clash as well as encumbrance of the carbonyl oxygen caused by the phenyl groups on the phosphorus. Increased steric encumbrance present in semi-stabilised ylides creates unfavourable interactions in both *cis*- and *trans*-OPA formation. The transition state being later and less flexible for *cis*-OPA formation, means less puckering can occur to alleviate the steric clash, poor selectivity is therefore observed. Electronic effects play a large role in the selectivity for stabilised ylides. In this case *trans*-OPA formation is significantly favoured due to the presence of dipole-dipole interactions between the carbonyl group of the aldehyde and the delocalised charge into the ylidic ester group.

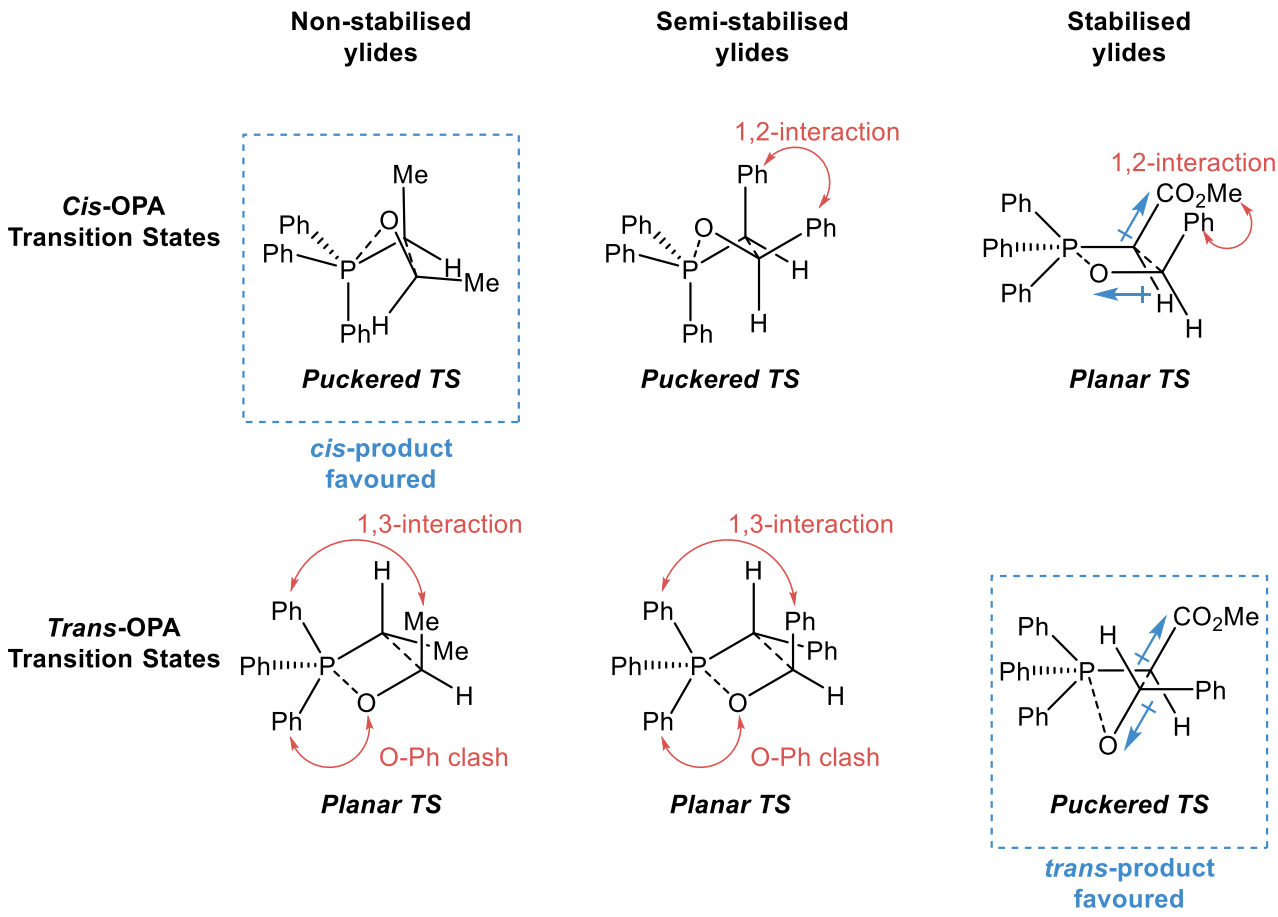


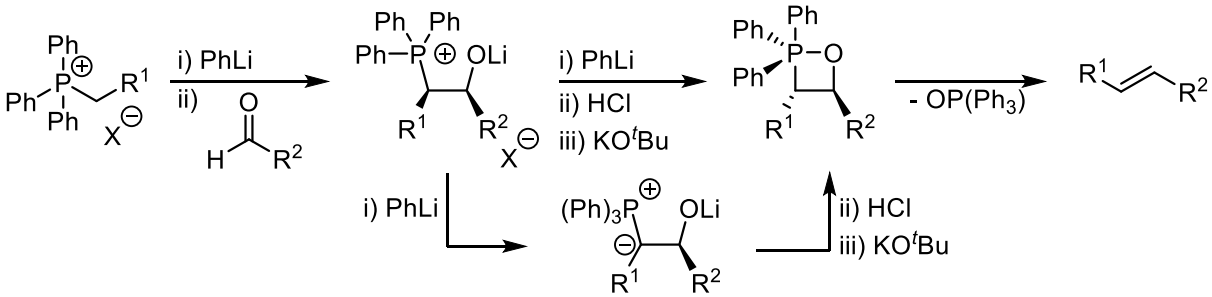
Figure 4. Transition state geometries in the Wittig reaction[18]

1.4 Modifications and related processes

The robustness and versatility of the Wittig reaction has inspired the development of modifications and related reactions which have expanded the scope and utility of this olefination process. The following section will briefly highlight some notable examples.

1.4.1 Schlosser modification

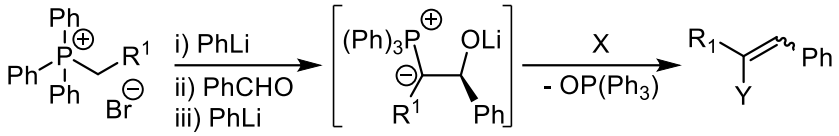
In 1966 Schlosser reported a modification for the Wittig reaction of non-stabilised ylides to give high selectivity for the *trans*-isomer of the alkene product.[19] They found that in the presence of lithium salts, OPA intermediates derived from non-stabilised ylides (which are stable at low temperatures) can be cleaved to form lithiobetaines. Epimerization of the lithiobetaine could be achieved by treatment with a organolithium base followed by reprotonation of the subsequently formed β-oxido phosphonium ylide, yielding the kinetically preferred *trans*-diastereioisomer almost exclusively. Cycloreversion (as seen in the standard Wittig) leads to the *trans*-alkene, the opposite stereoisomer of the reaction of non-stabilised ylides under lithium free conditions (**Scheme 5**).



Scheme 5. Mechanism of the Schlosser modified Wittig reaction[19]

Soon after this report, Schlosser demonstrated that intermediate β-oxido phosphonium ylides can be trapped with electrophiles to deliver trisubstituted alkenes (**Scheme 6**).[20] A range of electrophiles were explored, high

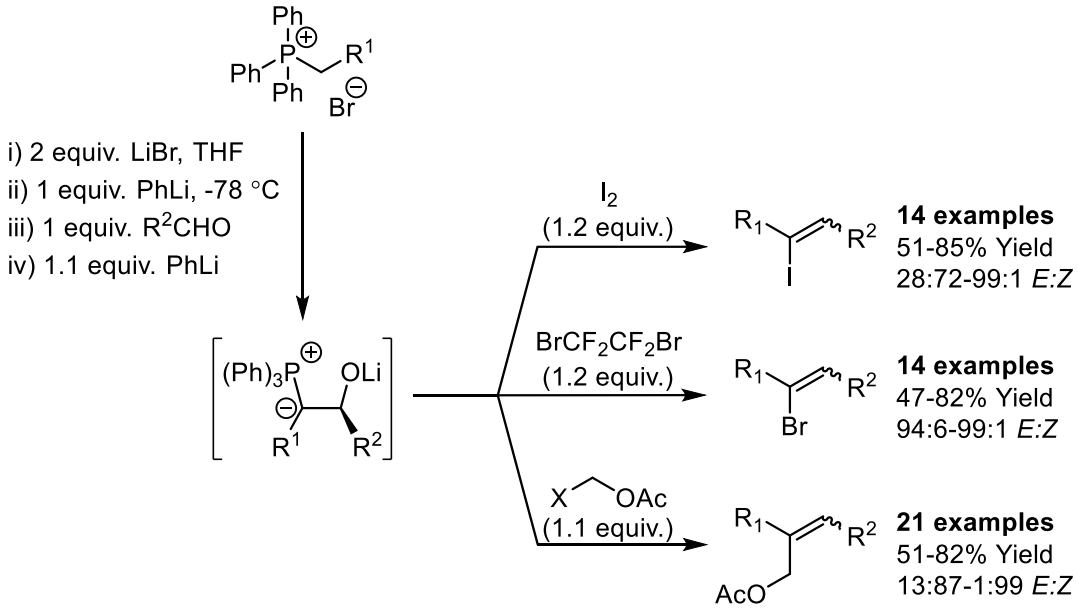
stereoselectivities were obtained for ylides where $R^1 \neq H$, though modest yields and a limited scope were reported.



R^1	X	Y	Yield	*E:Z*
H	DCl	D	65%	52:48
Et	MeI	Me	75%	95:5
Me	$FClO_3$	F	37%	2:98
Me	Cl_2IPh	Cl	55%	2:98
Me	Br_2	Br	26%	10:90

Scheme 6. Trapping β-oxido phosphonium ylides[20]

Building on this concept, Hodgson reported an improved protocol for the synthesis of trisubstituted alkenyl bromides and iodides from phosphonium salts.[21] They reported higher yields and better stereoselectivity than Schlosser's original report, thus further expanding the scope of the Wittig reaction. Furthermore, the same group later reported reactions with halogenated methyl esters to give allylic esters in good yields and excellent stereoselectivities (**Scheme 7**).[22]

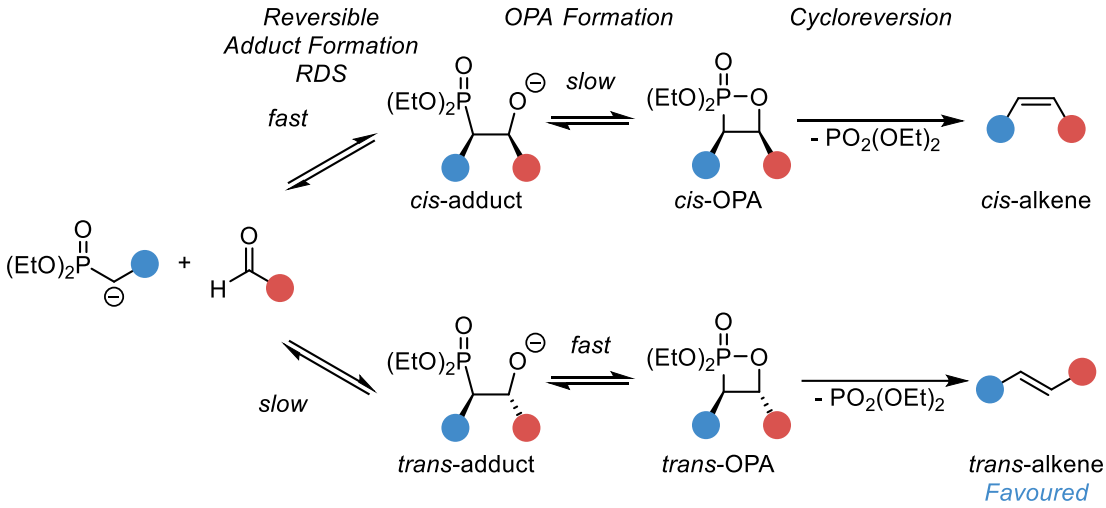


Scheme 7. Trapping of β-oxido phosphonium ylides reported by Hodgson[21,22]

1.4.2 Horner-Wadsworth-Emmons reaction

Soon after Wittig's seminal publication, it was found that phosphorous(V) reagents other than phosphonium ylides could be used in carbonyl olefinations. Horner demonstrated that carbanions derived from alkyl phosphine oxides and phosphonate esters were able to alkenylate ketones.[23] Wadsworth and Emmons further improved Horner's concept by exploring the scope and utility of carbanions derived from phosphonate esters in carbonyl olefinations,[24] introducing the Horner-Wadsworth-Emmons (HWE) reaction as a complementary olefination to the Wittig reaction. The HWE has a few distinct advantages over the Wittig reaction of stabilised ylides. Firstly, HWE reagents are more nucleophilic than stabilised ylides, hence ketones are suitable coupling partners. Secondly the phosphourus(V) by-product from an HWE reaction is water soluble, facilitating its removal upon aqueous extraction. HWE reagents are easily prepared *via* the Arbuzov[25] or the Michaelis-Becker reaction[26]. Furthermore, the respective reagents needed for these reactions, trialkyl phosphites or dialkyl

phosphites, are less expensive than phosphines used to prepare phosphonium ylides in Wittig reactions. The selectivity of the HWE reaction is due to the reversible and step-wise manner in which OPAs are formed.[17] The addition to the carbonyl compound has been found to be rate limiting[27,28], this step is faster for the formation of the *cis*-adducts than the *trans*-adducts. However, due to steric clash of R^1 and R^2 the subsequent OPA formation is faster for the trans-OPA. Hence (due to the reversibility of the first two steps) *trans*-alkenes are formed preferentially (**Scheme 8**).

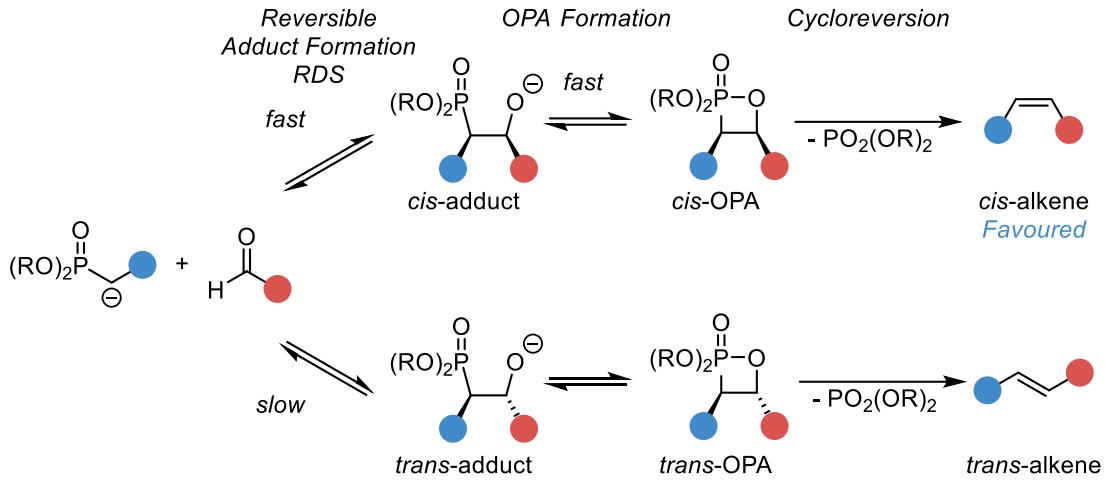


Scheme 8. Proposed Mechanism for HWE reaction

1.4.3 The Still-Genarri and Ando modifications

Still and Genarri reported that tuning the electronic properties of the phosphonate ester involved in HWE reactions could give *Z*-selectivity almost exclusively.[29] By employing more electrophilic bis(trifluoroethyl) phosphonate esters in the reaction, ring closure from the preferentially formed cis-adducts could be accelerated giving preference for *cis*-alkene formation (**Scheme 9**). Ando later reported the use of diphenyl phosphonate esters in HWE reactions

could give the same effect, providing a more simple method to generate *cis*-alkenes.[30]



R = CH_2CF_3 (Still-Genarri), Ph (Ando)

Scheme 9. Proposed Mechanism for Still-Genarri modification of HWE reaction

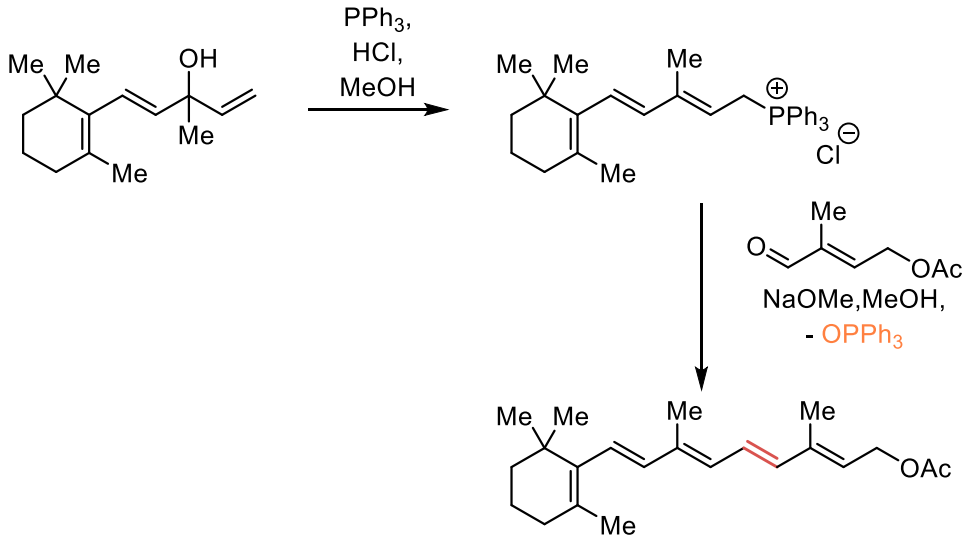
1.5 Industrial Relevance of the Wittig Olefination

The versatility of the Wittig reaction in the synthesis of substituted alkenes, has made it a staple in medicinal chemistry, process chemistry and natural product synthesis. The enabling role of Wittig chemistry in natural product synthesis cannot be understated, perhaps best described by K.C. Nicolaou in his seminal review.[31]

Despite the disadvantages associated with the Wittig reaction, namely in the generation of stoichiometric triphenylphosphine oxide waste and the complications it may cause in purifying compounds, it remains a valuable method in the preparation of fine chemicals on industrial scales.

Not long after its discovery the significance of this olefination was apparent to the chemical industry. Chemical manufacturer BASF used the reaction in their efforts to synthesise vitamin A, patenting a route in 1956 (**Scheme 10**).[32] This

process was so effective that a production plant for the multi tonne scale synthesis of vitamin A was opened in 1971.[33] BASF remains one of the main global producers of vitamin A, other carotenoids such as β-carotene are also produced on industrial scales by Wittig reactions.[34]



Scheme 10. BASF synthesis of vitamin A acetate from vinyl-β-ionol, and β-formylcrotyl acetate

Several olefin containing drugs are produced on industrial scales using the Wittig reaction (**Figure 5**). The HMG-CoA reductase inhibitor rosuvastatin, is an important cholesterol lowering drug. Key to its synthesis is a Wittig reaction to couple the *syn*-1,3 diol moiety key to the drugs activity to the heterocyclic core of the drug.[35-37] Additionally the synthesis, the T-cell lymphoma treatment bexarotene[38], the antibiotic ceftrobiprole[39,40] and the vitamin D analogue calcipotriol[41,42] all involve Wittig olefinations. It should be noted that the olefins highlighted in **Figure 5** would be difficult to synthesise on industrial scales by other olefinations, either due to the access to the starting material or the functional group compatibility.

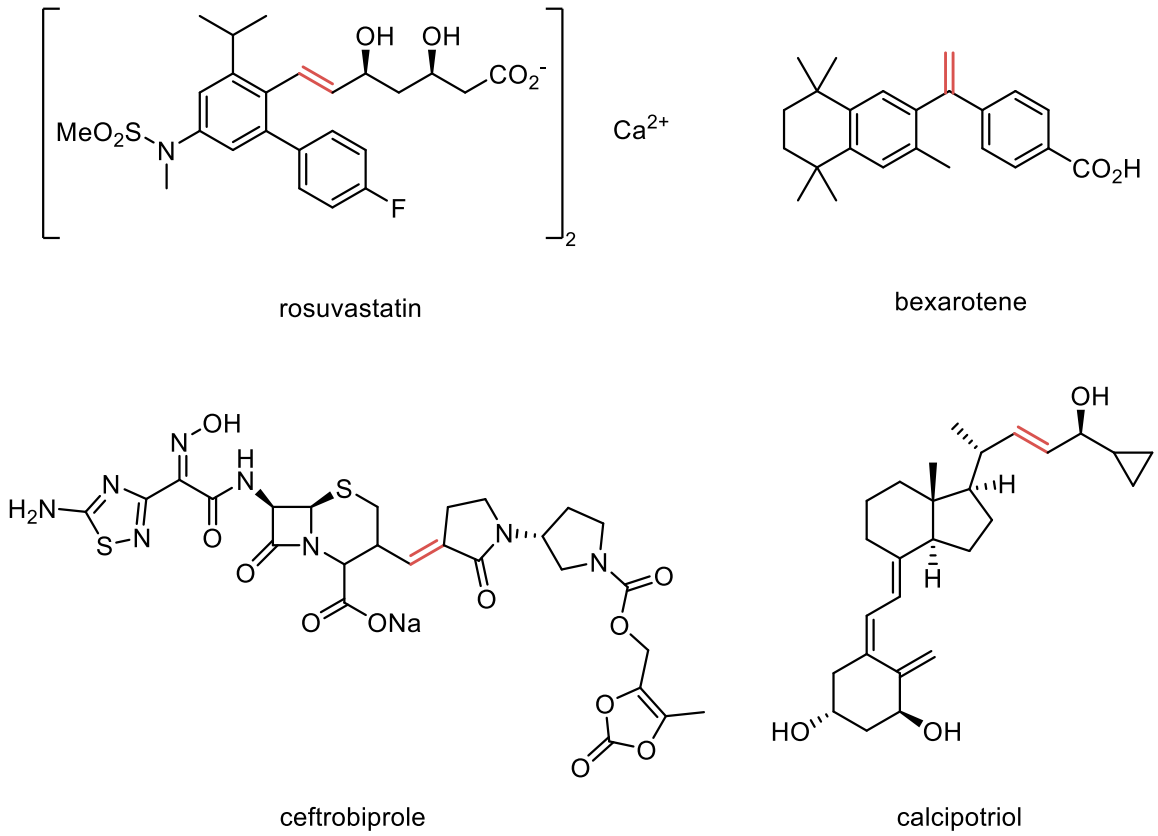


Figure 5. Selected examples pf small-molecule drugs produced on a process scale with a Wittig reaction, (alkene linkage made by Wittig reaction highlighted in red)

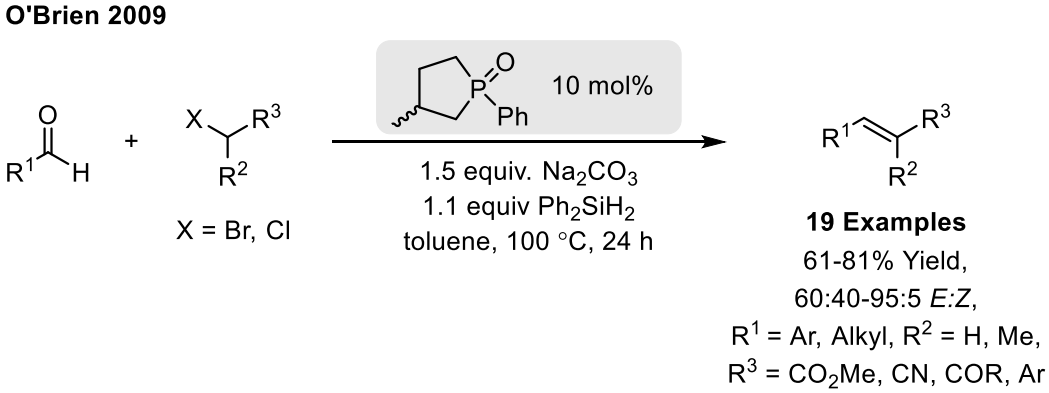
1.6 Limitations and Disadvantages of the Wittig reaction

Despite the versatility and robustness of the Wittig reaction, it remains hampered by the stoichiometric generation of phosphine oxide. Removal of triphenylphosphine oxide can be cumbersome, sometimes requiring column chromatography which becomes impractical on industrial scales. Chromatography-free methods of triphenylphosphine oxide removal sometimes can address these issues.[43,44] More importantly the generation of triphenylphosphine oxide waste on industrial scales is problematic due to its limited uses. Recycling of triphenyl phosphine oxide by reduction back to triphenyl phosphine requires, expensive or harsh reagents.[45] Triphenyl phosphine production is also problematic as it is derived directly from

phosphorus trichloride, an increasingly unfavourable feedstock for organophosphorus reagents[46]; the reaction involves addition of chlorobenzene to phosphorus trichloride in a solution of molten sodium and toluene.[33]

1.7 Wittig Reactions Catalytic in Phosphine

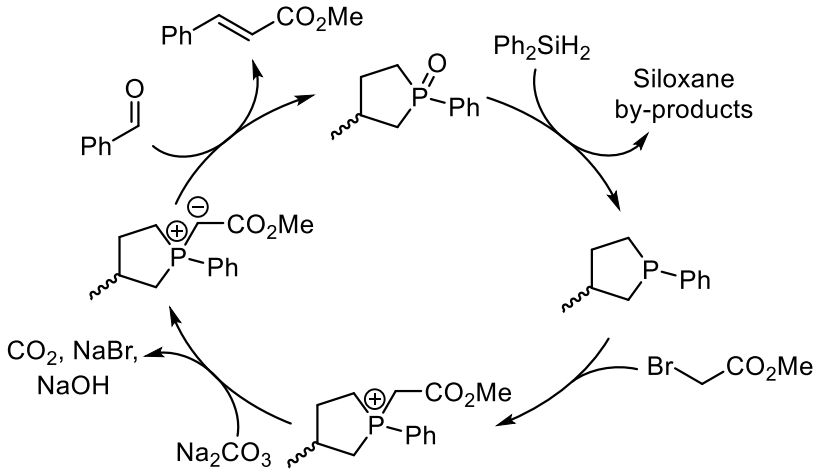
One of the most pioneering advances towards tackling the problematic generation of phosphine oxide waste in organophosphorus mediated transformation was O'Brien's development of the first Wittig reaction using sub stoichiometric amounts of phosphine (**Scheme 11**).[6] The key challenge in designing this phosphorous (III/V) redox manifold was to achieve chemoselective reduction of the phosphine oxide in the presence of other reductively labile functionalities, such as the aldehyde and the alkene product. While a variety of reagents are known to reduce phosphine oxides,[45] O'Brien demonstrated that hydrosilanes could achieve this reduction without reducing the aldehyde or alkene.



Scheme 11. The first Wittig reaction catalytic in phosphine[6]

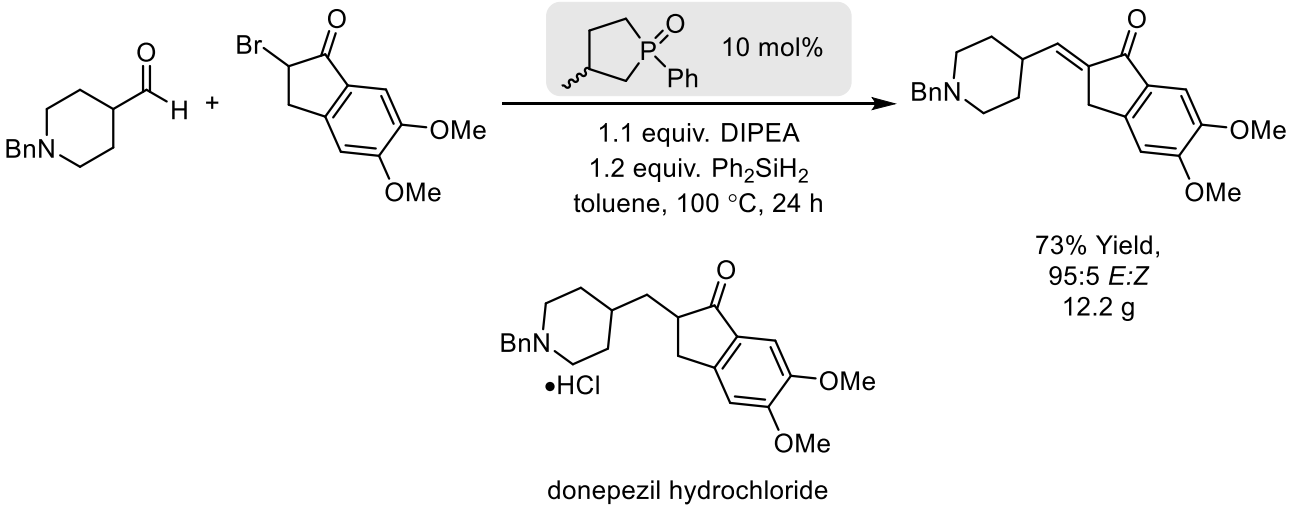
The catalytic cycle is proposed to occur via the following sequence (**Scheme 12**). Firstly, phosphine oxide reduction by the hydrosilane generates the free phosphine. Alkylation with the alkyl bromide gives the corresponding

phosphonium salt, which is subsequently deprotonated forming the stabilised ylide. Finally, Wittig reaction with the aldehyde generates the product and reintroduces the phosphine oxide to the catalytic cycle.



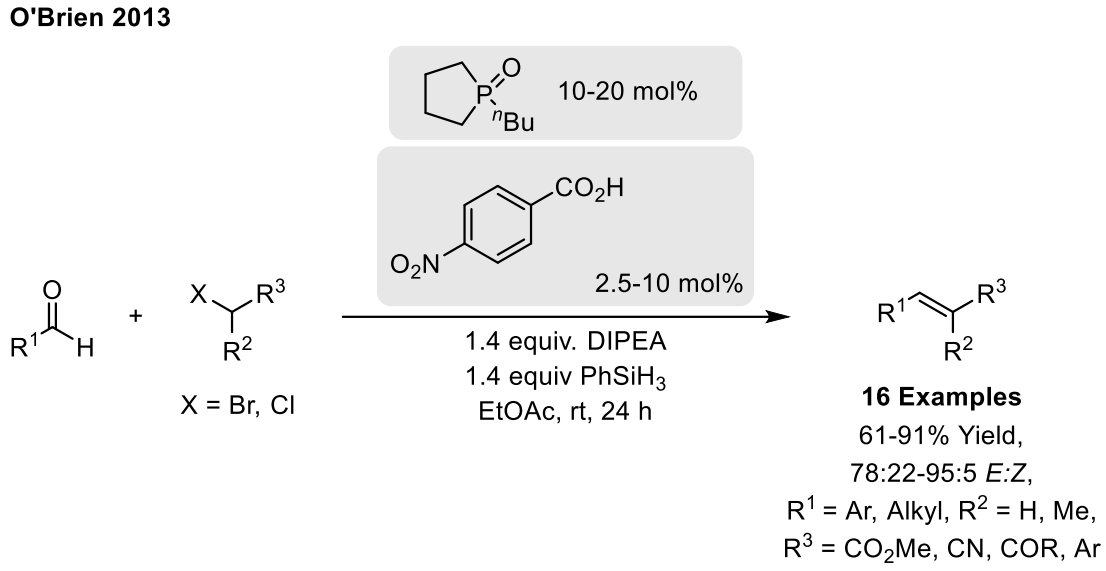
Scheme 12. Proposed Catalytic Cycle for CWR

A subsequent study by the group was undertaken to further optimize this reaction.[47] It was found that acyclic phosphine oxides were not competent catalysts in their system, due to the slow rate of phosphine oxide reduction. The employment of DIPEA as a soluble base further improved the reaction yield from 74% to 90% for the same substrate. The authors also demonstrated the scalability of the protocol, with the synthesis of a precursor to the Alzheimer's medication donepezil hydrochloride on a 43.6 mmol scale in a good yield of 73% (**Scheme 13**).



Scheme 13. Decagram scale synthesis of donepezil hydrochloride precursor by CWR

O'Brien reported a further improvement of his catalytic Wittig methodology with the introduction of a room temperature variant (**Scheme 14**).[48] Key to this development was the combination of phenylsilane with a substoichiometric amount of 4-nitrobenzoic acid. Slight tweaking of the phospholane oxide catalyst structure employed also led to improved stereoselectivity for the *E* isomer. These conditions enabled catalytic Wittig reactions utilising commercially available acyclic alkyl phosphines oxides or even triphenyl phosphine oxide as the catalysts although at higher temperatures (100 °C).



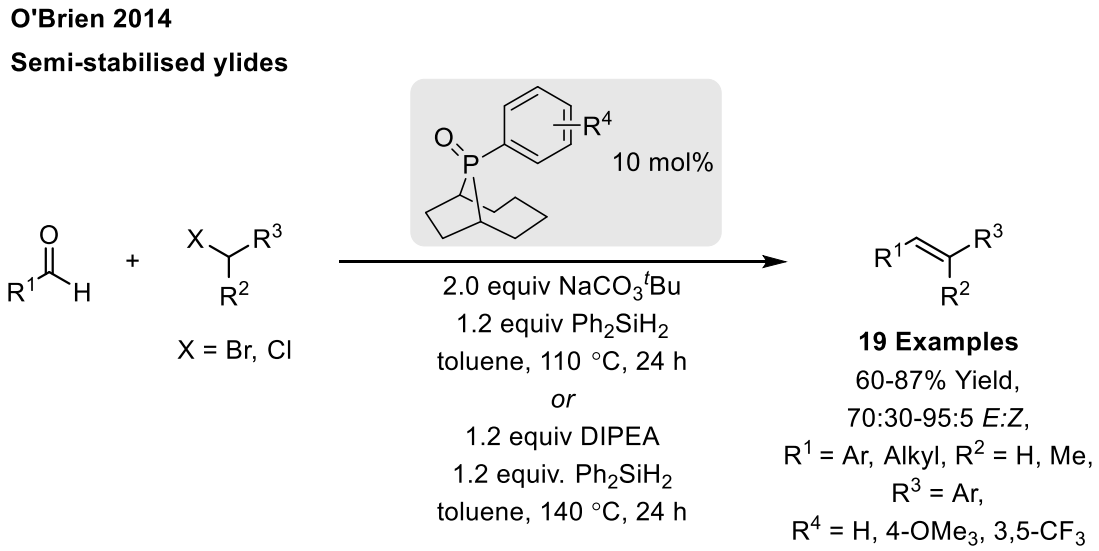
Scheme 14. Room temperature catalytic Wittig reaction

The authors suggest that the presence of a Brønsted acid facilitates the phosphine oxide reduction by activating the P–O bond of the phosphine oxide however no further investigation or mechanistic discussion is presented in their work.

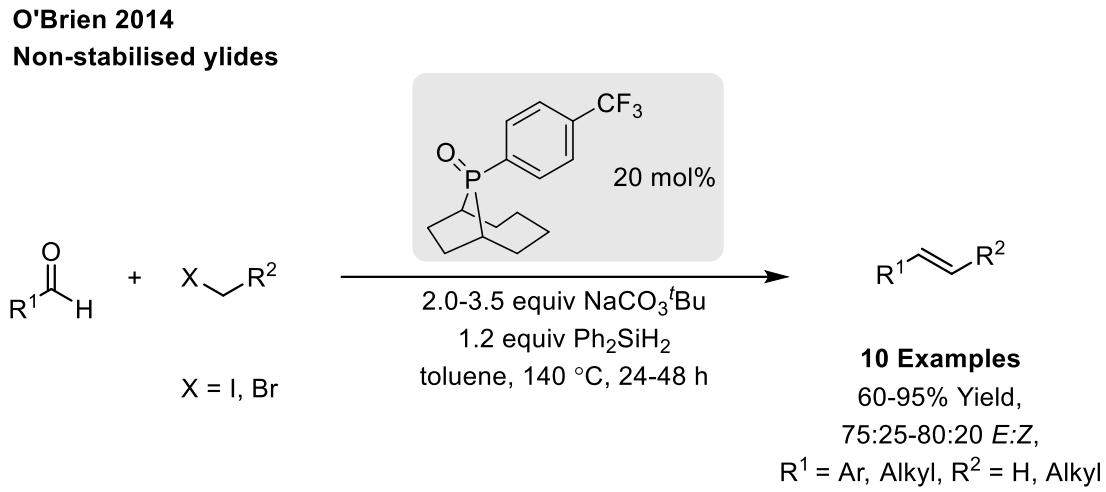
Alternative reaction manifolds have also been used for catalytic Wittig reactions. Microwave assisted catalytic Wittig reactions have been developed greatly reducing reaction times and allowing the use of commercially available alkyl phosphines without the need of a Brønsted acid additive.[49]

Tuning of phosphine oxide structure has been shown to enable diverse catalytic Wittig reactions. O'Brien demonstrated that by carefully tuning the steric and electronic properties of the phosphine oxide pre-catalyst, semi- and non-stabilised ylides could be use in catalytic Wittig reactions (**Schemes 15** and **16**).[50] A key challenge for this methodology was striking a balance between the nucleophilicity of the phosphine catalyst, and the acidity of the α-protons on the corresponding phosphonium salt. Elevated temperatures and diphenylsilane as

the terminal reductant were required. A general procedure was not applicable for the scope of semi-stabilized ylides, and different pre-catalysts and conditions had to be employed to maximize the yields. Impressively Wittig methylenations could be achieved in good yields by using methyl iodide as the alkyl halide, demonstrating a classic use of the traditional Wittig reaction could be adapted in a catalytic manifold. The bicyclic phosphine structure is based on the work of Vedejs who demonstrated its high *E* selectivity in Wittig reactions.[51] This same effect was noted in this study, as moderate to good *E* selectivity for both semi-stabilised and non-stabilised ylides. This selectivity would traditionally require the employment of the Schlosser modification in classical Wittig reactions.



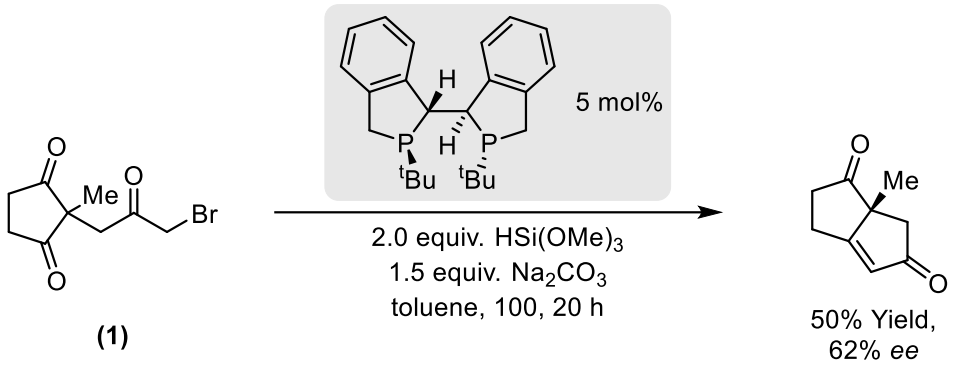
Scheme 15. CWR of semi-stabilised ylides



Scheme 16. CWR of non-stabilised ylides

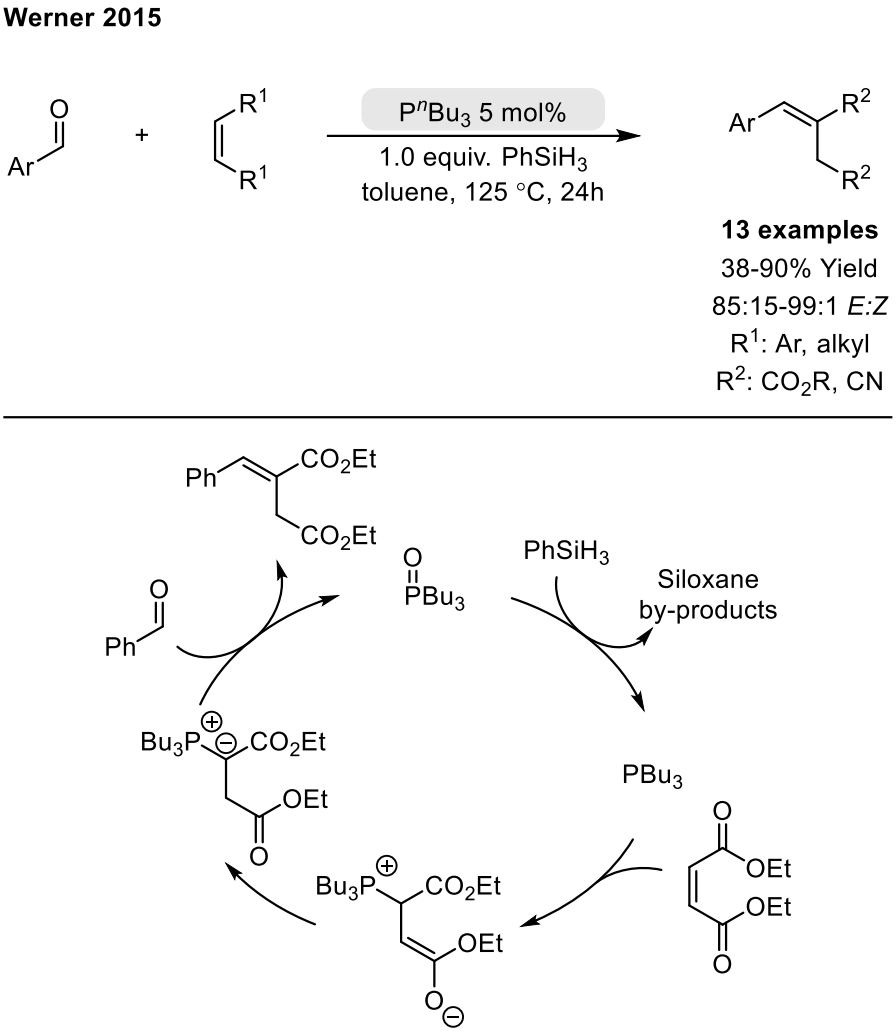
Since, any phosphine oxide which can be reduced under mild conditions can be theoretically employed in a catalytic Wittig reaction, the use of chiral phosphines as catalysts in catalytic Wittig reactions has been explored. Werner reported the first example of an enantioselective catalytic Wittig reaction.[52] Screening a range of chiral phosphines they demonstrated 5 mol% of Me-DuPhos was capable of de-symmetrise prochiral ketone (**1**) with an enantiomeric excess of 90% but a poor yield 10%. This implies the turnover of the catalyst to be rate limiting. A subsequent study demonstrated (DuanPhos to be competent catalyst for de-symmetrisation, giving a modest yield and enantiomeric excess (**Scheme 17**).[53]

Werner 2015



Scheme 17. Enantioselective catalytic Wittig reaction

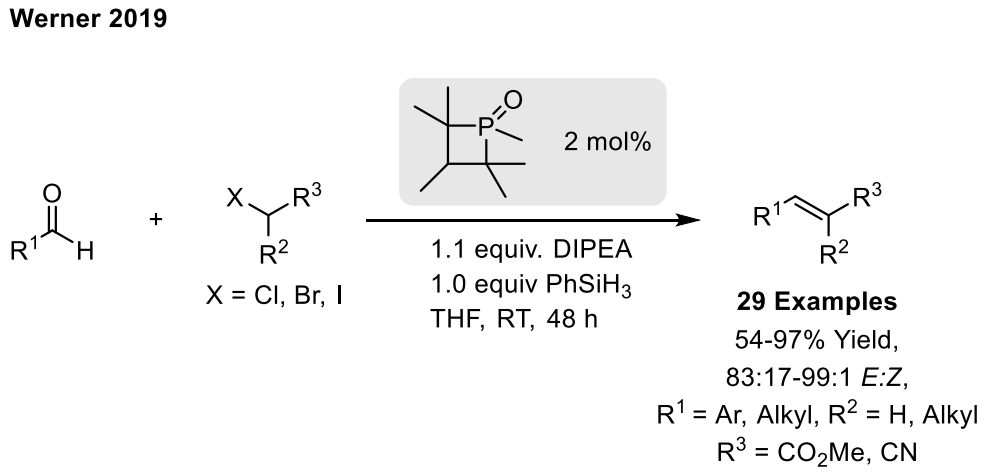
Alternative forms of ylide generation have also been explored, giving access to highly functionalized alkenes. Werner reported base-free catalytic Wittig reactions where ylide generation occurs via Michael addition onto a maleate followed by proton transfer (**Scheme 18**).[54] Improved conditions to this method were found later by employing a cyclic phospholane oxide and benzoic acid as an additive.[55] Subsequent methods have employed acrylates,[56] acetylenes,[57-59] allenes[60] and enones[61] as Michael acceptors. These have been used for the rapid synthesis of functionalized heterocycles[57,58,60,61] and carbocycles.[59]



Scheme 18. "Base-free" catalytic Wittig and proposed mechanism

The initial development of the catalytic Wittig reaction and the subsequent methods are largely dependent on the use of a cyclic 5-membered phospholane oxide to facilitate P–O reduction. Recently, more strained phosphetane oxides have been demonstrated as effective in catalytic Wittig reactions. Werner was the first to employ phosphetane oxide catalysts in catalytic Wittig reactions (**Scheme 19**).[62] This phosphetane oxide has been recently popularised by Radosevic.[63,64] They demonstrated that phosphetane were effective catalyst at room temperature for several reactions, at low catalyst loadings. The authors highlight that (in comparison to O'Brien's 2013 room temperature method) no

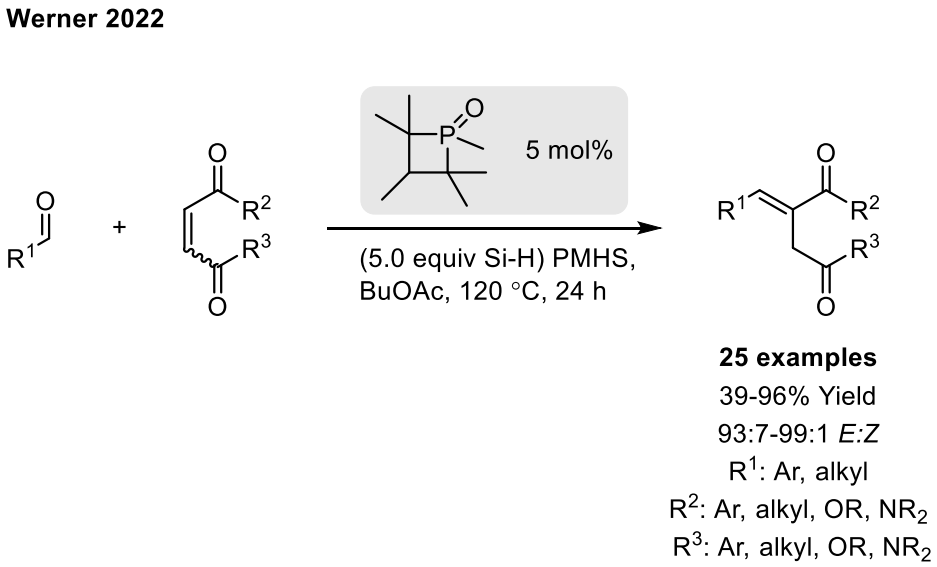
benzoic acid additive is needed to increase the rate of reaction. However, it should be noted that in their optimisation benzoic acid was used as an additive rather than 4-nitrobenzoic acid, as used in the O'Brien paper. Furthermore, an increase in yield was still observed, suggesting that the reaction could still be improved with a Brønsted acid additive.



Scheme 19. Phosphetane oxide catalysed Wittig reactions

While catalytic Wittig reactions reduce phosphine oxide waste associated with typical Wittig reactions, stoichiometric waste streams still result from the use of silane reductants. Nevertheless, It should be noted that catalytic Wittig reactions employing phenylsilane are predicted to reduce the cumulative energy demand (CED) and greenhouse gas emissions (GHG) by 18% and 35% respectively when compared to the traditional Wittig reaction.[65] Phenylsilane is the most prevalent terminal reductant especially in room temperature methodologies, however its relatively high cost, make the adoption of catalytic Wittig methodologies less appealing. Some effort has been made to employ cheaper silanes in organophosphorus catalysed transformations. To this end, PMHS has been identified as an ideal terminal reductant, due to its stability and low cost. Furthermore the use of PMHS in catalytic Wittig reactions is predicted to lower

CED and GHG by 62% and 66% respectively.[65] To date, it was found that only Werner has employed this silane in a catalytic Wittig system (**Scheme 20**).[66] The lower activity of PMHS required the use of elevated temperatures and higher silane loadings. Despite the limited scope of this methodology, this is a further step forward to establishing more sustainable Wittig reactions.



Scheme 20. Catalytic Wittig reactions employing PMHS as a terminal reductant

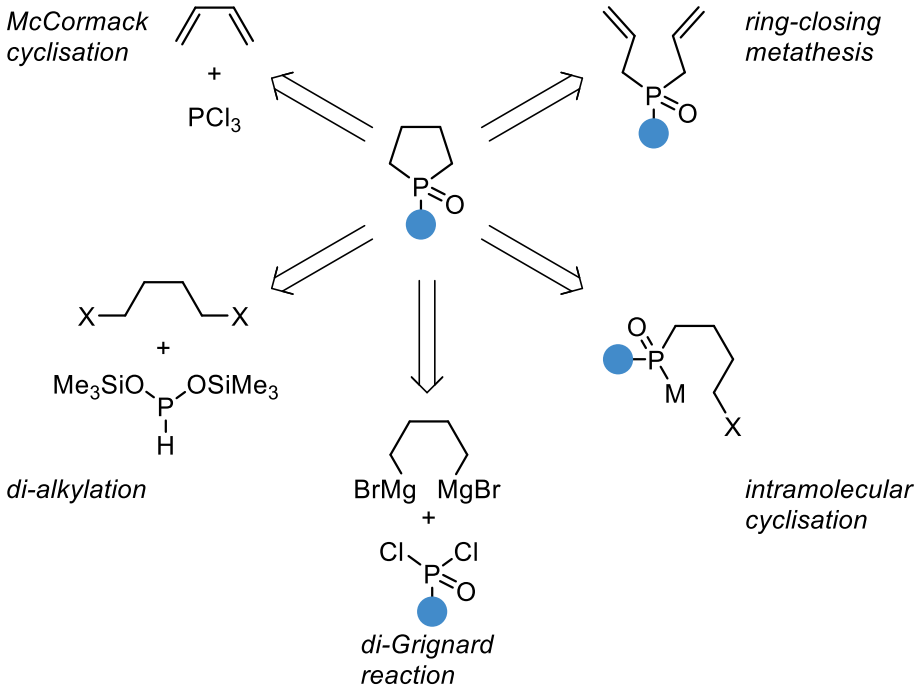
1.8 Project Aims

Despite the clear advantages catalytic Wittig reactions present in improved atom economy and ease of purification, these reactions seem to be limited to academic use. A few barriers to adoption are present; firstly, the selection and synthesis of the more active phosphine oxide precatalyts is non trivial and often involves harsh reagents and conditions. Secondly, the optimal pre-catalyst and silane reductant pairing is often not intuitive, although computational studies as well as some empirical evidence has given some insight. This project aims to provide the first kinetic study into catalytic Wittig reactions to gain further mechanistic insight. The original aim for this project was to perform the kinetic studies on un-published work conducted by O'Brien. Due to the difficulty in gaining consistent reproducible results, as well as the lack of homogeneity of the reaction, the project shifted to the study of O'Brien's 2013 room temperature variant of the catalytic Wittig reaction. The kinetic analysis will be conducted using the variable time normalization analysis (VTNA) methodology popularised by Bures. This technique will be used to determine the rate order in each reaction component.

2. Results and Discussion

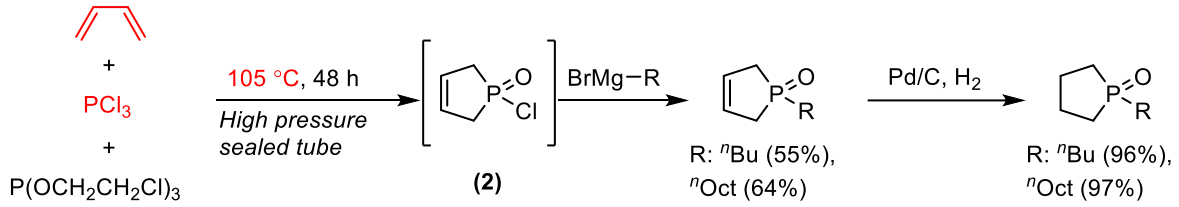
2.1 New route for the synthesis of phospholane oxide pre-catalysts

Before beginning the kinetic studies on catalytic Wittig reactions, we realised one of the largest barriers to entry in carrying out catalytic Wittig reactions is the synthesis of the phosphine oxide catalysts. Catalysts used in previous work are based on cyclic phosphine oxides structures, the majority of which are 5-membered phospholane oxides. Typical routes for the synthesis of phospholane oxides involve multi-step reactions, the handling of hazardous reagents, and can involve manipulations under Schlenk conditions, and are therefore cumbersome. Among these approaches are McCormack cyclisations[67], di-alkylations[68,69], di-Grignard reactions[70,71], intramolecular cyclisations, and ring closing metathesis[72] (**Scheme 21**).



Scheme 21. Strategies for the synthesis of Phospholane oxides

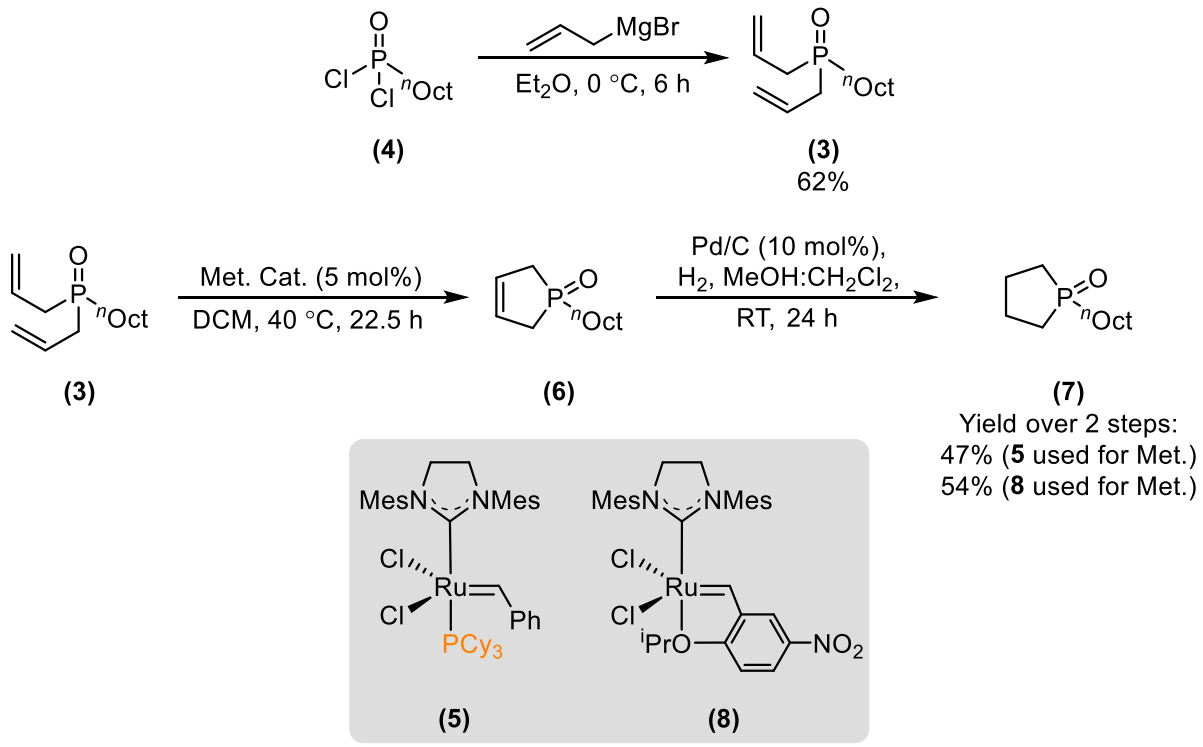
The synthesis of the original phospholane oxide pre-catalysts used by O'Brien is particularly problematic. This route involves a McCormack cyclisation between phosphorus trichloride (a toxic chemical weapons precursor), butadiene and tris(2-chloro-ethyl) phosphite at elevated temperatures, thus requiring the use of pressure rated glassware (**Scheme 22**). While the synthesis of 1-chloro-3-phospholene oxide (**2**) allows for facile catalyst diversification, the harsh conditions required for its synthesis make it unfavourable. In fact, other than O'Brien's group we could find no recent examples of this route being employed.



Scheme 22. O'Brien route to catalyst

As previously stated, our early work was attempting to study an unpublished reaction developed by O'Brien employing an n-octyl substituted phospholane oxide catalyst, and therefore some of the early phospholane synthesis studies were conducted on this system. Our initial strategy for the phospholane synthesis was *via* ring closing metathesis. Diallyl phosphine oxide (**3**) was prepared from the commercially available dichloride (**4**), in a satisfactory yield of 62%. Ring closing metathesis using 2nd generation Grubbs metathesis initator (**5**) led to quantitative conversion of the cyclised product (**6**), as evidenced by ^{31}P NMR spectroscopy. Although some effort was spent in purifying this intermediate by column chromatography, it was found that the trace impurities of tricyclohexylphosphine oxide in the crude product were difficult to separate without a significant loss in yield. Furthermore, column chromatography was not found to be effective in removing ruthenium impurities.

Removal of ruthenium impurities is a non-trivial problem when employing metathesis.[73] It was found that by telescoping the crude cyclised product from the metathesis into the next step and distilling the final product the pure phospholane oxide could be obtained. Although both the metathesis and hydrogenation were found to go to completion by analysing the crude NMR spectra of the compounds, significant amounts of product were lost during the distillation. We found that employing the nitro-Grela metathesis initiator (**8**) eliminated the problem of phosphine oxide impurity (as no phosphine ligands are present) however the higher cost of this catalyst makes this less practical on a larger scale.



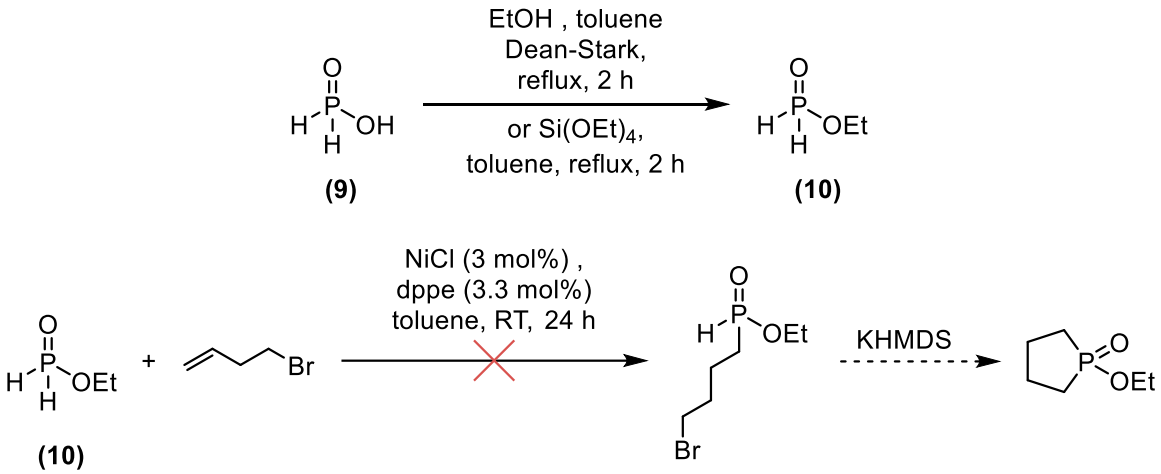
Scheme 23. Route for phospholane oxide pre-catalysts

While this route was successful, it is inherently limited to the commercially available phosphoryl dichlorides limiting catalyst tunability. Secondly the possibility of trace ruthenium content, and palladium could potentially affect the

catalysts effectiveness in the catalytic Wittig sequence as trace metal contaminants could potentially react with the organosilane reductant.

Therefore, a simpler method was sought with large-scale catalyst synthesis in mind. Our ideal route would use inexpensive, avoid the handling of phosphorus trichloride, and would make use of a simple method for catalyst purification.

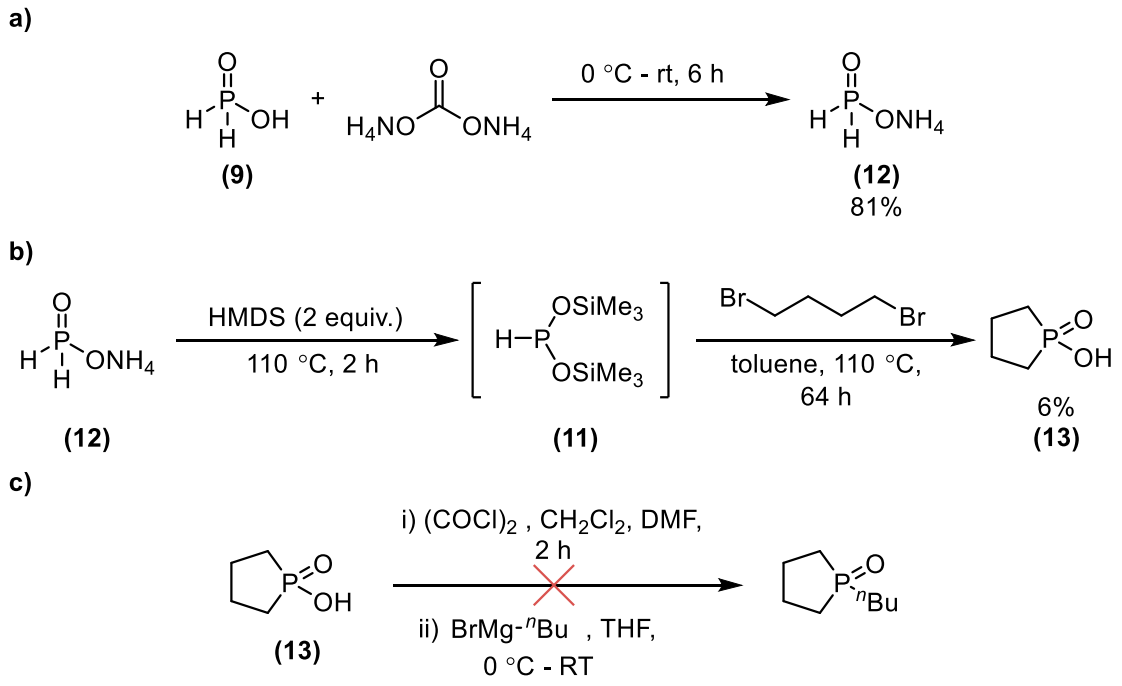
We were interested in using hypophosphorous acid (**9**) as a the phosphorus atom source for the catalyst, due to the fact it is inexpensive, easy to handle and not derived from PCl_3.[46] Taking inspiration from work by Montchamp and co-workers which described the hydrophosphination of terminal alkenes with H-phosphinate esters (**10**).[74] In our hands however the H-phosphinate esters did not seem to form quantitatively, and the subsequent hydrophosphination was found to be unsuccessful (**Scheme 24**).



Scheme 24. Attempted catalyst synthesis based on cyclisation

An alternate route from hypophosphorous acid was explored, *via* a double Arbuzov reaction with bis(trimethylsiloxy)phosphine (**11**) which is generated *in situ* from ammonium hypophosphite (**12**). While compound (**12**) could be readily prepared in good yield the subsequent double Arbuzov reaction resulted in a

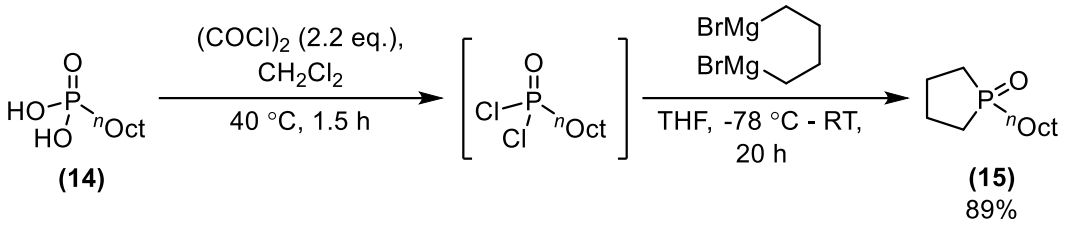
number of impurities evident in the ^{31}P NMR spectrum of the crude material (**Scheme 25a** and **25b**). Isolation of the pure hydroxy phospholane oxide (**13**) was cumbersome, due to the limited methods in visualising the compound *via* TLC, giving an overall poor yield of (**13**). When the isolated (**13**) was used in the subsequent chlorination and Grignard addition, a mixture of products was seen which could not be separated. (**Scheme 25c**).



Scheme 25. Attempted synthesis from ammonium hypophosphite

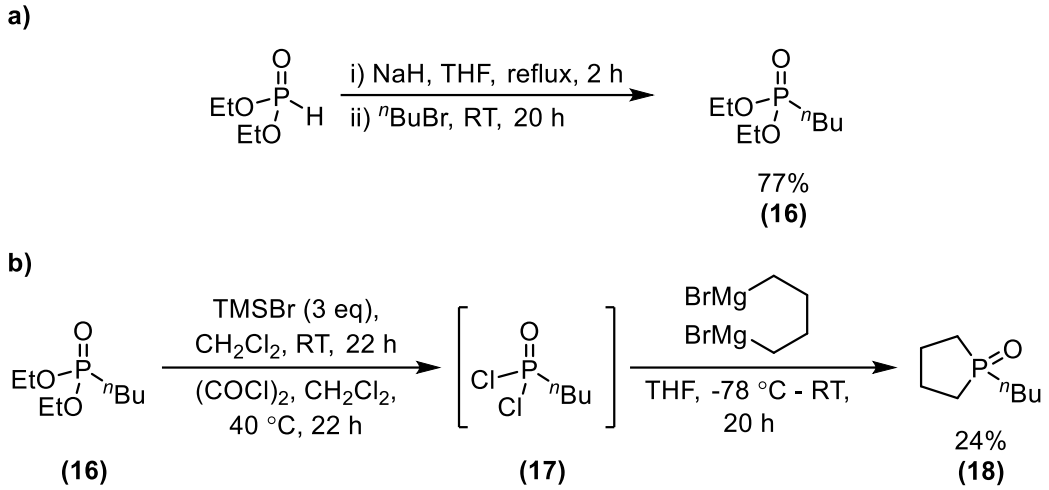
Finally, we thought of using a double Grignard addition to a phosphorous electrophile to form the ring. Double-Grignard additions to form phospholane oxides have generally suffer from impractical conditions, or low yields, the main problem in these reactions being unproductive oligomerization.[70] A more recent study found that performing the Grignard addition at low temperatures resulted in good yields of phospholanes.[71] However in this report, the purity of the compounds was not established (no ^{31}P NMR spectra were supplied on the supporting information), and their methodology is limited to commercially

available phosphoryl dichlorides. When reproducing their method, we found it to be effective while using n-octyl phosphonic acid (**14**) with only trace amounts of impurities being present (**Scheme 26**).



Scheme 26. Double-Grignard addition to form phospholane (**15**)

We thought phosphonate esters could be simple precursors for the phosphonic acids. A simple method for the synthesis of the corresponding alkyl phosphonate ester (**16**), via a Michaelis-Becker type alkylation was found in good yield without the need for column chromatography (**Scheme 27a**). In our hands however isolation of phosphonic acids was difficult due to their high solubility in aqueous media. We therefore thought to avoid the direct isolation of phosphonic acids and to directly prepare the phosphoryl dichloride. To this end we developed a one pot method where, phosphoryl dichlorides could be prepared *in-situ* by the sequential de-alkylation and chlorination (**Scheme 27b**). Inspection of the ^{31}P NMR of the crude dichloride (**17**) demonstrated near quantitative conversion only trace impurities were present. After removal of all volatiles and dilution of (**17**) with THF, the freshly prepared di-Grignard reagent was added to the same reaction vessel. After a few attempts at purifying phospholane (**18**) we found distillation to be suitable method delivering the phospholane (**18**) in a modest 24% yield after three steps.

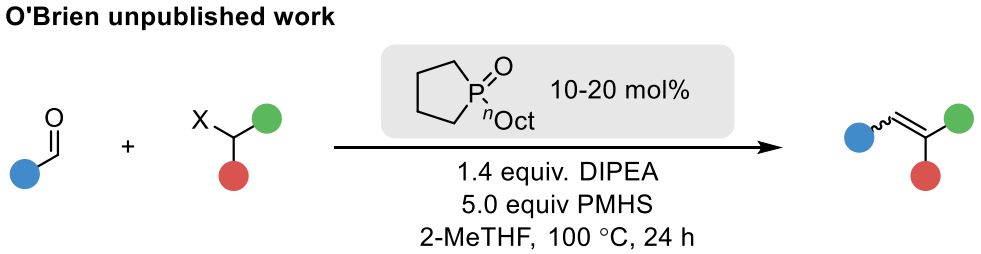


Scheme 27. a) Michaelis-Becker type alkyation of diethyl phosphite b) preparation of phospholanes (**18**) by di-Grignard addition

While we believe this sequence is already a good improvement on O'Brien's route, further optimization of the reaction needs to be undertaken to improve the yield. If the phospholane oxide product would be solid, recrystallization could be used as a much simpler method for purification.

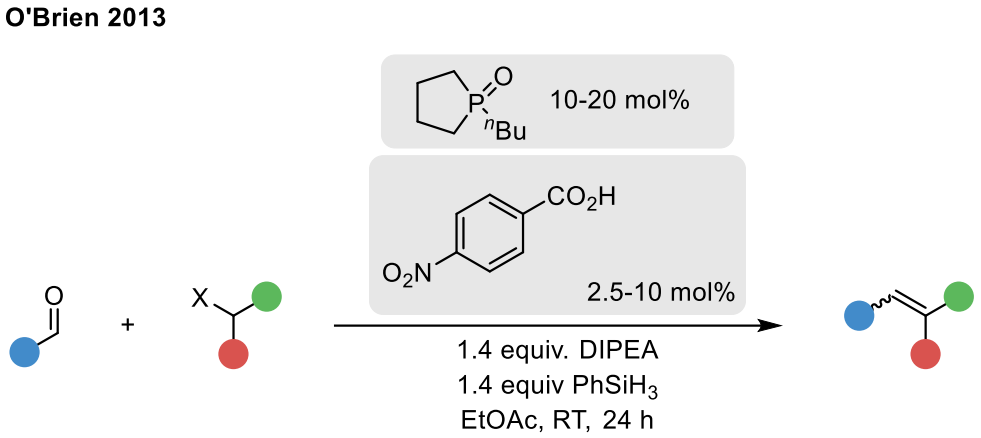
2.2 Investigation into Room Temperature Catalytic Wittig reaction

The initial aim of the project was to study the kinetics of unpublished work by O'Brien (**Scheme 28**), which employed PMHS as a cost-effective and sustainable silane reductant. However, we found this reaction to be capricious and not suitable for kinetic study. The reaction medium was heterogeneous, as a result of gummy solids being produced over the course of the reaction, therefore rendering any *in-situ* and *ex-situ* reaction monitoring methods unfeasible.



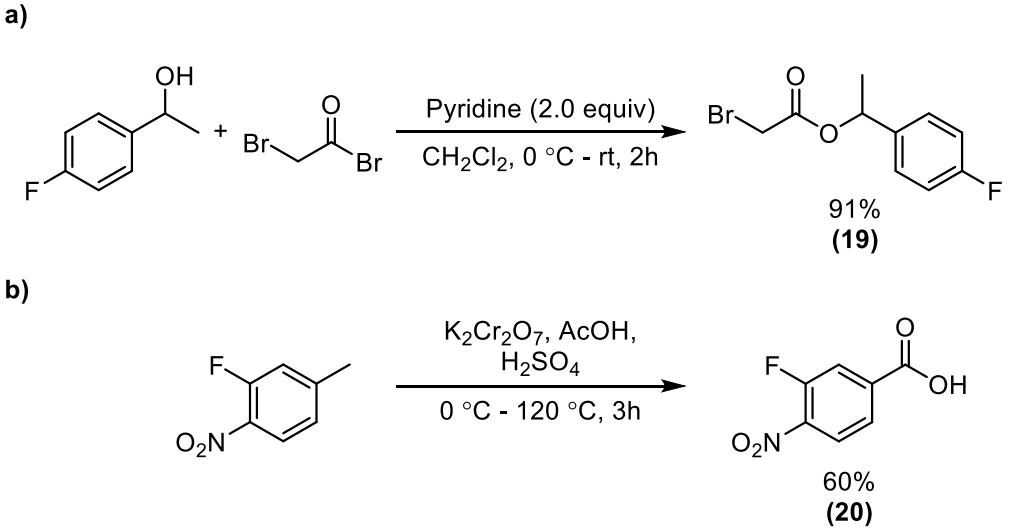
Scheme 28. O'Brien's catalytic Wittig reaction employing PMHS as a terminal reductant

Therefore, it was decided to investigate O'Brien's 2013 room temperature catalytic Wittig reaction (**Scheme 29**). We envisaged a kinetic study could provide valuable information in helping further development catalytic Wittig reactions, by determining which step is rate limiting and if other factors such as catalyst decomposition or product inhibition affect this reaction. Additionally, we wanted to gain a better understanding on the role of the benzoic acid additive in the catalytic process. We believe O'Brien's suggestion that the acid activates the phosphine oxide to increase the rate of reduction to not be possible due to the conditions of the reaction. Due to our group's experience in organosilicon chemistry, we believe the role of the benzoic acid is to activate the silane reductant instead of the phosphine oxide.



Scheme 29. O'Brien's room temperature catalytic Wittig

We reasoned that ^{19}F NMR spectroscopy could enable simple monitoring of the progression of the reaction. The small Hammett σ_p value (0.06) for the fluorine group, ensures the that it would not exert an electronic effect on the reaction under study.[75] Fluorine labelling each component in our model reaction would allow for monitoring of each step of the proposed catalytic sequence. Furthermore, ^{31}P NMR could be used to probe the resting state of the phospholane catalyst. Fluorinated α-bromo ester (**19**) and 3-fluoro 4-nitro benzoic acid (**20**) were therefore prepared (**Scheme 30**).

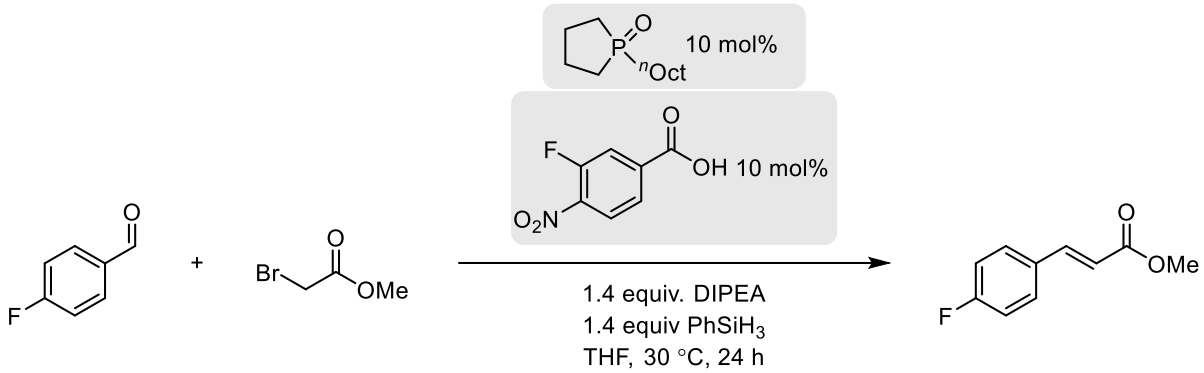


Scheme 30. a) preparation of fluorinated α-bromo ester, b) preparation of fluorinated benzoic acid

2.2.1 Reaction Monitoring and Kinetic Studies

In their original publication O'Brien conducts the room temperature catalytic Wittig at high concentrations (3.0 M in aldehyde). However, this concentration is not suitable for reaction monitoring by NMR spectroscopy, where ideally for high data density the reaction would be carried out in an NMR tube. Initial tests were conducted running the reaction at lower concentrations in an NMR tube however a few practical challenges were encountered (**Table 1**). Firstly, the reaction generates the DIPEA hydrobromide salt as a precipitate which prevents the acquisition of reliable NMR data. When attempting to acetonitrile as a solvent as the DIPEA salt was soluble, we observed much worse conversion. Furthermore, the evolution of a significant amount of hydrogen gas also made running the reaction in a sealed tube unsafe. Although we could perform the reaction in a pressure rated NMR tube the continuous bubbling of gas also gave problems with the acquisition of NMR data. These factors as well as the lack of mixing possible while performing a reaction in an NMR tube made the reaction poorly reproducible even when setting the reaction up under identical conditions different results were obtained (**Table 1** entries **2** and **3**)

Table 1. Attempts at *in-situ* reaction monitoring using NMR tube



Entry	Concentration (M)	Conversion*
1	0.25	88%
2	0.20	87%
3	0.20	89%

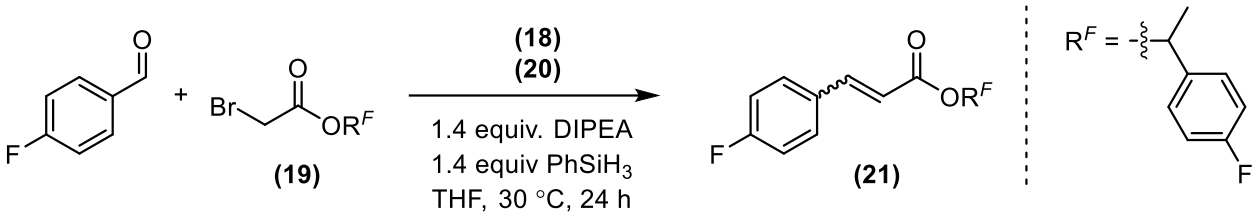
*Conversion determined by quantitative ^{19}F NMR spectroscopy of crude mixture using 4,4'-bis(trifluoromethyl)-1,1'-biphenyl as an internal standard. Concentration in $mgmL^{-1}$

With the aim of performing the reaction monitoring *in-situ* we attempted to use Bruker insight flow NMR system which would allow for monitoring under normal reaction conditions. Unfortunately, after some preliminary experiments, we noticed the hydrogen gas evolved during the course of the reaction was found to interrupt the flow of the piston pump so the mixture could not be effectively flowed into the spectrometer.

We therefore to use *ex-situ* monitoring by taking aliquots of the reaction mixture. A brief conditions screening was performed to obtain the best conditions for convenient reaction monitoring (**Table 2**). Although good conversion was observed under similar conditions to the original publication (Entries 1 and 2), to obtain the best kinetic data we wanted to observe the reaction to go to over 99% conversion. It should be noted that the catalytic

Wittig reaction is heterogeneous as a white precipitate forms during the course of the reaction, which was later identified as the DIPEA hydrobromide salt. As this was anticipated to complicate sampling we attempted the reaction in MeCN as the DIPEA salt was found to dissolve in this solvent however very poor conversion was observed under the same conditions when using this solvent. This was interesting as it suggests that the precipitation of the salt may be necessary to drive the formation of the ylide. We found by doubling the concentration of catalyst and benzoic acid the catalytic Wittig reaction could go to over 99% conversion in 6 hours.

Table 2. optimisation of *ex-situ* monitoring



Entry	**(18)**	**(20)**	Concentration	Solvent	Time	Conversion*
1	10 mol%	10 mol%	1.0 M	THF	5.5 h	63%
2	10 mol%	10 mol%	2.0 M	THF	6 h	77%
3	10 mol%	10 mol%	1.0 M	MeCN	6 h	25%
4	20 mol %	20 mol %	1.0 M	THF	6 h	99%
5	20 mol %	20 mol %	0.5 M	THF	6 h	99%
6	20 mol %	20 mol %	0.5 M	THF	8 h	99%

*Conversion determined by quantitative ^{19}F NMR spectroscopy of crude mixture 4,4'-bis(trifluoromethyl)-1,1'-biphenyl as an internal standard.

With these standard conditions in hand reaction monitoring was performed in triplicate, to asses reproducibility. Despite the reaction being heterogeneous we found very good agreement between three runs conducted under the same conditions.

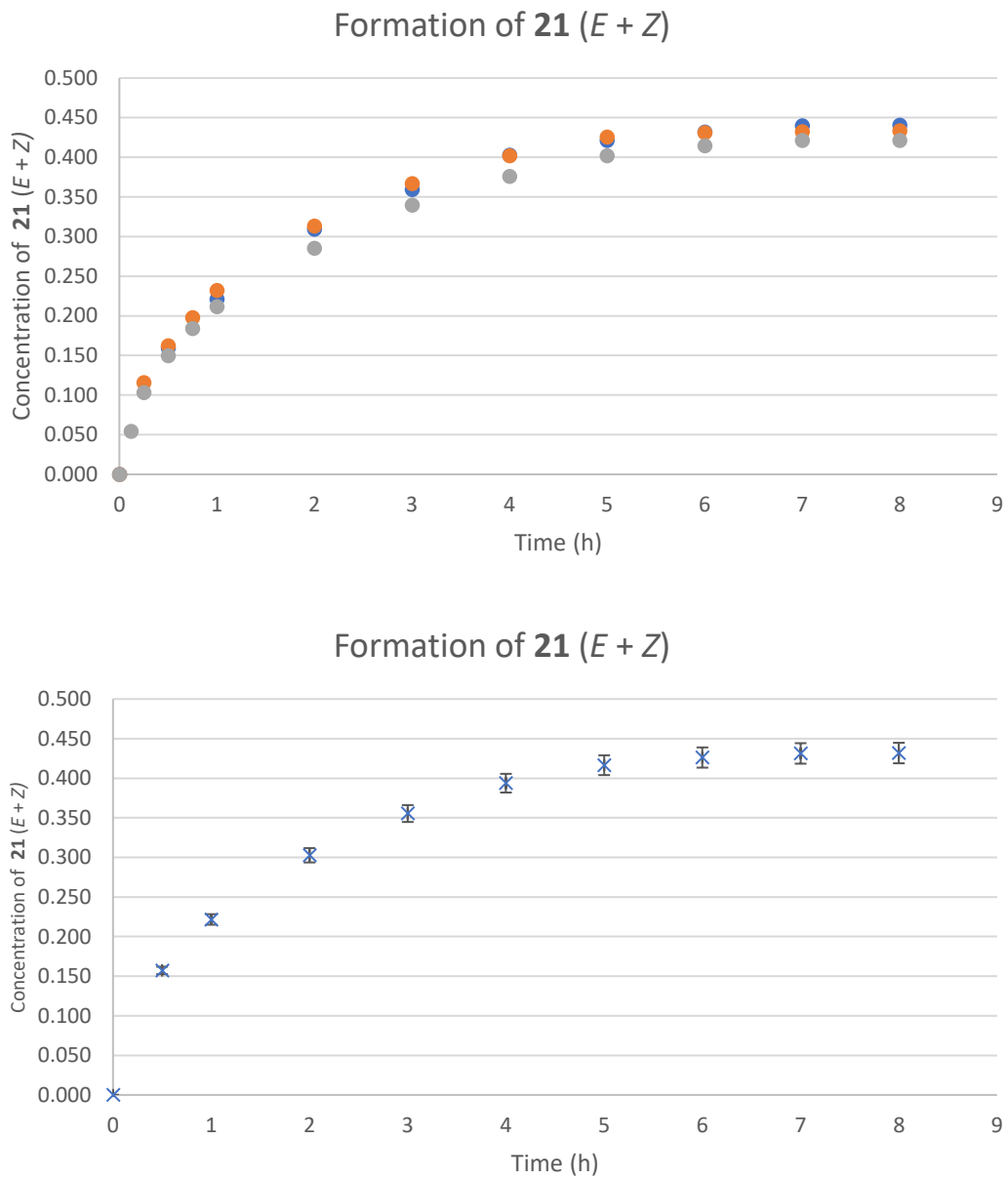


Figure 6. (top) Time plot for formation of **21** (sum of *E* + *Z* alkene products) from three runs using standard conditions. (bottom) Average time plot from three runs including standard deviation of three runs. Concentration of *E* + *Z* alkene products denoted in $mgmL^{-1}$

We next sought to determine the order of each substrate on the reaction. To do this we believed visual time normalization analysis (VTNA) would be the best method due to the low amount of data needed for analysis.[76] A number of different excess experiments were performed (**Table 3**). Unfortunately, due to time constraints we were not able to perform the different excess experiments on the silane or the benzoic acid.

Table 3. Summary of different excess experiments performed. Concentration reagents products denoted in $mgmL^{-1}$.

Entry	Aldehyde (M)	**(19)** (M)	**(18)** (M)	**(20)** (M)	DIPEA (M)	$PhSiH_3$ (M)
1	0.501	0.651	0.100	0.100	0.704	0.699
2	0.373	0.500	0.100	0.102	0.704	0.699
3	0.501	0.650	0.100	0.100	0.502	0.699
4	0.501	0.651	0.075	0.100	0.704	0.699

The time normalized plots were compared until divergence in product yield was observed. The visual comparison for the plots shown below suggest that the reaction is zero order in α-bromo ester, DIPEA and aldehyde (**Figure 7**). Thus suggesting that the alkylation of the phosphine, deprotonation of the phosphonium salt and the Wittig reaction are not rate limiting. Although it was difficult to distinguish by visual analysis, the reaction rate is clearly dependent on the concentration of the catalyst, a first order fitting fit best. Although we were not yet able to perform the different excess experiments on the benzoic acid additive, the results thus far still suggest that the reduction of the phosphine oxide is rate limiting. We expect the exact nature of the silane reductant to be difficult to observe from kinetic studies. It has been suggested that the silanol by-products from phenyl silane reduction are better reductants.

Therefore, it can be expected that the reduction rate may increase during the course of the reaction which complicates the derivation of a rate order in phenyl silane.

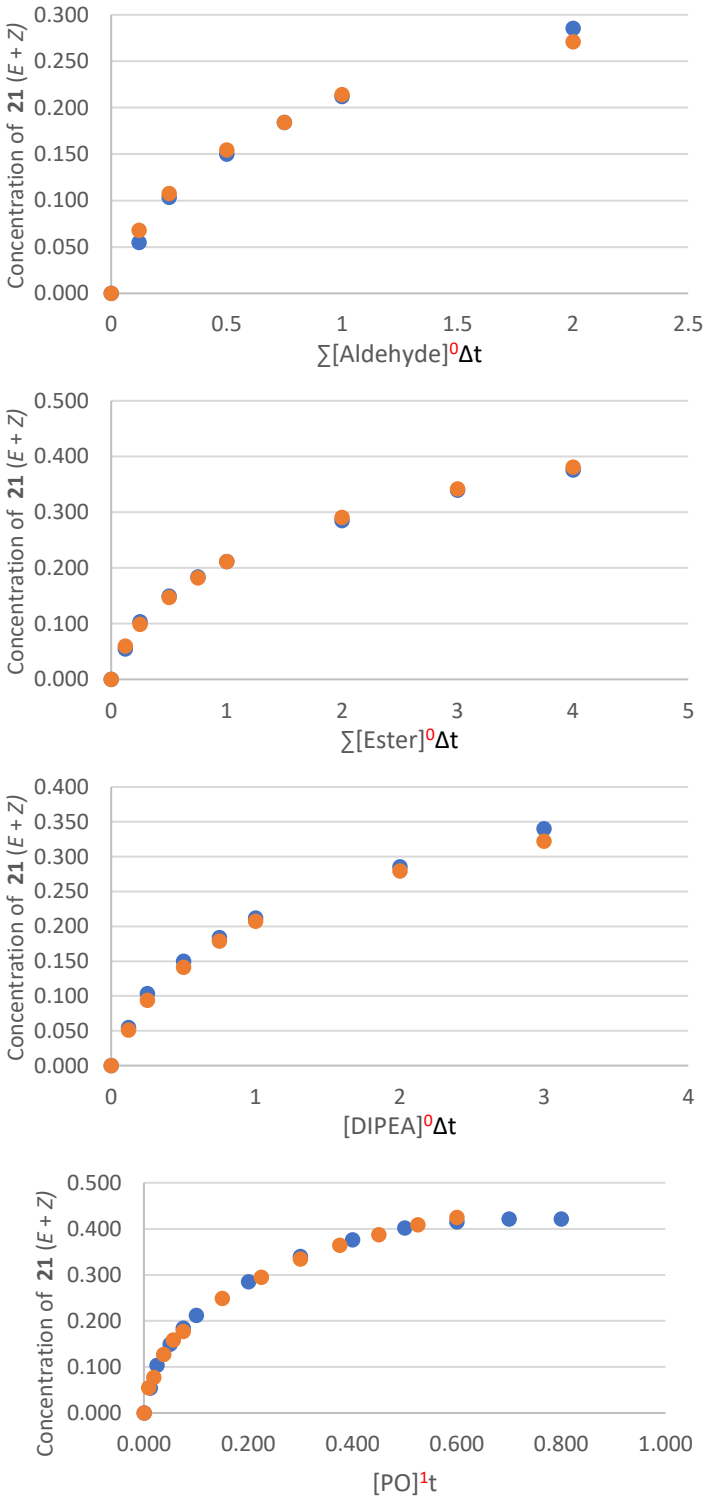
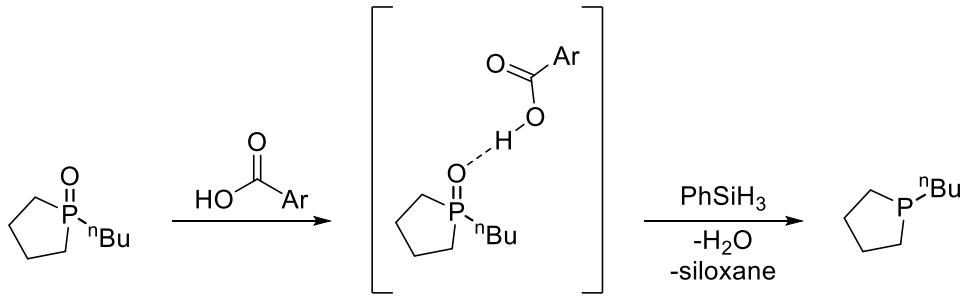


Figure 7. Different Excess experiments for substates (Full visual comparisons in SI)

2.2.2 Investigation on the Role of the Benzoic Acid Additive.

O'Brien has implied that the benzoic acid additive acts as a proton donor to activate the phosphine oxide (**Scheme 31**).



Scheme 31. Previous postulated mechanism of activation of phosphine oxide by Brønsted acid catalyst

We believe this cannot be the case under the reaction conditions, as a sub stoichiometric amount of benzoic acid is used in comparison to the amount of base (10 mol% of benzoic acid compared to 1.4 equivalents of base). To disprove the role of phosphine oxide activation a simple NMR experiment was performed. As is shown below when the acid is added to the phosphine oxide a shift is observed in the ^{31}P spectra of circa 5 ppm (**Figure 8b**). However, once the stoichiometric amount of DIPEA is added to the reaction mixture the shift returns to its original position (**Figure 8c**).

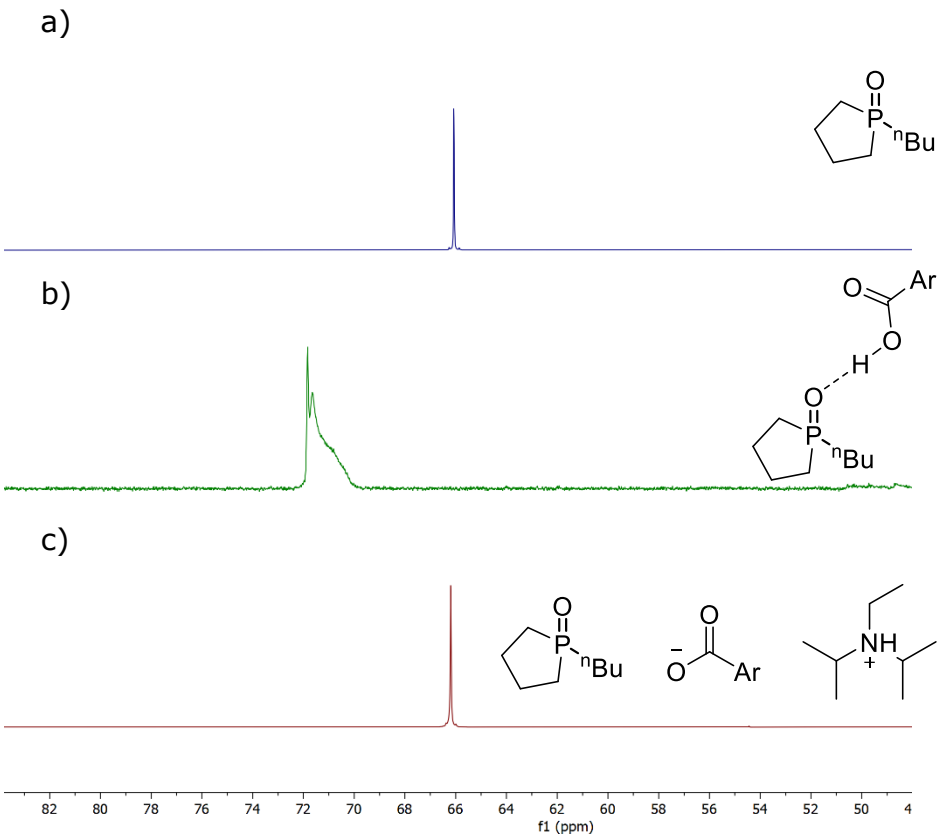
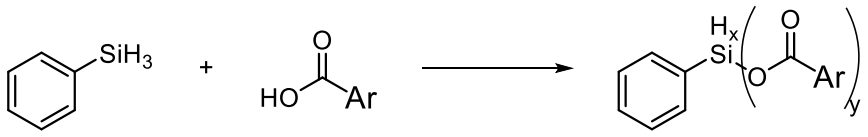


Figure 8. ^{31}P spectra of phosphine oxide a) phosphine oxide (**18**)
b) 1 equiv. of phosphine oxide (**18**) + 1 equiv. of acid (**20**).
c) 1 equiv. of phosphine oxide (**18**) + 1 equiv. of acid (**20**) + 7 equiv. DIPEA

From our group's experience in organosilicon chemistry, we believed that the increase in reduction rate observed in this reaction was due to the activation of the organosilane (to make it a better reductant) not the phosphine oxide. We believed this activation was from the of an *in-situ* generation of silyl esters (**Scheme 32**).



Scheme 32. Generation of silyl esters

We first investigated this silane activation by computationally modelling the energy barriers for phosphine oxide reduction using density functional theory. This modelling demonstrated a significant decrease of 5.28 kcal/mol in the reduction barrier when a silyl ester was used compared to phenyl silane (**Figure 9**).

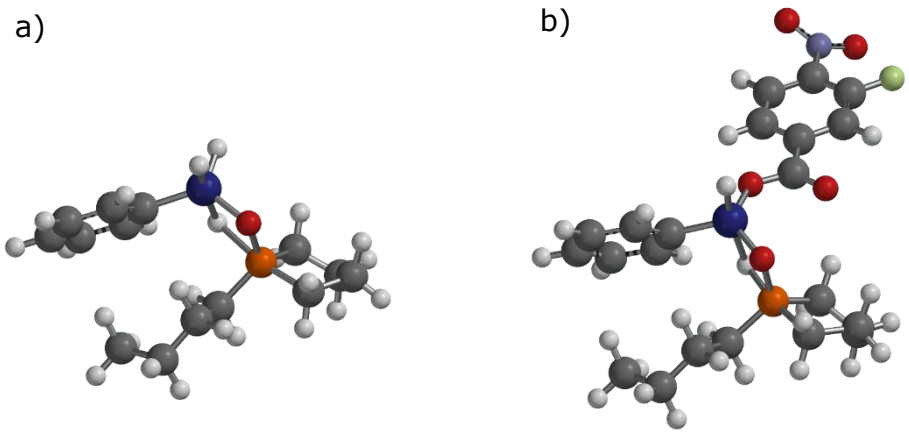
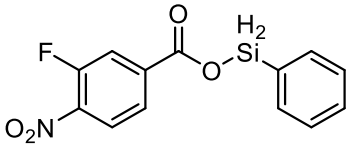


Figure 9. Comparison of phopshine oxide reduction barriers by phenyl silane (a) vs silyl ester (b) (DFT Calculations done at ωB97X-D level of theory with 6-31+G* basis set, all energies in kcal/mol)

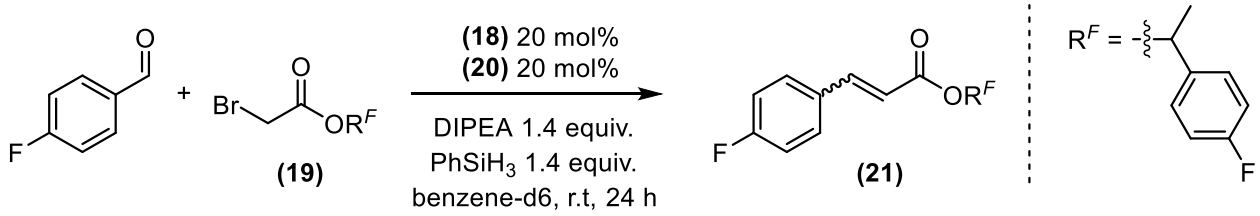
From both *in-situ* and *ex-situ* reaction monitoring, we observed a significant change in shift for the fluorine labelled benzoic acid. owever, we did not observe characteristic complex speciation associated with the formation of a number of silyl esters.[77] We therefore prepared the fluorine labelled silyl ester (**22**) (**Figure 10**) to compare the ^{19}F NMR shift with that of a catalytic Wittig reaction monitored *in-situ* (**Scheme 33**).



(22)

Figure 10: Fluorinated silyl ester

By conducting a catalytic Wittig reaction in an NMR tube, we found a significant change in chemical shift for the fluorinated benzoic acid (**20**) occurring during the course of the reaction (**Figure 11**). Before addition of phenylsilane a sharp singlet is observed at -119.2 ppm (**Figure 11b**) in the $^{19}F\{^{1}H\}$ NMR spectra, upon addition of phenyl silane the chemical shift changes into a broad range of shifts spanning (-116.8)-(-117.9) ppm in the $^{19}F\{^{1}H\}$ NMR spectra. Previous work in our group has demonstrated this broadening is characteristic of the formation of silyl esters. The isolated silyl ester **22** was found to have a $^{19}F\{^{1}H\}$ chemical shift of -116.9 ppm providing strong evidence for its presence in the reaction.



Scheme 33. Catalytic Wittig reaction performed in NMR tube for *in-situ* monitoring.

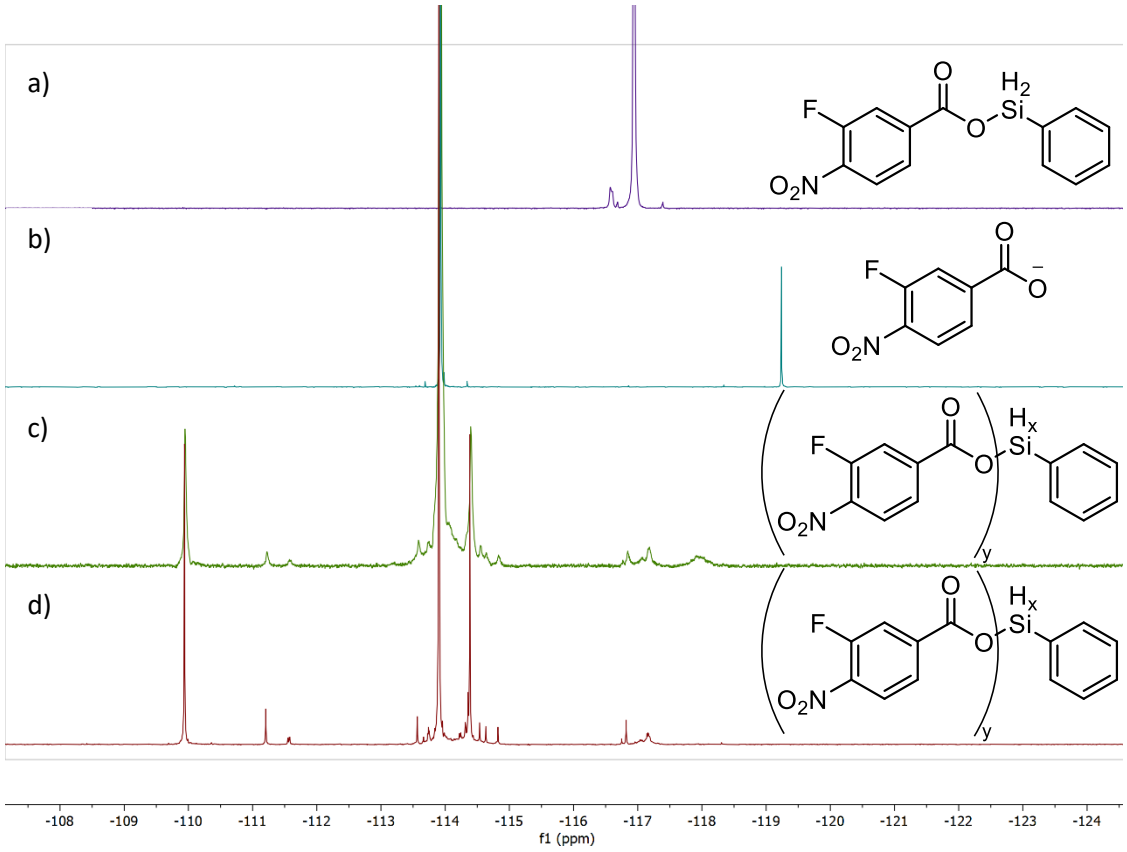


Figure 11. a) ^{19}F spectra of silyl ester (**22**)
b) ^{19}F spectra of catalytic Wittig reaction before addition of phenyl silane conducted in benzene-d_6 showing carboxylate
c) ^{19}F spectra of catalytic Wittig reaction 30 min after addition of phenyl silane showing complete consumption of carboxylate and generation of silyl esters
d) ^{19}F spectra of catalytic Wittig reaction 2 h after addition of phenyl silane showing change in silyl esters

2.3 Computational Screening of Phosphine Oxide Catalysts

As previously mentioned, the structure of phosphine oxide catalysts can have a dramatic effect on their performance in catalytic Wittig reactions. In previous work catalyst selection is often not rationalised, but rather dependent on what is commercially available or easily synthesised. Work by O'Brien[50], Werner[52] and Kwon[60] have already demonstrated that rational catalyst design can expand the scope of Wittig reactions, increase the rate of phosphine oxide reduction, and enable desymmetrisation reactions. Synthesis and subsequent experimental screening of libraries of phosphine oxides would be cumbersome and time-

consuming. As our results thus far suggest, the reduction of phosphine oxides is rate-limiting in catalytic Wittig, even under enhanced reducing conditions. We therefore sought to employ QM modelling of the reduction of phosphine oxides to screen most effective catalyst structures. In this regard, we took inspiration from work done by Krenske modelling the mechanism of the reduction of phosphine oxides mediated by phenyl silane[78] (**Figure 12**). Krenske showed, the rate determining step in this sequence is the hydride transfer from the silane to the phosphine. This goes *via* an asynchronous 4-membered transition state, where the forming Si-O bond is more developed than the P-H bond. The authors demonstrated that more electron rich phosphine oxides are reduced fastest. This was rationalized due to the increased negative charge on the oxygen of the phosphine oxide making it more nucleophilic to attack the Si centre.

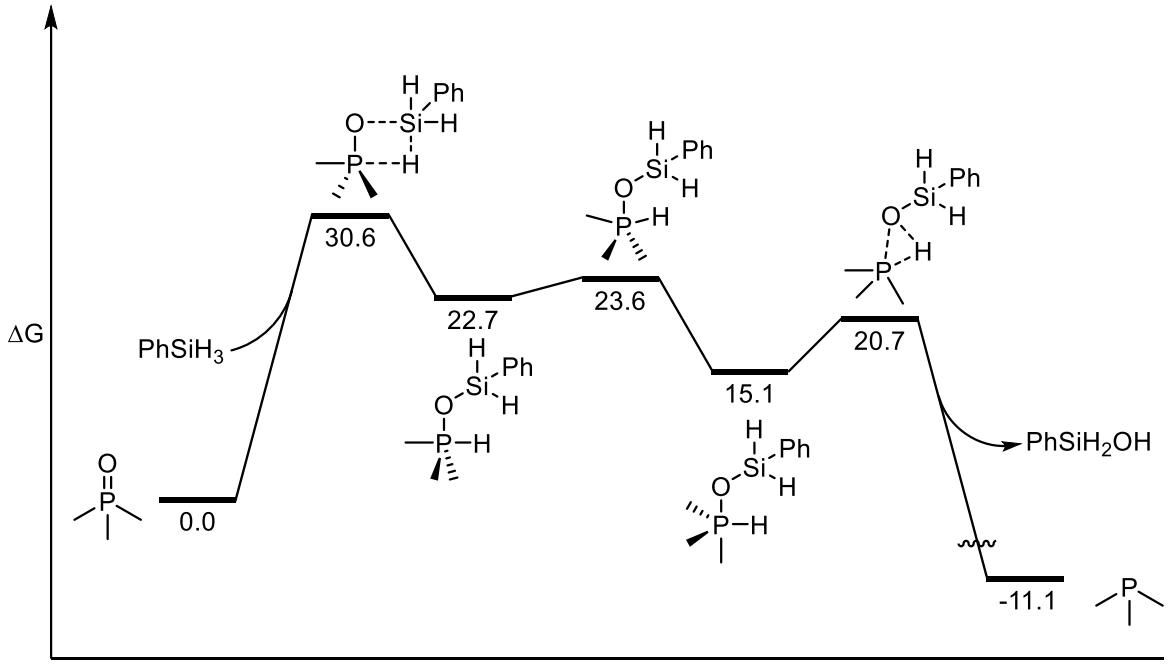
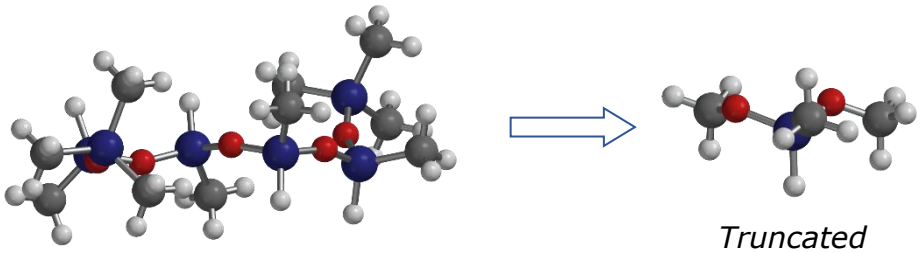


Figure 12. Free energy profile for phenylsilane mediated reduction of trimethyl phosphine oxide calculated by M06-2X/6-311+G(d,p) (energies in kcal/mol, presented relative to trimethyl phoshphine oxide, scheme adapted from Krenske[63]).

Given the interest in employing PMHS cost-effective terminal reductant for use in catalytic Wittig reactions, we chose to explore the phosphine oxide reduction barriers using a model system based on PMHS. In our model system, a few approximations were made to make the calculations less computationally expensive. As demonstrated by Krenske, the hydride transfer in the reduction of phosphine oxides is rate determining with all subsequent barriers being small. We therefore determined the energy barriers only for this first step. As PMHS is a polymeric silane, we chose to represent it as a truncated monomer (**Figure 13a**). For less expensive calculations we also performed the calculations without a solvent model. We understand these approximations cannot give quantitative data which accurately reflect the absolute energy barriers for the PMHS mediated reduction of phosphine oxides. However, the relative comparison of these results could still provide valuable information on how the geometry and substitution of phosphine oxides can impact the reduction barrier.

a)



b)

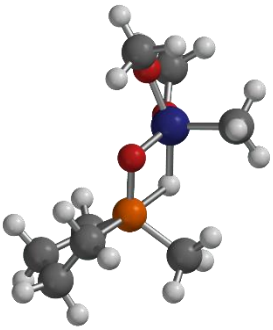
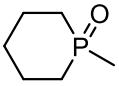
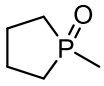
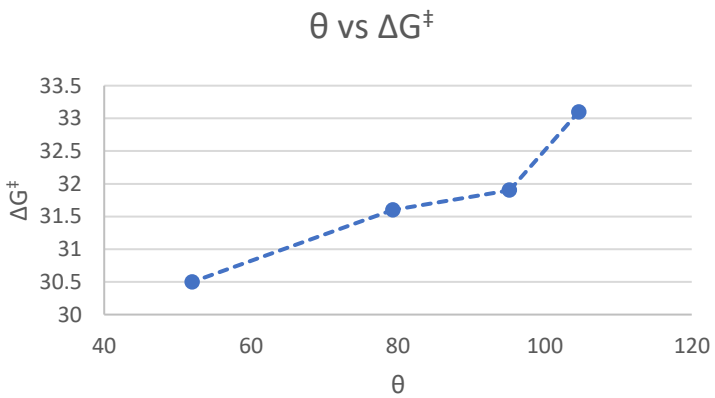


Figure 13. a) Truncated PMHS model used in study
b) Transition state geometry of rate-limiting hydride transfer

To begin with, the effect of phosphine oxide ring strain was examined. We found acyclic phosphine oxides possess the highest activation barriers for reduction. We then found correlation between the increased ring strain and decrease in the energy barrier (**Table 4**). These results are in agreement with Krenske's phenyl silane-based study[78] as well as kinetic studies conducted by Van Delft.[79] Phospholane (**25**) was anticipated to have the lowest barrier for reduction due to the internal C-P-C of the 5-membered ring to being closest to 90°, which is the angle present in the trigonal bipyramidal transition state. Therefore, according to our results, ground state destabilization seems not to be an important factor in lowering the reduction barrier, in contrast to what has been suggested by Kwon.[60] Phosphirane (**27**) showed the lowest barrier to reduction, however the general instability of these compounds (unless sterically and electronically stabilized[80]), makes them unsuitable catalysts.

Table 4. Effect of ring strain on phosphine oxide reduction barrier. Ordering based on magnitude of activation barrier for reduction. (energies in kcal/mol, θ: C-P-C is the internal angle of the cyclic structure in degrees)

Phosphine Oxide	 **(23)**	 **(24)**	 **(25)**	 **(26)**	 **(27)**
$\Delta G^{\ddagger}$	33.1	33.1	31.9	31.6	30.5
θ	104.6	104.6	95.2	79.3	52.0



Next, we aimed to investigate the effect of substitution on the reduction barrier of various cyclic phosphine oxides (**Table 5**). We found that more strained systems did not always have the lowest transition state barriers, as evidenced by comparing phospholane oxides (**30**) and (**31**). Methyl substitution on the ring system was shown to lower the energy barrier, for phospholanes, phosphetanes and phosphiranes. Incorporating the tert-butyl group was shown to increase the energy barrier, presumably due to greater steric incumberance with the methyl groups on the silane. On the other hand, the trimethyl silyl group drastically lowered the energy barrier, however at this time the significant reduction in barrier is not clear. Phosphetane (**35**) was found to have the lowest barrier to reduction amongst all other screened phosphine oxides (**Table 6**). This is in line with Werner's findings that (**35**) enables room temperature catalytic Wittig reactions at low catalyst loadings without the need of a benzoic acid additive.[53] By probing phosphetane oxides with similar ring strain, we find increasing methyl substitution decreases the reduction barrier. This is suggested to be due to an increased negative charge on the oxygen of phosphine oxides making it more nucleophilic.

Table 5. Effect of substitution on phosphine oxide reduction barrier. Ordering based on magnitude of activation barrier for reduction. (energies in kcal/mol, θ: C-P-C is the internal angle of the cyclic structure in degrees, natural charges are given in units of electrons)

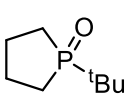
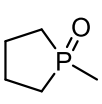
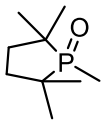
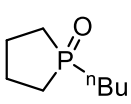
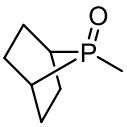
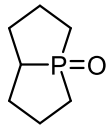
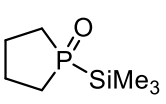
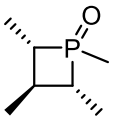
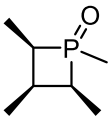
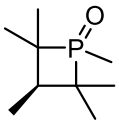
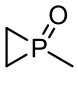
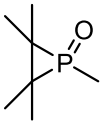
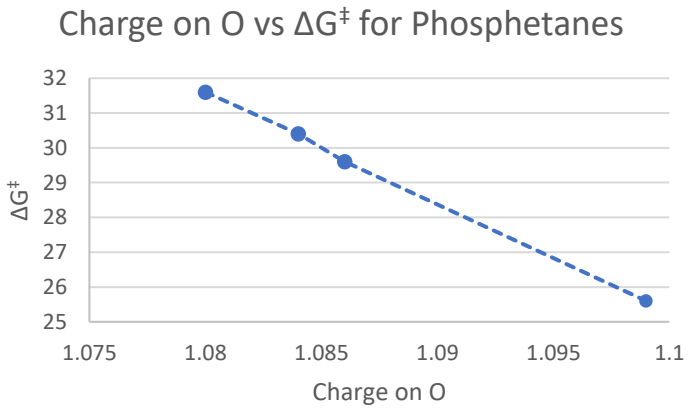
Phosphol-ane Oxide	 **(28)**	 **(25)**	 **(29)**	 **(18)**	 **(30)**	 **(31)**	 **(32)**
$\Delta G^{\ddagger}$	32.7	31.9	30.2	29.2	29.4	27.9	26.5
θ	95.1	95.2	97.0	95.1	83.1	95.5	94.1
Charge on P	2.013	1.961	2.036	1.982	1.987	1.982	1.501
Charge on O	-1.109	-1.099	-1.108	-1.102	-1.099	-1.091	-1.111

Table 6. Effect of substitution of phosphetane and phosphirane oxides on reduction barrier (energies in kcal/mol, θ: C-P-C is the internal angle of the cyclic structure in degrees, natural charges are given in units of electrons)

Phosphine Oxide	 **(26)**	 **(33)**	 **(34)**	 **(35)**	 **(27)**	 **(36)**
$\Delta G^{\ddagger}$	31.1	30.4	29.6	25.6	30.5	28.1
θ	79.3	79.1	80.6	81.2	52.0	52.4
Charge on P	1.949	1.985	1.982	2.026	1.893	1.941
Charge on O	-1.080	-1.084	-1.086	-1.099	-1.064	-1.077



At this point a discernible trend to predict novel more effective phosphine oxide catalysts could not be made. As Krenske notes the energies of the P-C σ* orbital and the lone pair on oxygen are also key in explaining the reduction of phosphine oxides. Attempts were made to correlate these orbital energies, however as the computational software (Spartan '20) used in this study does not contain natural bond order (NBO) methods, the analysis of the correct orbitals was nontrivial.

We therefore believe that the most easily reduced phosphine oxides for use in catalytic Wittig reactions should build off the structure of phosphetane (x), and further exploration of the effect of the exocyclic substituent on the reduction barrier should be conducted. We have already found longer alkyl substituents do lower the reduction barrier.

3. Conclusions and Future work

To conclude, despite its promise, catalytic Wittig reactions remain an underutilised method to prepare olefins. In this work we demonstrated a more practical route for the synthesis of phospholane oxides. While we only achieved modest yields, due to the difficulty in purification, it is nevertheless a step forward in preparing phospholane oxides from easily accesable phosphonate esters. From our initial results from the kinetic studies, it is suggested that phosphine oxide reduction is the rate limiting step. Furthermore, we probe the rate enhancing effect benzoic acid additives have in room temperature catalytic Wittig reactions. We suggest the benzoic acid additive forms silyl esters *in-situ* which have been demonstrated computationally to be significantly better reductants. Finally computational screenings of the rate limiting hydride transfer in phosphine oxide reduction demonstrates phosphetane (**35**) to have the lowest barrier to reduction. We suggest this to be a result of both the strain of the phosphetane ring as well as the inductive donation by methyl substituents increasing the charge on the oxygen of the phosphine oxide.

Future improvements on catalytic Wittig reactions can therefore begin from exploring more diverse catalyst structures based on phosphetane (**35**). Furthermore, the concept of silane activation may be used to perform catalytic Wittig reactions with more cost-effective silanes such as PMHS. While Brønsted

acid activation has been shown not be as effective with PMHS[81], other methods of activation such as carbonate bases and fluoride sources have been reported.[82,83] Using these strategies in tandem with a catalytic Wittig sequence could produce a more sustainable and practical olefination sequence.

4. Supporting Information

4.1 General Procedures

All reactions were performed in conventional glassware. Unless otherwise indicated all reagents and solvents were purchased from commercial suppliers and used without further purification. When required dry solvents were obtained from solvent towers or by drying over 3 Å molecular sieves. Degassing of solvents was achieved by sparging solvents with argon or nitrogen for 15 minutes. Moisture and air sensitive reactions were performed with standard Schlenk conditions. All water was deionised before use. DIPEA was distilled over KOH before use. Aldehydes were distilled or used fresh from chemical suppliers. Room temperature varied between 18 °C and 30 °C. Column chromatography was carried out using Fluorochem silica gel 60A (40-63 mesh). Analytical TLC was performed on Merck aluminium-backed silica gel 60 F^{254} plates. Methods used to visualise compounds are specified in the experimental details below. NMR spectra were recorded at 298 K on Bruker AV 400 and AV 500 spectrometers, and internally referenced to residual solvent signals ($CDCl_3$ δ 7.26 (1H) and 77.16 (13C); DMSO-d_6 δ 2.50 (1H) and 39.52 (13C); THF-d_8 δ 1.72, 3.58 (1H) and 25.31, 67.21 (13C); benzene-d_6 δ 7.16 (1H) and 128.84 (13H); MeCN-d_3 1.94 (1H) and 1.32, 118.26 (13C). Chemical shifts (δ) are reported in ppm, coupling constants (*J*) are reported in Hz, where relevant heteronuclear coupling is indicated. Assignments were only made where possible and for unambiguous peaks. IR spectra were obtained neat on a Bruker ALPHA FTIR spectrometer. HRMS spectra were acquired on a Bruker MicrOTOF II ESI-TOF instrument.

4.2 General Procedures for Kinetic Studies

Ex-situ reaction monitoring

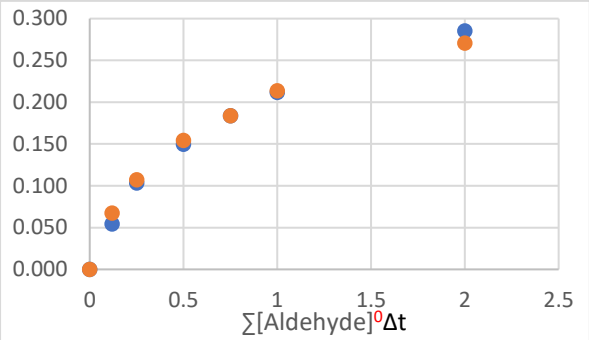
In a 20 mL microwave vial was added 1-butyl phospholane 1-oxide (64.1 mg, 0.40 mmol), 3-fluoro 4-nitrobenzoic acid (74.0 mg, 0.40 mmol), 1-(4-fluorophenyl)ethyl 2-bromoacetate (679 mg, 2.60 mmol) finally 4,4'-bis(trifluoromethyl)-1,1'-biphenyl (28.0 mg, 0.10 mmol) as an internal standard. A magnetic stirrer bar was added and the vial was then sealed. The vial was evacuated and backfilled three times with nitrogen then place under a balloon of argon. THF (4.0 mL) was introduced, then 4-flurobenzaldehyde (215 µL, 2.00 mmol) was added and the mixture was stirred until homogeneous. At this point a t0 measurement was taken by taking 0.1 mL aliquot was taken and diluted with 0.5 mL of MeCN-d_3. DIPEA (490 µL, 2.81 mmol) was then added, the mixture was stirred and warmed to 30 °C. Once the mixture reached the correct temperature phenylsilane (345 µL, 2.80 mmol) was added initiating the reaction. Aliquots were taken at 7, 15, 30, 45, and 60 minutes, after which an aliquot was taken every hour for 8 hours. Each aliquot after the t0 were prepared in the following way: 0.1 mL of the reaction mixture was removed with an inert needle, this was added to an NMR tube where MeOH (0.1 mL) was added to quench the silane, then diluted with MeCN-d_3 (0.4 mL). The NMR sample was sonicated until all bubbling subsided and a proton decoupled ^{19}F spectrum was taken. ^{19}F spectra were recorded with 8 scans and 30 second relaxation delays.

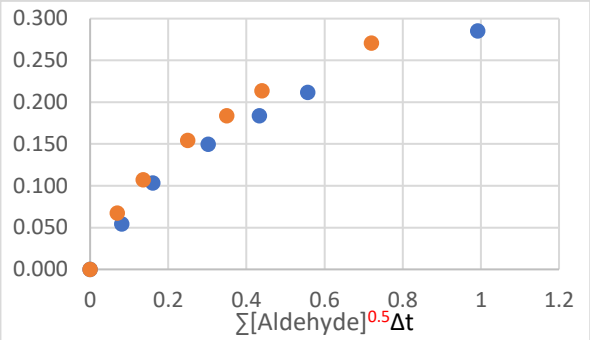
In-situ reaction monitoring

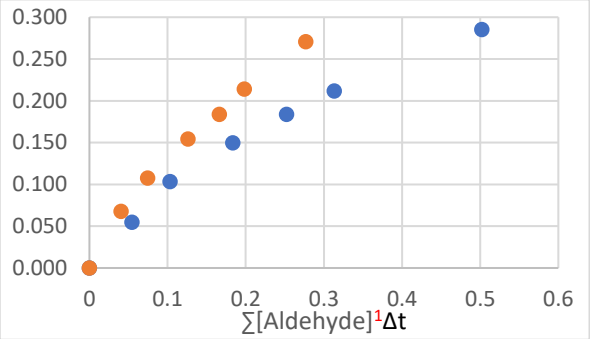
In an oven dried NMR tube were added 3-Fluoro 4-nitrobenzoic acid (5.5 mg, 0.03 mmol), 1-butyl phospholane 1-oxide (5.0 mg, 0.03 mmol), 1-(4-fluorophenyl)ethyl 2-bromoacetate (51.0 mg, 0.19 mmol) finally 4,4'-bis(trifluoromethyl)-1,1'-biphenyl (3.0 mg, 0.010 mmol). Benzene-d6 (0.6 mL) was added followed by 4-fluorobenzaldehyde (16 µL, 0.15 mmol) and DIPEA (35 µL, 0.20 mmol). The headspace in the NMR tube was flushed with a stream of nitrogen, then the sample was inserted into the NMR spectrometer and a t0 ^{19}F spectra was taken. Then the NMR tube was removed from the spectrometer and phenylsilane (25 µL, 0.20 mmol) was added and the NMR tube was sealed and sonicated. Due to potential build-up of gas pressure during the course of the reaction, the NMR tube reaction was conducted outside of the NMR spectrometer, inserting it periodically to take ^{19}F NMR spectra.

VTNA different excess full plots

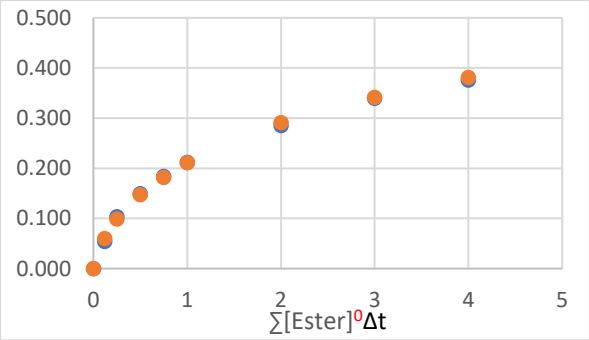
Different Excess in Aldehyde

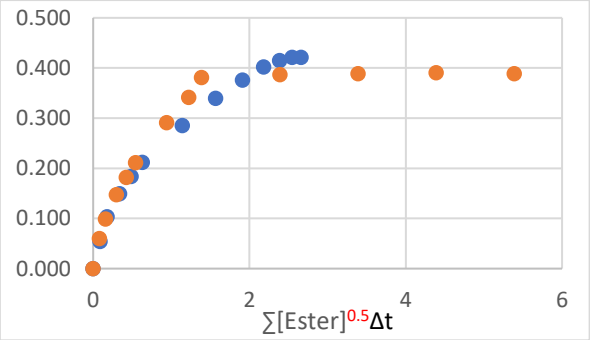


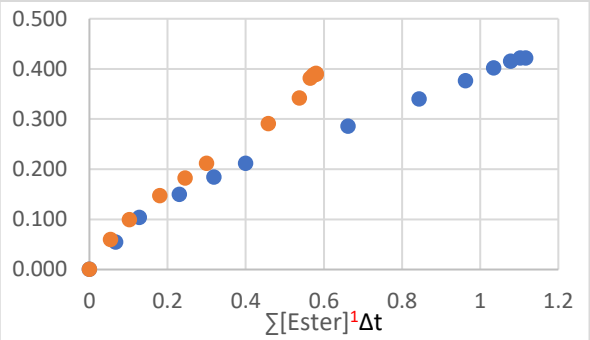




Different Excess in α-Bromo Ester

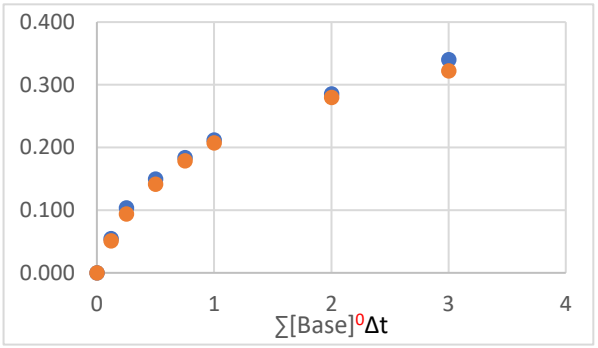




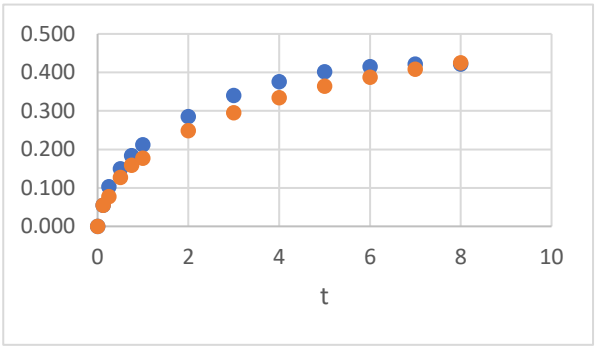


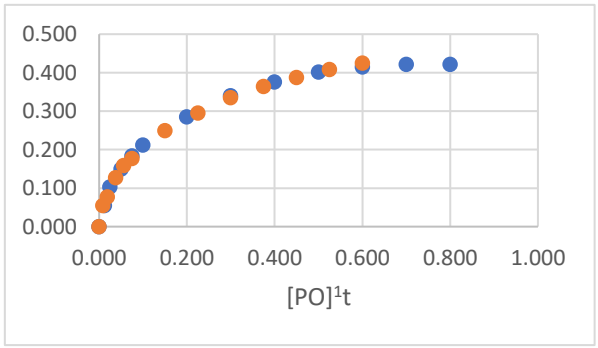
Different Excess Base

Note: As the change in concentration of DIPEA could not be monitored by our sampling method full visual analysis could not be performed, however overlap of the two plots without normalization implies zero order in DIPEA



Different Excess Phosphine Oxide pre-catalyst



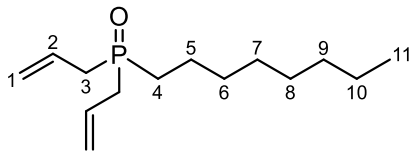


4.3 Computational Methods

DFT calculations were performed using Spartan'20 software. Geometry optimisations, frequency calculations and single point energy calculations were conducted using ωB97X-D/6-31+G* level of theory in the gas phase. Optimized structures were confirmed to be at a minimum by vibrational mode analysis. Which showed no imaginary frequencies. All transition states had a single imaginary frequency corresponding to movement along the hydride transfer reaction coordinate.

4.4 Experimental procedures

Diallyl(n-octyl)phosphine oxide (3)



To a solution of 1-octylphosphonic dichloride (5.00 g, 21.6 mmol) in Et_2O (30 mL) was added allyl magnesium bromide solution (100 mL, 100 mmol of a 1.0 M solution in Et_2O) dropwise at 0° C over a period of 30 minutes. After complete addition the reaction was stirred at 0° C for 6 hours. The reaction was quenched with saturated NH_4Cl solution (30 mL), extracted with Et_2O (5 x 30 mL) and the combined organic extracts were then dried over Na_2SO_4 and concentrated. The crude residue was purified by flash column chromatography (SiO_2, 0-5% MeOH in EtOAc) to afford the title compound as a yellow oil (3.26 g, 62%).

TLC: R*f* = 0.19 (1% MeOH in EtOAc, visualisation by $KMnO_4$ stain).

^{1}H NMR (400 MHz, DMSO-*d*$_6$): δ 5.78 (m, 2H, H^2), δ 5.18 (m, 4H, H1), 2.57 (m, 4H, H3), 1.62 (m, 2H, C*H*$_2$), 1.49 (m, 2H, C*H*$_2$), 1.26 (m, 10H, C*H*$_2$), 0.87 (t, *J* = 6.9 Hz, 3H, H11).

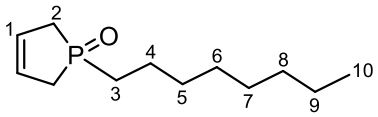
^{13}C{^{1}H} NMR (101 MHz, DMSO): δ 129.7 (d, *J* = 8.4 Hz, C1), 119.9 (d, *J* = 11.0 Hz, C2), 34.0 (d, *J* = 61.4 Hz, C3), 31.7 (s, *C*H_2), 30.9 (d, *J* = 13.2 Hz, *C*H_2), 29.0 (s, *C*H_2), 28.9 (s, *C*H_2), 27.1 (d, *J* = 65.9 Hz, C^4), 22.6 (s, *C*H_2), 21.3 (d, *J* = 4.1 Hz, *C*H_2), 14.4 (s, C^{11}).

^{31}P{^{1}H} NMR (162 MHz, DMSO-*d*$_6$): δ 42.1 (s).

HRMS(TOF-ESI$^+$): calcd. for $C_{14}H_{28}OP^+$ $[M+H]^+$ = 243.1872, found 243.1872.

FTIR: (neat) ν_{max}/cm^{-1} 3418, 3080, 2924, 2854, 1636, 1420, 1226, 1158 (P=O), 910.

1-(n-Octyl)phospholane-1-oxide (6)



To a solution of the diallyl(n-octyl) phosphine oxide (969 mg, 4 mmol) in anhydrous CH_2Cl_2 (80 mL), was added a prepared solution of Grubbs catalyst 2nd generation (170 mg, 0.2 mmol, 5 mol%) in CH_2Cl_2 (20 mL). The mixture was heated to 40 °C for 24 h. The mixture was allowed to cool then it was filtered through a plug of activated charcoal and Celite® rinsing with CH_2Cl_2. The volatiles were removed, the resultant viscous brown oil was shown to consist of 1-octyl-2,5-dihydrophosphole 1-oxide (x) which was used without purification in the next step.

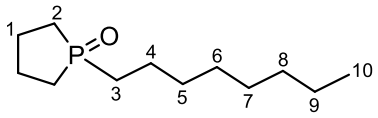
^{1}H NMR (400 MHz, $CDCl_3$) δ 5.90 (d, *J* = 27.2 Hz, 2H, H1), 2.65 - 2.43 (m, 4H, H2), 1.91-1.84 (m, 2H) 1.69- 1.62 (m, 2H) , 1.46-1.42 (m, 2H), 1.32-1.27(m, 8H), 0.90 (t*, J* =7.0 Hz, 3H)

^{13}C NMR {^{1}H} (101 MHz, $CDCl_3$) δ 127.4 (d, $^2J_{CP}$ = 11.0 Hz, C^1), 31.8 (s, *C*H_2), 31.55 (s, *C*H_2), 31.07 (s, *C*H_2), 30.90, 30.14, 29.13, 29.05, 22.62, 21.92, 14.09.

^{31}P NMR{^{1}H} (162 MHz, $CDCl_3$): δ 68.4 (s).

HRMS(TOF-ESI$^+$): calcd. for $C_{12}H_{23}OP^+$ $[M+H]^+$ = 215.1559, found 215.1558.

1-(n-Octyl)phospholane-1-oxide (7)



Crude 1-(n-octyl)phospholane-1-oxide (**6**) (913 mg, 4.26 mmol) was dissolved in 10% solution of CH_2Cl_2 in MeOH (107 mL) and transferred to a sealed Schlenk

flask charged with Pd/C (10% wt., 50% wet) (907 mg, 10 mol%) and a magnetic stirrer bar. The vessel was evacuated and backfilled twice with hydrogen, then placed under a balloon of hydrogen. The suspension was stirred at room temperature for 48 h, after which the flask was evacuated and backfilled once with nitrogen. The crude mixture was filtered over a plug of celite rinsing with MeOH. The volatiles were removed, and the product was purified by Kugelrohr distillation to give the *title compound* as a colourless oil (407 mg, 47% over two steps)

^{1}H NMR (400 MHz, $CDCl_3$): δ 2.03-1.99 (m, 2H, C*H*$_2$), 1.81-1.62 (m, 10H, C*H*$_2$), 1.43-1.40 (m, 2H, C*H*$_2$), 1.28-1.27 (m, 8H) 0.87 (t, *J* = 7.1 Hz, 3H, H10).

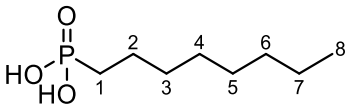
^{13}C NMR: (101 MHz, $CDCl_3$) δ 31.8 (s, *C*H$_2$), 30.9 (d, $^{1}J_{CP}$ = 61.9 Hz, C^{3}), 31.0 (d, $^{3}J_{CP}$ = 13.6 Hz, C^{5}), 29.1 (s, *C*H$_2$), 29.0 (s, *C*H$_2$), 26.9 (d, $^{1}J_{CP}$ = 64.7 Hz, C^{2}), 24.6 (d, $^{2}J_{CP}$ = 7.7 Hz, C^{1}), 22.59 (s, *C*H$_2$), 22.2 (d, $^{2}J_{CP}$ = 4.2 Hz, C^{4}), 14.0 (s, C^{10}).

^{31}P{^{1}H} NMR (162 MHz, $CDCl_3$): δ 71.0 (s).

HRMS(TOF-ESI^{+}): calcd. for $C_{12}H_{26}OP^{+}$ $[M+H]^{+}$ = 217.1716, found 217.1714.

FTIR: (neat) ν_{max}/cm^{-1} 3424, 2922, 2853, 1464, 1266, 1163 (P=O), 1109, 861, 721

n-Octylphosphonic Acid (14)



Procedure adapted from literature.[84]

A 250 mL Schlenk flask was charged with anhydrous $ZnCl_2$ (750 mg, 5.50 mmol), the flask was evacuated and backfilled with Nitrogen (3 times) then

flame dried. The flask was let cool then anhydrous Et_2O (20 mL) was added. The solution was cooled using a bath of ice then freshly prepared n-octyl magnesium bromide* (16.8 mL of a 1.0 M solution) was then added dropwise over a period of 15 minutes. The flask was then let warm to room temperature and stirred for 16 h. The reaction mixture was cooled once more using a bath of ice and $POCl_3$ (1.57 mL, 16.8 mmol) was added dropwise over a period of 15 minutes. The reaction mixture was let warm to room temperature and stirred for 24 h, after which the reaction mixture was cooled using a bath of ice and quenched with deionized water (10 mL), then let stir again for 24 h. The crude mixture was diluted with CH2Cl2 (100 mL), the organic layer was separated and washed with HCl (3 x 33 mL of a 1% aqueous solution). The organic layer was then dried over $MgSO_4$ and the volatiles were removed *in vacuo*. The crude product was purified by recrystallization in hot heptane giving the title compound as a colourless solid (251 mg, 8%)

Melting point: 83-85 °C

^{1}H NMR (400 MHz, $CDCl_3$): δ 10.27 (s, 2H, O*H*), 1.81-1.73 (m, 2H, CH_2), 1.68-1.58 (m, 2H, CH_2), 1.40-1.29 (m, 10H, CH_2), 0.90 (t, J = 6.7 Hz, 3H, H8).

^{13}C NMR{ 1H} (101 MHz, $CDCl_3$): δ 31.8 (s, *C*H_2), 30.4 (d, 2 JCP = 17.5 Hz, C2), 29.03 (s, *C*H_2), 29.00 (s, *C*H_2), 25.2 (d, 1 JCP = 144.7 Hz, C1), 22.6 (s, *C*H_2), 22.0 (d, 1 JCP = 5.1 Hz, C3), 14.1 (s, C8).

^{31}P NMR{1H} (162 MHz, $CDCl_3$): δ 37.6 (s).

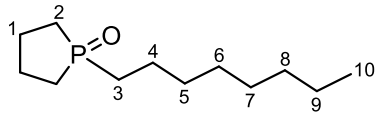
HRMS(TOF-ESI+): calcd. for $C_8H_{20}O_3P^+$ $[M+H]^+$ = 195.1145, found 195.1138

*Preparation of n-octyl magnesium bromide

A 100 mL Schlenk flask was charged with magnesium turnings (514 mg, 20.2 mmol) and a magnetic stirrer bar. The flask was flame dried in vacuo, then let cool and iodine (one crystal) was added against a current of nitrogen). The iodine was sublimed while stirring the turnings neat. Anhydrous Et_2O (16.8 mL) was then added. The suspension was cooled using a bath of ice and 1-

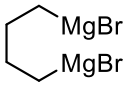
bromooctane was added dropwise over a period of 20 minutes. Once the addition was complete the reaction mixture was let warm to room temperature and stirred for 2 h.

1-(n-octyl)phospholane-1-oxide (7) (preparation via di-Grignard addition)



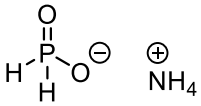
A Schlenk flask was charged with n-octylphosphonic acid (194 mg, 1.00 mmol) and sealed, then evacuated and backfilled with nitrogen three times. Anhydrous CH_2Cl_2 (2 mL) followed by oxalyl chloride (190 µL, 2.22 mmol) and finally DMF (1 drop). Once the effervesence subsided the reaciton mixture was se to heat at 40 °C for 1.5 h. The mixture was allowed to cool to room temperature, then conected to a Schlenk line and the volatiles were removed in vacuo. The crude product was then diluted with anhydrous THF (5 mL). The solution was cooled using a liquid N_2/ Acetone bath, then freshly prepared *di-Grignard reagent (4.4 mL of a 0.22 M solution) was then added dropwise over a period of 5 minutes. The mixture was then let warm to room temperature and stirred for 20 h. The reaction was then quenched with deionized water (8 mL). The aqeuous layer was extracted with EtOAc (3 x 30 mL), then the combined organic layers were dried over $MgSO_4$. The crude product was purified by flash column chromatography (SiO_2, 0%-10% 7 N NH3 (in MeOH) in EtOAc in Pentane) to give the title compound as an orange oil (194 mg, 81%) with identical characterisation data as above.

***Preparation of di-Grignard reagent**



A 500 mL Schlenk flask was charged with magnesium turnings (292 mg, 12.2 mmol) and a magnetic stirrer bar, then flame dried in vacuo. Iodine was added against a current of nitrogen then sublimed while stirring neat. Anhydrous THF was added (5 mL), then the suspension was cooled using a bath of ice, and 1,4 dibromobutane (0.60 mL, 5.02 mmol) was added dropwise over 10 minutes. The mixture was the let warm to room temperature and stirred for 2.5 h, then diluted with anhydrous THF (5 mL). The di-Grignard reagent was then titrated against I_2 in a 1.0 M solution of LiCl in THF. The concentration of the di-Grignard reagent was found to be 0.22 M after three successive titrations.

Ammonium Hypophosphite (12)

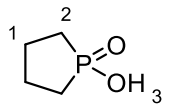


To a stirred solution of hypophosphorus acid (4.40 mL mL of a 50% wt. H_2O solution, 40 mmol) at 0 °C was added ammonium carbonate (1.92g, 20 mmol) portion wise. After complete addition the reaction was stirred for 6 hours at room temperature. The reaction mixture was concentrated *in vacuo* and the resultant white precipitate was collected by filtration washing with cold acetone. The solid was dried in a vacuum desiccator over P_2O_5 at room temperature for 24 h and the *title compound* was isolated as a colourless solid (2.69 g, 81%).

^{1}H NMR (400 MHz, D_2O): δ 6.95 (d, $^1J_{HP}$ = 518.2 Hz, 2H)

^{31}P NMR (162 MHz, D_2O): δ 7.0 (t, $^1J_{HP}$ = 518.2 Hz)

1-hydroxyphospholane 1-oxide (13)



A two neck round bottom flask fitted with a condenser was charged with ammonium hypophosphite (1.66 mg, 20.0 mmol). The flask was sealed and the atmosphere was purged with a stream of argon. HMDS (8.38 mL, 40.4 mmol) was added and the suspension was heated at 110 °C for 2 hours. The resulting solution was diluted with toluene (4 mL) and then 1,4-dibromobutane (2.39 mL, 20.0 mmol) was added. The mixture was then refluxed for 64 hours. The reaction was then quenched with MeOH (10 mL), the yellow precipitate was filtered off, the filtrate was collected and concentrated. The filtrate was then taken up in EtOAc (15 mL) and washed with (20 mL of a 1.0 M aqueous solution). The organic layer was separated, and the aqueous layer was washed with EtOAc (3 x 15 mL). The aqueous layer was then acidified to a pH of 1 with 6 M HCL, then saturated with NaCl. The aqueous layer was then extracted with EtOAc (5 x 20 mL). The combined organic layers were dried over Na_2SO_4 and concentrated in vacuo. The crude was then purified by reverse phase flash chromatography (10-30% MeCN in H_2O) to give the *title compound* as a colourless solid (149 mg, 6%).

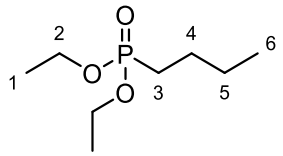
^{1}H NMR (400 MHz, $CDCl_3$): δ 9.31 (bs, 1H, H^3) 1.90-1.85 (m, 4H, C*H*$_2$), 1.77-1.74 (m, 4H, C*H*$_2$).

^{13}C{^{1}H} NMR (101 MHz, $CDCl_3$): δ 25.7 (d, $^1J_{CP}$ = 92.2 Hz, C^2), 23.3 (d, $^2J_{CP}$ =12.5 Hz, C^1).

^{31}P{^{1}H} NMR (162 MHz, $CDCl_3$): δ 82.2.

HRMS(TOF-ESI$^+$): calcd. for $C_4H_9O_2P^+$ $[M+H]^+$= 121.0413, found 121.0421

Diethyl butylphosphonate (16)



A two neck round bottom flask was charged with NaH (2.00 g, 50.0 mmol of a 60% w/w dispersion in oil). The flask was fitted with a condenser, sealed and the atmosphere was purged with a stream of argon. Anhydrous THF (80 mL) was added, and the suspension was cooled using an ice bath, diethyl phosphite (5.15 mL, 40.0 mmol) was then added dropwise. The mixture was refluxed for 2 hours, then cooled once more on an ice bath and 1-bromobutane (4.72 mL, 43.9 mmol) was added dropwise. The mixture was stirred at room temperature for 20 hours, after which the reaction was quenched with deionized water (40 mL) extracted with CH_2Cl_2 (3 x 80 mL). The combined organic extracts were dried over Na_2SO_4 and concentrated *in vacuo*. The residual mineral oil was removed by loading the crude product onto a plug of silica, rinsing with pentane, then finally eluting the compound with 10% MeOH in CH_2Cl_2. Giving the *title compound* as a yellow oil (5.95g, 77%)

^{1}H NMR (400 MHz, $CDCl_3$): δ 4.11 (q, *J* = 7.0 Hz, 4H, H2), 1.78-1.70 (m, 2H, H3), 1.65- 1.55 (m, 2H, H5), 1.42 (m, 2H, H4), 1.34 (t, *J* = 7.0 Hz , 6H, H1), 0.93 (t, *J* = 7.2 Hz , 3H, H6).

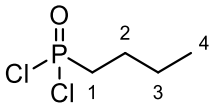
^{13}C{^{1}H} NMR (101 MHz, $CDCl_3$): δ 61.4 (d, $^2J_{CP}$ = 6.6 Hz, C2), 25.4 (d, $^1J_{CP}$ = 140.6 Hz, C3), 24.5 (d, $^2J_{CP}$ = 5.5 Hz, C4), 23.7 (d, $^3J_{CP}$ = 17.3 Hz, C5), 16.5 (d, $^3J_{CP}$ = 5.9 Hz, C1), 13.5 (s, C6).

^{31}P{^{1}H} NMR (162 MHz, $CDCl_3$): δ 32.7 (s).

HRMS(TOF-ESI$^+$): calcd. for $C_8H_{20}O_3P^+$ $[M+H]^+$= 195.1145, found 195.1146.

FTIR: (neat) ν_{max}/cm^{-1} 2933, 1467, 1279 (P=O), 1022 (P-OR), 953, 790, 731, 534.

butylphosphonic dichloride (17)



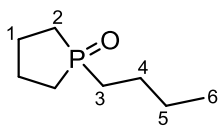
A 250 ml Schlenk flask was charged with diethyl butylphosphonate (3.88 g, 20.0 mmol, 1 equiv.) and a magnetic stirrer bar. The flask was then sealed and evacuated and backfilled three times with nitrogen, then placed under a balloon of nitrogen. Anhydrous CH_2Cl_2 (5 mL) was added, then bromotrimethylsilane (7.92 mL, 60.0 mmol, 3 equiv.) was added dropwise at room temperature. The reaction mixture was stirred at room temperature for 22 hours, after which the flask was connected to a Schlenk line and the volatiles were removed under vacuum. The crude mixture was then dissolved in anhydrous CH_2Cl_2 (20 mL) and oxalyl chloride (3.72 mL, 44.0 mmol) and DMF (15 µL, 0.2 mmol) were then added. The reaction mixture was set to reflux for 22 hours, after which the flask was let cool, and the reaction mixture was concentrated on a Schlenk line, to give crude phosphonyl dichloride as an orange oil.

^{1}H NMR (400 MHz, $CDCl_3$): δ 2.64-2.56 (m, 2H), 1.91-1.79 (m, 2H), 1.59, 1.49 (m, 2H), 1.00 (t, *J* = 7.2 Hz, 3H, H4).

^{13}C NMR{^{1}H} (101 MHz, $CDCl_3$): δ 42.8 (d, $^1J_{CP}$ = 96.4 Hz, C1), 22.9 (d, $^2J_{CP}$ = 6.6 Hz, C2), 22.9 (d, $^3J_{CP}$ = 22.4 Hz, C3), 13.4 (s, C4).

^{31}P NMR{^{1}H} (162 MHz, $CDCl_3$): δ 51.3 (s).

1-butyl phospholane 1-oxide (18)



Previously prepared butylphosphonic dichloride (**17**) was diluted in THF (40 mL), the solution was cooled on an EtOAc/liquid nitrogen bath. Freshly prepared di-

Grignard reagent* (100 mL of 0.2 M solution, 20.0 mmol) was added to the flask over a period of 10 minutes. The EtOAc/liquid N_2 was then removed, and the solution was stirred at room temperature for 20 hours. The reaction mixture was then quenched with NH_4Cl (50 mL of a saturated aqueous solution). The mixture was transferred to a separatory funnel where the organic layer was collected. The aqueous layer was extracted further with EtOAc (3 x 50 mL). The combined organic layers were dried over Na_2SO_4 and then concentrated *in vacuo*. The product was then purified by Kugelrohr distillation (0.30-0.33 mbar at 130-135 °C) to give a colourless oil. The product was found to have small amount of impurities remaining it was distilled a second time using a Hickmann still (2.0-2.1 mbar at 180-185 °C), to give the *title compound* as a colourless oil (779 mg, 24%).

^{1}H NMR (400 MHz, $CDCl_3$): δ 2.06-1.98 (m, 2H) , 1.86-1.60 (m, 10H) 1.50-1.40 (m, 2H), 0.94 (t, J = 7.3 Hz, 3H, H^6).

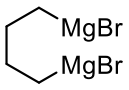
^{13}C{^{1}H} NMR (101 MHz, $CDCl_3$): δ 30.6 (d, $^1J_{CP}$ = 62.1 Hz, C^3) , 26.5 (d, $^1J_{CP}$ = 65.1 Hz, C^2) , 24.6 (d, $^2J_{CP}$ = 8.1 Hz, C^1) , 24.2 (d, $^2J_{CP}$ = 5.1 Hz, C^4), 24.2 (d, $^3J_{CP}$ = 23.4 Hz, C^5), 13.6 (s, C^6).

^{31}P{^{1}H} NMR (162 MHz, $CDCl_3$): δ 71.0 (s).

HRMS(TOF-ESI$^+$): calcd. For $C_8H_{18}OP^+$ $[M+H]^+$= 161.1090, found 161.1087.

FTIR: (neat) ν_{max}/cm^{-1} 2955, 1643, 1265, 1146 (P=O), 901, 726, 513.

***Preparation of di-Grignard reagent**

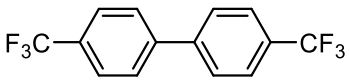


A 500 mL Schlenk flask was charged with magnesium turnings (3.06 g, 126 mmol) and a magnetic stirrer bar, then flame dried *in vacuo*. Anhydrous THF (20 mL) was added followed by 1,2-dibromoethane (0.2 mL, 2.3 mmol) and the

mixture was heated until bubbling was observed. More anhydrous THF (100 mL) was added, the suspension was cooled to 0 °C, and 1,4-dibromobutane (7.16 mL, 60.0 mmol) was added dropwise. The mixture was then stirred at 0 °C for 1.5 h, then let warm to room temperature and stirred overnight. The di-Grignard reagent was then titrated with a 1.0 M solution of anhydrous sec-butanol in toluene, using 1,10-phenanthroline as an indicator.[66] The concentration of the di-Grignard reagent was found to be 0.2 M after three successive titrations.

Note: the low concentration of prepared Grignard reagent was due to decomposition and precipitation of magnesium bromide. Better conditions to prepare the di-Grignard reagent were found later on during this study, using a 3 equivalent excess of magnesium turnings to 1,4-dibromobutane.

4,4'-bis(trifluoromethyl)-1,1'-biphenyl



A 100 mL round-bottom flask equipped with a stir-bar was charged with magnesium turnings (292 mg, 12 mmol), then flame-dried in vacuo. Iodine (one crystal) was added against a current of nitrogen, then sublimed. Anhydrous THF (10 mL) was introduced, then 4-bromobenzotrifluoride (1.40 mL, 10 mmol) was added dropwise to the suspension, upon complete addition the reaction mixture was refluxed for 2 hours. In a separate flask a suspension of $FeCl_3$ was (80 mg, 0.5 mmol) prepared in anhydrous THF (10 mL), to which dibromoethane (1.10 mL, 13 mmol) was added dropwise. The Grignard reagent was then added to the flask and the mixture was refluxed for 40 minutes. The reaction was then quenched with a saturated solution of NH_4Cl (10 mL). The aqueous layer was

extracted with Et_2O (3 x 15 mL). The combined organic extracts were dried over $MgSO_4$, filtered, concentrated *in vacuo*. The crude product was then purified by Kugelrohr distillation (1.0-0.9 mbar at 130-133 °C) to give the *title compound* as a colourless solid (924 mg, 64%).

Melting point: 82-84 °C

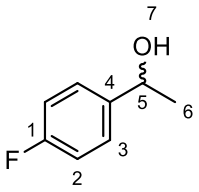
^{1}H NMR (400 MHz, $CDCl_3$): δ 7.77-7.72 (m, 8H, Ar*H*).

^{19}F{^{1}H} NMR (376 MHz, $CDCl_3$): δ -62.6 (s).

HRMS(TOF): *Not found by HRMS*

FTIR: 1667, 1315, 1160, 1126, 1066, 1018, 825.

1-(4-fluorophenyl)ethan-1-ol



A solution of 4-fluoroacetophenone (13.8 g, 100 mmol) in MeOH (100 mL) was cooled to 0 °C using an ice bath. Sodium borohydride (4.16 g, 110 mmol) was added portion-wise to the stirred solution over a period of 30 minutes. After complete addition the reaction mixture was let warm to room temperature and stirred for 1.5 h. The reaction was then quenched with HCl (100 mL of a 1.00 M aqueous solution). EtOAc (200 mL) was added, and the organic layer was separated and collected. The remaining aqueous layer was extracted with EtOAc (100 mL x 2). The combined organic layers were then washed with a $NaHCO_3$ (100 mL x 2 of a saturated aqueous solution), then dried over $MgSO_4$, filtered, and concentrated *in vacuo* to afford the racemic alcohol as a yellow oil (12.0 g, 86%).

^{1}H NMR (400 MHz, $CDCl_3$): δ 7.38-7.35 (m, 2H, H3), 7.07-7.03 (m, 2H, H2), 4.91 (q, *J* = 6.5 Hz, 1H, H5), 1.87 (bs, 1H, H7), 1.50 (d, *J* = 6.5 Hz, 3H, H6).

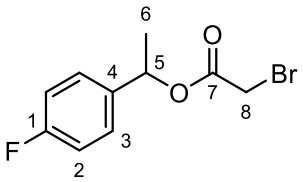
^{13}C{^{1}H} NMR (101 MHz, $CDCl_3$): δ 162.1 (d, $^{1}J_{CF}$ = 245.1 Hz, C1) 141.5 (d, $^{4}J_{CF}$ = 3.3 Hz, C4), 127.0 (d, $^{3}J_{CF}$ = 7.8 Hz, C3), 115.3 (d, $^{2}J_{CF}$ = 21.6 Hz, C2) 69.8 (s, C5), 25.3 (s, C6).

^{19}F{^{1}H} NMR (376 MHz, $CDCl_3$): δ -115.3 (s).

HRMS(TOF): *Not found by HRMS*

FTIR: (neat) ν_{max}/cm^{-1} 3340, 2974, 1603, 1508, 1219 (C-OH), 832, 540.

1-(4-fluorophenyl)ethyl 2-bromoacetate (19)



To a solution of 1-(4-fluorophenyl) ethanol (2.80 g, 20.0 mmol) in CH_2Cl_2 (100 mL) was added pyridine (3.24 mL, 40.0 mmol). The solution was cooled to 0 °C, and 2-bromo acetyl bromide (3.5 mL, 40 mmol) was added dropwise over a period of 20 minutes. The reaction was let warm to room temperature and stirred for 2 hours, after which the reaction was quenched with NH_4Cl (50 mL of a saturated aqueous solution) at 0 °C. The organic layer was collected, and the remaining aqueous layer was extracted with CH_2Cl_2 (3 x 50 mL). The combined organic fractions were washed once with $CuSO_4$ (100 mL of a saturated aqueous solution) then dried over $MgSO_4$, and concentrated. The crude product was purified by flash chromatography (SiO_2, 0-5% EtOAc in Pentane) to afford the *title compound* as a colourless oil (4.73 g, 91%).

TLC: R*f* = 0.31 (5% EtOAc in pentane, visualisation by UV)

^{1}H NMR (400 MHz, $CDCl_3$): δ 7.39-7.36 (m, 2H, H3), 7.09-7.05 (m, 2H, H2), 5.93 (q, *J* = 6.6 Hz, 1H, H5), 3.85 (s, 2H, H8), 1.60 (d, *J* = 6.6 Hz, 3H, H6).

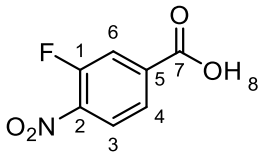
^{13}C{^{1}H} NMR (101 MHz, $CDCl_3$): δ 166.4 (s, C7), 162.5 (d, $^{1}J_{CF}$ = 246.0 Hz, C1), 136.4 (d, $^{4}J_{CF}$ = 3.4 Hz, C4), 128.0 (d, $^{3}J_{CF}$ = 8.1 Hz, C3), 115.5 (d, $^{2}J_{CF}$ = 21.2 Hz, C2), 73.8 (s, C5), 26.1 (s, C8), 21.9 (s, C6).

^{19}F{^{1}H} NMR (376 MHz, $CDCl_3$): δ -113.7 (s).

HRMS(TOF-ESI^{+}): calcd. For $C_{10}H_{10}O_2FBrNa$ $[M+Na]^+$= 282.9740, found 282.9733

FTIR: (neat) ν_{max}/cm^{-1} 2983, 1732 (C=O), 1606, 1511, 1453, 1422, 1378, 1272 (C-O), 1223 (C-F), 1157, 1106. 1056, 1001, 950, 833, 546 (C-Br).

3-fluoro 4-nitrobenzoic acid (20)



To a suspension of potassium dichromate (3.92 g, 13.3 mmol, 1.33 equiv.) in glacial acetic acid (12.0 mL), was added 2-Fluoro-4-methyl-1-nitrobenzene (1.55 g, 9.99 mmol, 1 equiv.) portion wise. The suspension was stirred for 15 min, then cooled on a bath of ice, concentrated sulfuric acid (18.0 mL) was added dropwise to the suspension. Once the addition was completed, the mixture was heated at 120 °C for 3 h. The mixture was let cool to room temperature and poured into cold deionized water (40 mL), while rinsing the reaction vessel with cold deionized water. The yellow precipitate was isolated by filtration to give 3-fluoro 4-nitrobenzoic acid as a pale-yellow solid (1.11 g, 60%).

Melting point: 164-170 °C

^{1}H NMR (400 MHz, DMSO): δ 13.90 (bs, 1H, H8), 8.26 (t, *J* = 8.1 Hz, 1H, Ar*H*), 8.00-7.93 (m, 2H, Ar*H*).

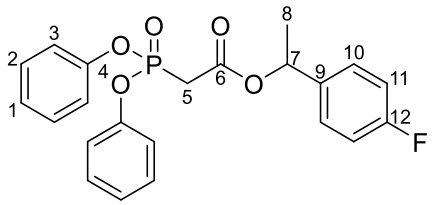
$^{13}C\{^1H\}$ NMR (101 MHz, DMSO): δ 165.3 (s, C7), 154.8 (d, $^1J_{CF}$ =263 Hz, C1), 139.9 (d, J_{CF} = 8.1 Hz, Ar*C*), 138.2, (d, J_{CF} = 7.7 Hz, Ar*C*), 127.2 (d, $^4J_{CF}$ = 2.9 Hz, C4), 126.3 (d, $^3J_{CF}$ = 4.0 Hz, C3), 119.4 (d, $^2J_{CF}$ = 21.7 Hz, C6)

$^{19}F\{^1H\}$ NMR (376 MHz, DMSO): δ -118.3 (s).

HRMS: calcd. for $C_7H_3NO_4F^-$: 184.0052 $[M]^-$, found 184.0054 (ESI^-).

FTIR: (neat) ν_{max}/cm^{-1} 2848 (broad), 1692 (C=O), 1599 (N-O), 1353, 1294, 740

1-(4-fluorophenyl)ethyl 2-(diphenoxyphosphoryl)acetate



To a suspension of NaH (60 mg, 1.5 mmol of a 60% w/w dispersion in oil) in dry THF (1.5 mL) was added diphenyl phosphite (285 µL, 1.5 mmol) dropwise at 0 °C. The mixture was then stirred at room temperature for 1.5 h. A 0.5 M solution of 1-(4-fluorophenyl)ethyl 2-bromoacetate in THF was prepared. 3 mL of this solution were added dropwise to the reaction mixture. The mixture was then stirred for 4 h at room temperature. The reaction was quenched NH_4Cl (4 mL of a saturated aqueous solution). The reaction mixture was then extracted with Et_2O (3 x 10 mL) dried over $MgSO_4$ and concentrated in vacuo. The crude product was purified by flash chromatography (SiO_2, 5-20% EtOAc in Pentane) to afford the *title product* as a colourless oil (243 mg, 39%)

TLC: R*f* = 0.17 (20% EtOAc in pentane, visualisation by UV)

^1H NMR (400 MHz, $CDCl_3$): δ 7.39-7.36 (m, 2H, H10), 7.36-7.30 (m, 4H, H3), 7.23-7.13 (m, 6H, H1 and H2), 7.03-6.99 (m, 2H, H11), 5.98 (q, *J* = 6.7 Hz, 1H, H^7) 3.30 (d, $^2J_{PH}$ = 21.8 Hz, 2H, H5), 1.58 (d, *J* = 6.7 Hz, 3H, H8).

$^{13}C\{^1H\}$ NMR (101 MHz, $CDCl_3$): δ 164.0 (d, $^2J_{CP}$ = 6.6 Hz, C6), 162.5 (d, $^1J_{CF}$ = 246.6 Hz, C^{12}), 149.9 (m, C4), 136.5 (d, $^4J_{CF}$ = 3.0 Hz, C9), 129.8 (d, $^4J_{CP}$ =

2.6 Hz, C2), 128.2 (d, $^{3}J_{CF}$ = 8.1 Hz, C10), 125.6 (s, C1), 120.6 (m, C3), 115.4 (d, $^{2}J_{CF}$ = 21.7 Hz, C11), 73.60 (s, C7), 34.40 (d, $^{1}J_{CP}$ = 136.7 Hz, C5), 22.0 (s, C8).

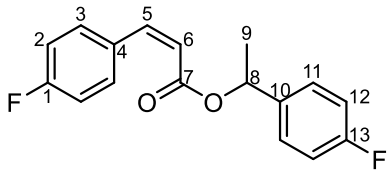
$^{19}F\{^{1}H\}$ NMR (376 MHz, $CDCl_3$): δ -113.9 (s).

^{31}P NMR (162 MHz, $CDCl_3$): δ 12.5 (t, $^{2}J_{PH}$ = 21.8 Hz)

HRMS(TOF-ESI$^+$): calcd. For $C_{22}H_{20}O_5FPNa$ $[M+Na]^+$= 437.0925, found 437.0923

FTIR: (neat) ν_{max}/cm^{-1} 1734 (C=O), 1590, 1487, 1283 (P=O), 1219, 1184, 927, 759, 637

1-(4-fluorophenyl)ethyl (Z)-3-(4-fluorophenyl)acrylate (21-*Z*)



A microwave vial was charged with a magnetic stirrer bar 1-(4-fluorophenyl)ethyl 2 (diphenoxyphosphoryl)acetate (83 mg, 0.2 mmol) and 18-crown-6 (284 mg, 1.1 mmol). The vial was sealed, then evacuated and back-filled with nitrogen three times. THF (4 mL) was added and the solution was cooled on an EtOAc/liquid N_2 bath. KHMDS (0.22 mL of a 1.0 M in THF, 0.22 mmol) was added, the solution was stirred for 10 minutes then 4-fluorobenzaldehyde (24 µL, 0.22 mmol) was added. The reaction mixture was stirred at -78 °C for 30 minutes, then quenched with NH_4Cl (4 mL) then let warm to room temperature. The mixture was extracted with Et_2O (3 x 5 mL), the combined organic layers were then dried over $MgSO_4$, and the volatiles were removed *in vacuo*. The crude material was purified by flash chromatography (SiO_2, 0-10% Et_2O in Cyclohexane) to give the *title compound* as a colourless oil (23 mg, 40%).

TLC: R*f* = 0.39 (10% Et_2O in pentane, visualisation by UV)

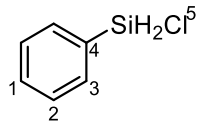
^{1}H NMR (400 MHz, $CDCl_3$): δ 7.63-7.53 (m, 2H, H3), 7.34-7.29 (m, 2H, H11), 7.09-6.96 (m, 4H, H2 and H12), 6.92 (d, *J* = 12.6 Hz, 1H, H5), 5.97 (d, *J* = 12.6 Hz, 1H, H6), 5.92 (q, *J* = 6.6 Hz, 1H, H8), 1.54 (d, *J* = 6.6 Hz, 3H, H9).

^{13}C NMR (101 MHz, $CDCl_3$): δ 165.2 (s, C7), 163.0 (d, $^1J_{CF}$ = 249.7 Hz, Ar*C*), 162.3 (d, $^1J_{CF}$ = 245.9 Hz, Ar*C*), 142.5 (s, C5), 137.2 (d, $^4J_{CF}$ = 3.2 Hz, Ar*C*) 131.9 (d, $^3J_{CF}$ = 8.4 Hz, C3), 130.9 (d, $^4J_{CF}$ = 3.5 Hz, Ar*C*) 128.0 (d, $^3J_{CF}$ = 8.1 Hz, C11), 119.6 (s, C6), 115.3 (d, $^2J_{CF}$ = 21.3 Hz, Ar*C*), 115.0 (d, $^2J_{CF}$ = 21.7 Hz, Ar*C*), 71.76 (s, C8), 22.2 (s, C9).
^{19}F{^{1}H} NMR (376 MHz, $CDCl_3$): δ -111.4 (s), -114.3 (s).

HRMS(TOF): *Not found by HRMS*

FTIR: (neat) ν_{max}/cm^{-1} 1716, 1628, 1600, 1507, 1223, 1151, 1101, 832.

Phenyl chlorosilane



Method adapted from: W. Wang, Y. Tan, Z. Xie and Z. Zhang, *J. Organomet. Chem.*, 2014, **769**, 29–33.

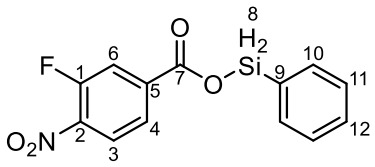
An oven dried 250 mL round bottom flask fitted with a large magnetic stirrer bar was charged with activated 4 Å molecular sieves (40 g), and anhydrous $CuCl_2$ (13.4 g, 100 mmol, 2 equiv.). The flask was sealed and dried further by heating under high vacuum. Then CuI (381 mg, 2.0 mmol, 4 mol%) was added against a counter current of dry N_2. 35 mL of dry Et_2O and phenylsilane (6.17 mL, 50 mmol, 1 equiv.). The resulting mixture was filtered through a cannula to remove the copper salts and molecular sieves, and the solid was washed with diethyl ether (5 × 10 mL). The solution was then distilled, initially under a flow of N_2 to remove Et_2O, and then under reduced pressure (6 mbar) to give phenylchlorosilane (683 mg, 9%) contaminated with ca 4.5% phenylsilane and ca 4% Et_2O (see ^{1}H NMR spectrum) as a colourless oil.

^{1}H NMR (400 MHz, C_6D_6): δ 7.38-7.35 (m, 2H, Ar*H*), 7.12-7.09 (m, 1H, Ar*H*), 7.06-7.02 (m, 2H, Ar*H*), 5.06 (s, 2H, H^5).

^{13}C{^{1}H} NMR (101 MHz, C_6D_6): δ 134.3 (s, Ar*C*), 131.1 (s, Ar*C*), 130.0 (s, Ar*C*), 128.2 (s, Ar*C*).

^{29}Si{^{1}H} NMR (79 MHz, C_6D_6): δ -17.9 (s).

phenylsilyl 3-fluoro-4-nitrobenzoate (22)



An oven dried microwave was charged with potassium 3-fluoro 4-nitrobenzoate (78.1 mg, 0.35 mmol, 1 equiv.). The tube was sealed and evacuated and backfilled with N_2 (3 x). Dry degassed C_6D_6 (0.7 mL) was then added, and finally phenyl chlorosilane (47 µL, 0.35 mmol, 1 equiv.) was added. The mixture was heated to 80 °C for 1 h, then allowed to cool to room temperature. An aliquot (0.2 mL) of the reaction mixture was taken and diluted with dry C_6D_6 (0.4 mL) in an oven dried NMR tube under a flow of N_2. The silyl ester was confirmed to be formed by ^{1}H-^{1}H COSY, ^{1}H-^{13}C HSQC, and ^{1}H-^{13}C HMBC spectra. ^{1}H-^{13}C HMBC cross-peak between H8 and C5 suggests formation of silyl ester. The silyl ester was found to be contaminated with ca 7% phenylsilane.

^{1}H NMR (400 MHz, C_6D_6): δ 7.66-7.63 (m, 2H, Ar*H*), 7.29-7.26 (m, 1H, H6), 7.17-7.10 (m, 5H, Ar*H*), 5.21 (s, 2H, H8).

^{13}C{^{1}H} NMR (101 MHz, C_6D_6): δ 163.77 (s, C7), 155.44 (d, $^{1}J_{CF}$ = 265.2 Hz, C1), 140.0 (d, J_{CF} = 8.4 Hz, Ar*C*), 135.8 (s, Ar*C*), 135.4 (s, Ar*C*), 134.0 (s, Ar*C*), 131.5 (s, Ar*C*), 130.4 (s, Ar*C*), 129.4 (s, Ar*C*), 125.5 (s, Ar*C*), 119.6 (d, $^{1}J_{CF}$ = 22.2 Hz, C6).

^{19}F{^{1}H} NMR (376 MHz, C_6D_6): δ -117.0 (s).

^{29}Si{^{1}H} NMR (79 MHz, C_6D_6): δ -18.0 (s).

4.5 Computational Data

Phenylsilane Ground State (**Figure 9**)

H	2.152830	-0.019423	-0.410083
C	1.202577	-0.008317	0.119428
C	-1.205462	0.001471	1.512733
C	0.000000	-0.009223	-0.602421
C	1.205462	0.001471	1.512733
C	0.000000	0.007156	2.211019
C	-1.202577	-0.008317	0.119428
H	2.147456	0.000787	2.053871
H	0.000000	0.011747	3.297220
H	-2.152830	-0.019423	-0.410083
H	-2.147456	0.000787	2.053871
Si	0.000000	0.007954	-2.479415
H	0.000000	1.396711	-3.009638
H	1.214591	-0.681690	-2.984332
H	-1.214591	-0.681690	-2.984332

Gibbs Energy: -522.758426 au

No imaginary frequencies present

Phenyl Silane hydride transfer TS (**Figure 9**)

Si	-0.279797	-2.075272	1.214183
O	1.145162	-1.870713	0.109460
P	1.705490	-0.395372	0.282310
H	0.302277	-0.576093	1.663835
C	3.178728	-0.433986	-0.841520
C	2.680118	0.071451	1.767576
H	-0.555598	-3.394038	0.516637
C	4.396052	-0.516819	0.091251
H	3.110991	-1.269606	-1.541286
H	3.214852	0.495272	-1.423982
C	4.099566	0.403219	1.284300
H	4.521236	-1.547311	0.444957
H	5.319880	-0.233832	-0.422232
H	4.148720	1.450802	0.959902
H	4.829857	0.280026	2.090350
H	2.670933	-0.805424	2.424923
H	2.180965	0.881343	2.305179
H	-0.036172	-2.552179	2.612807
C	-1.970617	-1.251954	0.898288

C	-2.871990	-1.806576	-0.020107
C	-2.369235	-0.092272	1.579159
C	-4.120952	-1.227928	-0.253317
H	-2.593260	-2.709678	-0.560687
C	-3.623020	0.478409	1.375061
H	-1.681277	0.366433	2.289456
C	-4.501200	-0.086838	0.450066
H	-4.799667	-1.671174	-0.978511
H	-3.913503	1.368293	1.928541
H	-5.475694	0.362822	0.276375
C	0.665101	0.936759	-0.406463
H	1.313985	1.814977	-0.531436
H	-0.115779	1.185139	0.314351
C	0.053047	0.522839	-1.752687
H	0.849552	0.208222	-2.440665
H	-0.595079	-0.348150	-1.598807
C	-0.764225	1.644085	-2.404610
H	-0.114619	2.511811	-2.588041
H	-1.094650	1.291324	-3.389594
C	-1.988104	2.065932	-1.589057

H	-1.707037	2.540880	-0.642232
H	-2.616186	1.200378	-1.347137
H	-2.598850	2.784800	-2.146596

Gibbs Energy: -1254.089658

1 imaginary frequency present: -236 cm^{-1}

Silyl Ester Ground State (**Figure 9**)

H	-0.890737	2.394433	-4.387772
C	-0.068179	1.748942	-4.092268
C	2.037395	0.094552	-3.332820
C	-0.319593	0.610982	-3.331762
C	1.235729	2.059292	-4.475143
C	2.291086	1.233244	-4.093697
C	0.730542	-0.235087	-2.940586
H	-1.338543	0.379931	-3.033557
H	1.429336	2.945755	-5.072115
H	3.308428	1.473770	-4.389037
H	2.870338	-0.543854	-3.045432
Si	0.432846	-1.776971	-1.947090
H	-0.773138	-2.520549	-2.360641

H	1.639258	-2.629588	-1.969671
O	0.286967	-1.440965	-0.258361
C	-0.778558	-0.779138	0.187812
O	-1.675466	-0.399095	-0.537099
C	-0.770237	-0.546388	1.665794
C	-0.816540	-0.092058	4.398884
C	0.286478	-0.994672	2.454790
C	-1.841826	0.143393	2.238169
C	-1.859227	0.375938	3.604264
C	0.257670	-0.767808	3.821767
H	1.130234	-1.517478	2.020013
H	-2.650439	0.490606	1.604694
H	-2.672065	0.916696	4.075526
N	-0.894159	0.129758	5.845264
O	-0.400873	-0.712374	6.574648
O	-1.477991	1.136045	6.219739
F	1.291266	-1.177310	4.555687

Gibbs Energy: -1245.869051

No imaginary frequencies present

Phenyl Silane enhanced reduction TS (Figure 9)

Si	-0.516395	-1.072379	-0.924254
O	0.833796	-0.634024	-1.891830
P	1.502692	0.686438	-1.198968
H	0.312127	0.316389	-0.062779
C	2.915507	0.822131	-2.432662
C	2.656061	0.618892	0.237563
C	4.161919	0.339717	-1.682293
H	2.711813	0.251663	-3.341043
H	3.046790	1.874747	-2.716080
C	4.066619	0.929966	-0.268464
H	4.161400	-0.755922	-1.621315
H	5.086399	0.639834	-2.186553
H	4.227742	2.015354	-0.311119
H	4.824447	0.514626	0.403575
H	2.591419	-0.406694	0.616526
H	2.285668	1.287588	1.020985
C	-2.063579	-0.011094	-0.940897
C	-2.991538	-0.175016	-1.978043
C	-2.357056	0.918975	0.065568

C	-4.166395	0.575867	-2.018360
H	-2.799456	-0.903249	-2.763814
C	-3.537928	1.654997	0.045378
H	-1.648989	1.064620	0.879086
C	-4.443066	1.487935	-1.002503
H	-4.869677	0.439845	-2.835369
H	-3.750473	2.364675	0.840340
H	-5.361476	2.068080	-1.026431
C	0.674036	2.303839	-1.468778
H	1.448831	3.074261	-1.351388
H	-0.075330	2.451615	-0.687897
C	0.038627	2.407097	-2.861745
H	0.800514	2.217380	-3.627627
H	-0.721878	1.624685	-2.974390
C	-0.607194	3.772210	-3.123640
H	0.146704	4.562450	-3.001438
H	-0.920011	3.804243	-4.174735
C	-1.817171	4.063949	-2.235935
H	-1.542557	4.142459	-1.178166
H	-2.563933	3.266387	-2.322344

H	-2.292633	5.008197	-2.522305
O	-0.438245	-1.813445	0.648913
C	0.593027	-2.444410	1.170051
O	1.684543	-2.536336	0.639396
C	0.305560	-3.037299	2.519165
C	-0.136020	-4.136619	5.026763
C	1.318081	-3.763401	3.141233
C	-0.933729	-2.870499	3.142766
C	-1.153542	-3.428089	4.393542
C	1.096661	-4.309528	4.394415
H	2.274505	-3.907435	2.650324
H	-1.716354	-2.309593	2.645574
H	-2.107281	-3.323905	4.898269
N	-0.398337	-4.679363	6.362314
O	-1.559257	-4.958289	6.628679
O	0.545136	-4.795499	7.125612
F	2.068859	-5.027838	4.954405
H	-0.889984	-2.271183	-1.717276

Gibbs Energy: -1977.208664

1 imaginary frequency seen: -232 cm^{-1}

Truncated PMHS (Figure 13)

Si	-0.427193	0.088049	-0.247262
H	-1.085838	1.343269	0.221224
C	-0.590452	-0.140168	-2.086798
H	-0.118981	-1.079660	-2.394856
H	-0.108290	0.679511	-2.632233
H	-1.643567	-0.173044	-2.386628
O	-1.112703	-1.225031	0.478278
O	1.158981	0.162295	0.245627
C	1.970727	1.302786	0.071041
H	2.892725	1.153953	0.639320
H	1.475701	2.212528	0.439202
H	2.233292	1.446787	-0.985738
C	-1.147828	-1.400087	1.881754
H	-0.137912	-1.538772	2.284305
H	-1.742496	-2.292502	2.093264
H	-1.616165	-0.539914	2.379500

Gibbs Energy: -560.155182 au

No imaginary frequencies present.

Phosphine oxide (**23**) **GS**

P	0.000448	0.000000	0.616998
O	0.000744	0.000000	2.114842
C	0.832077	-1.441802	-0.123796
H	0.809880	-1.402820	-1.217754
H	1.872064	-1.471448	0.215628
H	0.336007	-2.356463	0.215100
C	-1.664092	-0.000000	-0.123362
H	-2.209263	0.886396	0.215235
H	-1.618631	0.000000	-1.217305
H	-2.209263	-0.886396	0.215235
C	0.832077	1.441802	-0.123796
H	0.809880	1.402820	-1.217754
H	0.336007	2.356463	0.215100
H	1.872064	1.471448	0.215628

Energy: -536.195248 au

No imaginary frequencies present

Phosphine oxide (23) Reduction TS

P	-1.027109	-1.287235	-0.367656
H	0.703954	-0.967950	0.603174
O	-0.983891	0.261611	-0.078164
Si	0.622257	0.658231	0.689778
C	-1.259323	-2.411487	1.047808
H	-0.322085	-2.904679	1.308711
H	-2.032852	-3.152832	0.822439
H	-1.582057	-1.812189	1.904644
C	0.144201	-1.952170	-1.590667
H	0.827774	-2.655547	-1.111416
H	0.744188	-1.119911	-1.970056
H	-0.390276	-2.438138	-2.413246
C	-2.640862	-1.398428	-1.216930
H	-2.634980	-0.760479	-2.105345
H	-3.435008	-1.049158	-0.550629
H	-2.854156	-2.429406	-1.518096
O	0.230700	2.321737	0.649193
O	1.937632	0.635434	-0.375615
C	0.885929	0.576030	2.553251

H	1.721090	-0.092880	2.789434
H	-0.010367	0.156825	3.030522
H	1.065112	1.562997	2.990033
C	2.809034	1.735432	-0.535317
H	3.667469	1.396417	-1.125276
H	3.174638	2.107261	0.430704
H	2.330389	2.571341	-1.059788
C	-0.310253	2.969512	-0.469797
H	0.079506	2.573058	-1.421155
H	-0.056560	4.035536	-0.417212
H	-1.404097	2.871066	-0.493324

Gibbs Energy: -1096.297751

1 imaginary frequency present: -159 cm^{-1}

Phosphine Oxide (24) GS

C	-0.452957	1.283386	-1.275694
C	-0.450288	-1.284338	-1.275672
C	-0.014840	-0.000030	-1.994179
C	0.147524	-1.411966	0.135572
C	0.144585	1.412252	0.135554

H	-1.547357	1.305828	-1.201969
H	-1.544640	-1.309057	-1.201945
H	1.080274	0.001110	-2.103356
H	1.244819	-1.436057	0.086029
H	1.241828	1.438653	0.086024
H	-0.156794	2.155689	-1.870254
H	-0.152323	-2.156029	-1.870228
H	-0.428659	-0.000475	-3.009236
H	-0.186296	-2.335785	0.621018
H	-0.191195	2.335369	0.620988
H	1.770535	0.001929	2.344571
C	0.713285	0.000768	2.628452
H	0.502396	-0.886053	3.233730
H	0.500451	0.887115	3.233748
P	-0.378564	-0.000398	1.170945
O	-1.841785	-0.001910	1.505902

Gibbs Energy: -652.835844 au

No imaginary frequencies present

Phosphine Oxide (24) TS

P	-0.471972	-0.804700	-0.298949
H	-0.075926	-0.391466	1.544958
O	-0.668514	0.765621	-0.213313
Si	-0.149738	1.256877	1.443015
C	-1.689853	-1.890618	0.522486
H	-2.001910	-2.697590	-0.148754
H	-2.564137	-1.275445	0.761081
H	-1.291134	-2.298278	1.452491
C	1.243539	-1.451332	-0.285363
H	1.810404	-0.853675	0.432131
C	-0.920204	-1.074156	-2.068782
H	-0.551693	-0.225296	-2.654664
H	-2.012449	-1.065069	-2.157080
O	-0.125656	2.906877	1.003973
O	1.482183	1.164807	1.833805
C	-1.497854	1.242889	2.767656
H	-1.173966	0.620870	3.609326
H	-2.419214	0.795369	2.372193
H	-1.741718	2.243191	3.142245

C	2.366612	2.265687	1.914005
H	3.339099	1.878222	2.236596
H	2.020312	3.010196	2.639894
H	2.475480	2.762334	0.944117
C	-1.236773	3.575543	0.479390
H	-1.523255	3.174799	-0.504176
H	-0.982628	4.635690	0.362472
H	-2.114138	3.509585	1.144578
C	-0.323985	-2.391519	-2.581731
H	-0.765500	-2.649527	-3.550063
H	-0.604067	-3.209826	-1.903883
H	1.204931	-2.478412	0.099729
C	1.212243	-2.330096	-2.707599
H	1.486232	-1.991349	-3.713716
H	1.620446	-3.342603	-2.600927
C	1.873407	-1.393774	-1.682063
H	1.833355	-0.357133	-2.038953
H	2.938041	-1.636690	-1.596127

Gibbs Energy: -1212.935064 au

1 Imaginary frequency present at: -163 cm^{-1}

Phosphine Oxide (25) GS

P	-0.693964	0.733170	-0.577472
O	-1.850354	1.685971	-0.605011
C	-1.033238	-0.963154	0.053969
H	-1.203806	-1.680219	-0.754727
H	-1.953108	-0.899170	0.646621
C	0.657928	1.092636	0.629500
H	0.516329	2.092454	1.048367
H	1.627864	1.071827	0.118458
C	0.115456	0.509862	-2.196820
H	0.912606	-0.239375	-2.140046
H	0.539955	1.462094	-2.528551
H	-0.630796	0.188819	-2.929350
C	0.571626	-0.027539	1.681426
H	1.514817	-0.146806	2.224130
H	-0.199714	0.221464	2.420626
C	0.169155	-1.315706	0.943771
H	1.008242	-1.660614	0.324359
H	-0.068999	-2.125714	1.640748

Gibbs Energy: -613.553622 au

No imaginary frequencies present

Phosphine (25) TS

P	-0.705899	-0.931570	-0.098713
H	0.909195	-0.582782	0.693675
O	-0.696702	0.650565	-0.044209
Si	0.900969	1.074913	0.734275
C	-0.944832	-1.919454	1.423014
H	-1.678457	-2.713439	1.250775
H	-1.323186	-1.251454	2.203418
H	0.001738	-2.343711	1.762397
C	0.292982	-1.800401	-1.373522
H	0.748829	-2.674021	-0.893690
H	1.108690	-1.147734	-1.693509
C	-2.318867	-1.228805	-0.964385
H	-2.554662	-0.344494	-1.565506
H	-3.143164	-1.383504	-0.261334
O	0.839161	2.649995	0.111718
O	2.518485	0.819997	0.336300
C	0.566547	1.267962	2.576143
H	0.806638	0.363506	3.144802

H	-0.485544	1.521998	2.756403
H	1.173867	2.089865	2.973702
C	3.474375	1.860144	0.286501
H	4.460346	1.395636	0.175629
H	3.471407	2.455228	1.210299
H	3.289979	2.536163	-0.554593
C	-0.289525	3.480273	0.099120
H	-1.151680	2.989145	-0.370626
H	-0.045612	4.381965	-0.474891
H	-0.576542	3.789626	1.116106
C	-2.052549	-2.436455	-1.871732
H	-2.832934	-2.556156	-2.630046
H	-2.033742	-3.364095	-1.282147
C	-0.672458	-2.197458	-2.503274
H	-0.747640	-1.375953	-3.226115
H	-0.309211	-3.075492	-3.045983

Gibbs Energy: -1173.657998 au

1 imaginary frequency present at: -173 cm^{-1}

Phosphine (26) GS

P	-0.714090	0.000577	0.715900
C	-0.392287	1.174785	-0.665478
H	-1.340977	1.494280	-1.107410
H	0.232062	2.051081	-0.475807
C	-0.393651	-1.174658	-0.664910
H	0.229674	-2.051589	-0.474814
H	-1.342717	-1.493264	-1.106678
C	0.248846	-0.000505	-1.458087
H	1.337907	-0.001117	-1.353378
H	0.014564	-0.000626	-2.525762
C	0.799247	-0.000028	1.735095
H	1.703922	-0.000575	1.118876
H	0.796405	-0.887848	2.374319
H	0.797279	0.888008	2.374024
O	-1.976184	0.001481	1.514109

Gibbs Energy: -574.255209 au

No imaginary frequency present

Phosphine (26) TS

P	-0.727647	-1.243683	-0.435690
H	0.818377	-0.133485	-0.029853
O	-1.353938	0.063842	0.149648
Si	0.052539	1.156888	0.640544
C	-0.019138	-2.437990	0.742072
C	-0.032665	-1.411236	-2.119166
H	1.032161	-1.641932	-2.192311
H	-0.239920	-0.493658	-2.679219
C	-2.061342	-2.200005	-1.277604
H	-2.849944	-1.520296	-1.612878
H	-2.515665	-3.042536	-0.750415
O	-1.091557	2.394451	0.647829
O	1.276358	2.102624	-0.070391
C	0.455101	0.735025	2.432326
H	1.505463	0.437733	2.545684
H	-0.172330	-0.086198	2.799837
H	0.275753	1.599977	3.083167
C	2.598541	1.684755	-0.251865
H	3.056915	2.300172	-1.035220

H	2.659706	0.625963	-0.556263
H	3.184762	1.805929	0.671772
C	-0.798877	3.712730	1.036144
H	-0.554262	3.768035	2.109739
H	-1.692426	4.322704	0.861300
H	0.039806	4.131142	0.466177
C	-1.059696	-2.538136	-2.417190
H	-1.486599	-2.504757	-3.422757
H	-0.610392	-3.525778	-2.275204
H	0.138822	-3.392817	0.230030
H	-0.748175	-2.588125	1.545077
H	0.920267	-2.081337	1.164681

Gibbs Energy: -1134.360073 au

1 imaginary frequency present at: -178 cm^{-1}

Phosphine (27) GS

C	0.002030	0.857223	-1.125266
H	-0.650290	1.250963	-1.901087
H	0.846892	1.503390	-0.896809
C	0.279777	-0.688699	-1.202220

H	-0.209066	-1.207332	-2.023563
H	1.300300	-1.020610	-1.023663
P	-0.753135	-0.142769	0.156226
C	0.209647	-0.047793	1.691060
H	-0.194597	0.750270	2.319254
H	1.262608	0.153247	1.476844
H	0.120232	-0.995216	2.228998
O	-2.214399	-0.412674	0.300226

Gibbs Energy: -534.948945 au

No imaginary frequency seen

Phosphine (27) TS

P	-0.792560	-1.524868	-0.591939
H	0.689202	-0.390676	-0.316471
O	-1.456941	-0.273587	0.054634
Si	-0.041280	0.886140	0.444331
C	-0.007453	-2.771072	0.463687
C	-0.690044	-1.756273	-2.355605
H	0.057963	-2.436033	-2.756565
H	-0.836337	-0.864551	-2.961306
C	-1.957334	-2.367236	-1.685213

H	-2.899518	-1.870489	-1.904896
H	-2.027630	-3.453035	-1.681392
O	-1.200025	2.096159	0.388091
O	1.212610	1.837840	-0.200914
C	0.368307	0.481571	2.234465
H	1.292439	-0.102557	2.327563
H	-0.444704	-0.073652	2.715553
H	0.511669	1.414770	2.793089
C	2.537090	1.404048	-0.322356
H	3.091018	2.142068	-0.912321
H	2.604141	0.428977	-0.831353
H	3.024792	1.309841	0.660127
C	-0.910644	3.461483	0.564802
H	-0.327402	3.644348	1.479208
H	-1.864064	3.993827	0.651396
H	-0.346659	3.864299	-0.283477
H	0.241654	-3.649413	-0.139425
H	-0.723241	-3.061120	1.238506
H	0.894949	-2.370809	0.927780

Gibbs Energy: -1095.055665 au

1 imaginary frequency seen: -186 cm^{-1}

Phosphine Oxide (28) GS

P -0.108818 0.751447 -0.664101

C 1.206667 1.416915 0.445241

C 0.539937 1.613771 1.816595

C -0.912876 2.044516 1.555152

C -1.495914 1.077577 0.510027

H 1.500930 2.379063 0.010716

H 2.098387 0.784293 0.481570

H 0.545825 0.669333 2.376071

H 1.077453 2.350878 2.422115

H -0.921944 3.065655 1.154378

H -1.506231 2.051380 2.475341

H -2.340598 1.495693 -0.043561

H -1.829760 0.149871 0.987702

O -0.225827 1.422242 -2.003225

C 0.116085 -1.084605 -0.807899

C -1.158436 -1.657709 -1.449374

H -1.030110 -2.732941 -1.626856

H -1.368905 -1.174883 -2.408870

H -2.034451 -1.532032 -0.801809

C 1.314059 -1.326694 -1.740595

H 2.248798 -0.947815 -1.309917

H 1.164563 -0.840306 -2.708994

H 1.438576 -2.404094 -1.907266

C 0.369427 -1.750698 0.551256

H 1.283908 -1.380815 1.028622

H 0.491258 -2.831589 0.407065

H -0.462003 -1.608455 1.250614

Gibbs Energy: -731.383736 au

No imaginary frequencies present

Phosphine Oxide (28) TS

P -0.480127 -0.502605 -0.377072

H 1.244049 -0.088876 0.515896

O -0.446465 1.074242 -0.227741

Si 1.206562 1.532343 0.355925

C -0.898479 -1.496386 1.155846

C 0.663419 -1.342307 -1.547022

H 0.951712 -2.295468 -1.086979

H 1.569537 -0.741452 -1.649408

C -1.956745 -0.686366 -1.485813

H -2.070912 0.284435 -1.980024

H -2.890674 -0.888439 -0.955395

O 0.936363 3.162110 -0.094752

O 2.513344 1.296940 -0.678376

C 1.459985 1.742852 2.221500

H 0.549520 1.484434 2.779609

H 1.733686 2.770176 2.488726

H 2.253323 1.068656 2.565183

C 3.181857 2.315259 -1.397192

H 4.009474 1.842690 -1.937719

H 3.586445 3.083136 -0.727291

H 2.512567 2.806621 -2.111696

C -0.131049 3.918499 0.399818

H -1.098673 3.535693 0.041787

H -0.017134 4.952681 0.053474

H -0.156135 3.932668 1.502796

C -1.587688 -1.762100 -2.516870

H -2.221591 -1.694400 -3.406964

H -1.729612 -2.765271 -2.096549

C -0.106529 -1.547168 -2.860770

H -0.004731 -0.648230 -3.480513

H 0.306173 -2.383965 -3.433189

C -1.906404 -0.660328 1.962553

H -1.470078 0.286864 2.292049

H -2.206841 -1.225239 2.853083

H -2.811662 -0.432031 1.389576

C -1.545733 -2.828940 0.731503

H -0.868477 -3.441974 0.125978

H -2.479531 -2.695168 0.179134

H -1.782893 -3.403827 1.634066

C 0.321323 -1.820085 2.028900

H 0.767677 -0.924201 2.461458

H 1.101977 -2.340369 1.464245

H -0.000826 -2.475105 2.848229

Gibbs Energy: -1291.486852 au

1 imaginary frequency present: -168 cm-1

Phosphine Oxide (29) GS

P -0.539352 0.636598 -0.694365

O -1.681736 1.611925 -0.722278

C -0.949413 -1.061864 -0.039716

C 0.828534 1.030614 0.530087

C 0.205860 0.422287 -2.347204

H 1.025533 -0.301360 -2.360343

H 0.575477 1.390735 -2.696185

H -0.578726 0.089375 -3.032655

C 0.724400 -0.121633 1.558128

H 1.683546 -0.264892 2.070676

H -0.009027 0.139257 2.330422

C 0.278106 -1.397192 0.832301

H 1.094480 -1.766873 0.195585

H 0.040904 -2.203095 1.538010

C -2.220766 -0.940191 0.816931

H -2.121328 -0.201378 1.617710

H -2.445246 -1.912587 1.273690

H -3.074253 -0.632238 0.206389

C -1.176389 -2.109873 -1.133163

H -0.290362 -2.254551 -1.760558

H -2.015888 -1.837078 -1.782981

H -1.415620 -3.076819 -0.672839

C 0.564077 2.394726 1.175696

H 1.289287 2.567133 1.981525

H -0.444784 2.453535 1.593819

H 0.661903 3.206593 0.447189

C 2.222328 1.029990 -0.117331

H 2.971357 1.287002 0.641945

H 2.301350 1.769598 -0.921445

H 2.495751 0.052253 -0.529039

Gibbs Energy: -770.662489 au

No imaginary frequencies found.

Phosphine Oxide (29) TS

P -0.430870 -0.561811 0.121726

H 1.251128 -0.238578 0.940749

O -0.339359 1.022498 0.192874

Si 1.174678 1.417629 1.084464

C -0.801859 -1.418213 1.694579

H -1.371739 -2.332894 1.507674

H -1.412141 -0.746705 2.305957

H 0.112037 -1.658111 2.236888

C 0.592578 -1.617999 -1.047575

C -2.032201 -0.760898 -0.826410

O 0.962361 3.086182 0.803147

O 2.731089 1.345688 0.456752

C 0.943684 1.325869 2.958675

H 1.356619 0.405253 3.384974

H -0.121735 1.373932 3.223263

H 1.434271 2.181570 3.438015

C 3.539840 2.465700 0.150751

H 4.512780 2.082951 -0.176756

H 3.686884 3.110911 1.025844

H 3.097024 3.070541 -0.649075

C -0.205484 3.787522 1.127659

H -1.079553 3.395586 0.586966

H -0.067605 4.839184 0.848385

H -0.422506 3.750396 2.207887

C -1.851604 -2.158275 -1.444259

H -2.616407 -2.350254 -2.207098

H -1.979269 -2.933091 -0.674408

C -0.439121 -2.231165 -2.035976

H -0.412461 -1.675094 -2.978669

H -0.159222 -3.264243 -2.272684

C -2.118061 0.311401 -1.928804

H -1.211724 0.381626 -2.537281

H -2.287209 1.299369 -1.493675

H -2.954442 0.074389 -2.599167

C 1.630964 -0.768356 -1.790000

H 2.122354 -1.397316 -2.543120

H 2.389212 -0.370347 -1.109941

H 1.170344 0.078613 -2.310812

C 1.303991 -2.722080 -0.252946

H 1.949119 -2.299242 0.523704

H 1.935231 -3.300340 -0.937986

H 0.597793 -3.419286 0.213362

C -3.293505 -0.666585 0.038241

H -3.363571 -1.474820 0.773789

H -4.183240 -0.730805 -0.601292

H -3.339094 0.289695 0.571608

Gibbs Energy: -1330.769542 au

1 imaginary frequency found: -162 cm-1

Phosphine Oxide (18) GS

P 1.273192 0.223819 -1.383998

C 1.962550 -1.055043 -0.249576

C 2.149059 -0.355525 1.106640

C 2.577732 1.092184 0.811356

C 1.622555 1.646716 -0.260155

H 2.929532 -1.346670 -0.675500

H 1.338781 -1.952575 -0.196999

H 1.201756 -0.350756 1.661354

H 2.884570 -0.875371 1.729308

H 3.603390 1.093088 0.422082

H 2.574142 1.708851 1.716107

H 2.055159 2.463918 -0.843418

H 0.694337 2.010116 0.196134

O 1.886289 0.294965 -2.751413

C -0.543222 -0.002421 -1.435711

C -1.254292 -0.242110 -0.101103

H -0.860730 -1.149814 0.376237

H -1.050349 0.584056 0.593841

C -2.769527 -0.386333 -0.263946

H -2.979826 -1.208312 -0.960835

H -3.169604 0.523735 -0.730106

C -3.478920 -0.641087 1.065076

H -3.116519 -1.563963 1.532924

H -3.304235 0.181478 1.768599

H -0.947650 0.888267 -1.934243

H -0.717426 -0.842414 -2.120183

H -4.560742 -0.738797 0.927529

Gibbs Energy: -731.380584 au

No imaginary frequencies present

Phosphine Oxide (18) TS

P -0.114972 -0.646643 -0.831064

H 1.529841 -0.306849 0.188930

O -0.055748 0.928043 -0.707033

Si 1.539944 1.330158 0.052633

C -0.625878 -1.577272 0.658687

C 1.073439 -1.566573 -1.886514

H 1.407568 -2.432192 -1.302403

H 1.950415 -0.938535 -2.061016

C -1.545590 -0.903004 -1.971693

H -1.621243 -0.018895 -2.614225

H -2.495619 -1.010609 -1.440129

O 1.351059 2.980710 -0.350433

O 2.912306 1.081410 -0.885081

C 1.656046 1.437740 1.939349

H 0.805317 0.944245 2.425787

H 1.726866 2.462848 2.319408

H 2.553981 0.888746 2.248517

C 3.659062 2.099313 -1.522327

H 4.494307 1.614765 -2.040010

H 4.058717 2.818528 -0.797713

H 3.050175 2.650350 -2.246823

C 0.248947 3.740455 0.054071

H -0.669724 3.422349 -0.459801

H 0.439368 4.791831 -0.191107

H 0.071492 3.674152 1.140795

C -1.165954 -2.138337 -2.799704

H -1.794049 -2.235325 -3.690788

H -1.306824 -3.053376 -2.207756

C 0.318560 -1.977716 -3.161577

H 0.422267 -1.189419 -3.916805

H 0.736731 -2.893999 -3.589905

C -1.621435 -0.792761 1.520658

H -1.176887 0.164097 1.816971

H -2.515849 -0.544779 0.933893

H -1.085453 -2.509595 0.301986

H 0.264752 -1.836373 1.237021

C -2.034142 -1.571717 2.770785

H -1.136278 -1.816688 3.353743

H -2.482223 -2.529386 2.472436

C -3.015718 -0.788051 3.641358

H -2.575253 0.158878 3.975285

H -3.933039 -0.551963 3.088703

H -3.299283 -1.358562 4.532890

Gibbs Energy: -1291.489179

1 imaginary frequency found: -159 cm-1

Phosphine Oxide (30) GS

H 1.941501 -1.179853 0.320155

C 1.057687 -0.783351 0.831275

C -0.239835 1.223234 0.127109

C -1.436376 -0.783130 1.000834

C -1.436376 0.783130 1.000834

C -0.239835 -1.223234 0.127109

C 1.057687 0.783351 0.831275

H -0.263520 2.278457 -0.151641

H -1.326695 -1.186500 2.013767

H -2.373688 1.166337 0.588930

H 1.941501 1.179853 0.320155

H 1.080663 -1.179253 1.852408

H -2.373688 -1.166337 0.588930

H -1.326695 1.186500 2.013767

H -0.263520 -2.278457 -0.151641

H 1.080663 1.179253 1.852408

P -0.407377 0.000000 -1.242728

C 1.083481 0.000000 -2.291281

H 2.015808 0.000000 -1.722124

H 1.051394 0.885507 -2.932761

H 1.051394 -0.885507 -2.932761

O -1.674174 0.000000 -2.044017

Gibbs Energy: -690.904573 au

No imaginary frequencies seen

Phosphine Oxide (30) TS

P -0.775887 -0.750817 -0.171796

H 0.422135 -0.685201 1.483707

O -0.665794 0.763742 0.224030

Si 0.572543 0.945676 1.547993

C -1.870224 -1.757224 0.874267

H -2.862982 -1.843338 0.422382

H -1.950313 -1.283370 1.853634

H -1.441382 -2.753900 1.008787

C 0.578820 -1.693699 -0.982769

H 1.366482 -2.051189 -0.321791

C -1.446959 -0.665083 -1.884380

H -2.384177 -0.119124 -2.007571

O 0.615980 2.631801 1.216269

O 2.195323 0.678434 1.204947

C -0.039455 1.000338 3.337634

H 0.313499 0.129248 3.899386

H -1.137175 1.002108 3.380511

H 0.308445 1.911649 3.838441

C 3.162482 1.704695 1.088318

H 4.139990 1.222662 0.979889

H 3.178371 2.348724 1.975569

H 2.968579 2.338995 0.216554

C -0.530041 3.433309 1.191574

H -1.211885 3.140811 0.379452

H -0.227429 4.474527 1.029842

H -1.091721 3.388077 2.139714

C -0.249034 0.001953 -2.602002

H -0.237871 1.077301 -2.407738

H -0.334162 -0.142462 -3.684431

C 1.045783 -0.666982 -2.032309

H 1.707958 0.070546 -1.570475

H 1.615243 -1.180652 -2.814773

C -0.217101 -2.805445 -1.704514

H 0.406835 -3.240299 -2.492121

H -0.473117 -3.621349 -1.020273

C -1.504804 -2.143316 -2.296708

H -1.538328 -2.232745 -3.387583

H -2.408628 -2.628401 -1.911667

Gibbs Energy: -1251.013232 au

1 imaginary frequency seen: -174 cm-1

Phosphine Oxide (31) GS

H 0.902461 -0.062689 -1.976612

C 0.724814 -1.010504 -1.452343

C 1.795002 -1.236859 -0.371409

C 1.473347 -0.274956 0.784026

C -0.040875 -0.346436 1.089330

P -0.838914 -0.916712 -0.487792

H 0.667381 -1.813545 -2.191417

H 2.806206 -1.078177 -0.760634

H 1.741124 -2.274300 -0.018283

H 2.066452 -0.502523 1.676062

H 1.738348 0.747179 0.479509

H -0.241043 -1.080153 1.875988

C -1.684570 0.674137 -0.854532

C -0.991942 1.707403 0.049175

C -0.692471 1.014737 1.392734

H -2.734304 0.540649 -0.568568

H -1.654624 0.932191 -1.917191

H -1.610075 2.600485 0.186125

H -0.054260 2.040144 -0.415313

H -1.634756 0.859817 1.932814

H -0.051110 1.633740 2.031223

O -1.686190 -2.153628 -0.482890

Gibbs Energy: -690.916361 au

No imaginary frequencies found.

Phosphine Oxide (31) TS

P -0.429921 -0.649994 -0.192767

H 1.317925 -0.368642 0.663793

O -0.269256 0.910129 -0.187914

Si 1.388778 1.234433 0.623090

C -0.793968 -1.486193 1.398466

H -0.952934 -0.670147 2.114443

H 0.059527 -2.067413 1.752434

C 0.542424 -1.559564 -1.448643

H 0.850510 -2.523137 -1.025237

H 1.447456 -0.995705 -1.685806

C -2.090824 -1.010230 -0.943052

H -2.495585 -0.099974 -1.394958

O 1.359087 2.818649 0.000027

O 2.982031 0.937308 0.149996

C 1.079900 1.496753 2.467748

H 1.335122 0.605616 3.051605

H 0.028135 1.744406 2.661632

H 1.684087 2.334089 2.836667

C 3.955011 1.937936 -0.068579

H 4.911793 1.433019 -0.243234

H 4.059473 2.596520 0.803845

H 3.705426 2.558345 -0.935753

C 0.258620 3.681338 0.073984

H -0.588789 3.306511 -0.515372

H 0.559356 4.657366 -0.324175

H -0.081734 3.826899 1.111654

C -1.802261 -2.056012 -2.040275

H -2.588749 -2.055248 -2.802128

H -1.782896 -3.064569 -1.602841

C -0.422601 -1.740381 -2.631760

H -0.473081 -0.807474 -3.207204

H -0.075104 -2.523849 -3.312572

C -2.973319 -1.518571 0.207821

H -3.795153 -2.141709 -0.163836

H -3.423893 -0.667039 0.732018

C -2.076192 -2.301490 1.183341

H -2.585599 -2.490709 2.133631

H -1.822801 -3.281264 0.759912

Gibbs Energy: -1251.027069 au

1 imaginary frequency found: -121 cm-1

Phosphine Oxide (32) GS

P -0.903282 0.547946 0.562698

O -2.110049 1.457590 0.565811

C -1.189203 -1.158853 1.229008

H -1.299036 -1.908326 0.438374

H -2.139749 -1.109993 1.774227

C 0.421583 0.952877 1.799548

H 0.265921 1.969600 2.171227

H 1.407951 0.915316 1.319628

Si 0.054749 0.355685 -1.490957

C 0.314065 -0.125040 2.889957

H 1.233765 -0.199263 3.479827

H -0.497628 0.132958 3.581317

C -0.019861 -1.446752 2.182098

H 0.855728 -1.786780 1.612802

H -0.268876 -2.239622 2.895246

C -1.298002 -0.212916 -2.664206

H -0.937361 -0.226684 -3.699726

H -2.158659 0.462489 -2.610269

H -1.646888 -1.222206 -2.417674

C 1.448835 -0.911888 -1.387703

H 2.236595 -0.595693 -0.694198

H 1.912624 -1.051422 -2.372016

H 1.079408 -1.889272 -1.055710

C 0.709053 2.055880 -1.953713

H 1.505890 2.380126 -1.274510

H -0.094117 2.799504 -1.909321

H 1.116543 2.054740 -2.971764

Gibbs energy: -982.799159 au

No imaginary frequencies found.

Phosphine Oxide (32) TS

P -0.481322 -0.387580 -0.554075

H 1.078810 -0.023705 0.424376

O -0.457058 1.212338 -0.473822

Si 1.100863 1.656489 0.276227

Si -0.830738 -1.678040 1.298148

C 0.632109 -1.180331 -1.790936

H 1.043976 -2.088339 -1.334533

H 1.474544 -0.511630 -1.984361

C -2.011213 -0.612025 -1.597691

H -2.182038 0.315781 -2.153627

H -2.905755 -0.809908 -0.998659

O 0.983125 3.270097 -0.256839

O 2.583048 1.342827 -0.449258

C 1.053600 1.914642 2.145955

H 1.264629 1.008848 2.722445

H 0.073973 2.302295 2.454278

H 1.795095 2.676137 2.415499

C 3.505516 2.345657 -0.828337

H 4.406693 1.840524 -1.192588

H 3.780615 2.980279 0.024193

H 3.101589 2.990267 -1.615558

C -0.149188 4.075847 -0.096287

H -1.029292 3.643349 -0.592037

H 0.054588 5.055848 -0.543463

H -0.397084 4.235956 0.965542

C -1.660628 -1.755404 -2.557663

H -2.360920 -1.808096 -3.397831

H -1.712353 -2.721223 -2.037800

C -0.222036 -1.496326 -3.029626

H -0.216812 -0.632721 -3.705300

H 0.185726 -2.346257 -3.585916

C -1.679540 -0.570183 2.552933

H -1.039872 0.267226 2.844941

H -1.918586 -1.145501 3.455590

H -2.615567 -0.160076 2.157947

C -1.956419 -3.115590 0.824023

H -1.473882 -3.791745 0.109833

H -2.905939 -2.783270 0.391785

H -2.188977 -3.701136 1.722294

C 0.813915 -2.344970 1.903231

H 1.475068 -1.538837 2.232230

H 1.334704 -2.897701 1.113116

H 0.653034 -3.033813 2.741619

Gibbs Energy: -1542.912114 au

1 imaginary frequency found: -117 cm-1

Phosphine Oxide (33) GS

P -0.587676 0.000000 -1.412991

C -0.572517 1.174558 0.009018

C -0.096236 0.000000 0.913645

C -0.572517 -1.174558 0.009018

C 1.098710 0.000000 -2.113964

H 1.218413 -0.887488 -2.742172

H 1.872106 0.000000 -1.339836

H 1.218413 0.887488 -2.742172

C 0.244565 2.456146 -0.002570

H -0.153258 3.174997 -0.726622

H 1.292068 2.260221 -0.259607

H 0.229086 2.933336 0.984499

O -1.659128 0.000000 -2.457838

C 0.244565 -2.456146 -0.002570

H -0.153258 -3.174997 -0.726622

H 0.229086 -2.933336 0.984499

H 1.292068 -2.260221 -0.259607

C -0.621672 0.000000 2.342929

H -0.278826 -0.885761 2.890105

H -1.718122 0.000000 2.350961

H -0.278826 0.885761 2.890105

H 1.003337 0.000000 0.938457

H -1.625190 1.392770 0.236667

H -1.625190 -1.392770 0.236667

Gibbs Energy: -692.093972 au

No imaginary frequencies found.

Phosphine Oxide (33) TS

P -0.495044 -0.663974 0.097471

H 1.074698 0.483106 0.505026

O -1.107460 0.640483 0.710893

Si 0.273527 1.747805 1.193174

C 0.205290 -1.849207 1.286289

C 0.209085 -0.837634 -1.592189

C -1.843739 -1.579987 -0.764823

O -0.918928 2.938641 1.337673

O 1.381836 2.761842 0.393265

C 0.788811 1.341744 2.961739

H 1.796821 0.911474 3.009495

H 0.088637 0.627190 3.413399

H 0.774264 2.245782 3.582764

C 2.734461 2.462182 0.195361

H 3.101589 3.035196 -0.665224

H 2.896733 1.389726 -0.000644

H 3.332371 2.737421 1.077375

C -0.625710 4.270588 1.667803

H 0.014639 4.346413 2.561876

H -1.571916 4.781049 1.883637

H -0.118148 4.788055 0.844077

C -0.819294 -1.973763 -1.864665

H -0.356468 -2.933744 -1.590544

H 0.420954 -2.796595 0.781578

H -0.544223 -2.028762 2.064049

H 1.114560 -1.458133 1.742024

C 1.684189 -1.122442 -1.806122

H 2.296980 -0.265099 -1.514341

H 1.876491 -1.337652 -2.863940

H 2.010144 -1.991146 -1.221200

C -2.650752 -2.680250 -0.095257

H -2.002715 -3.458193 0.324820

H -3.319409 -3.162056 -0.818358

H -3.269799 -2.279234 0.713738

C -1.351586 -2.069358 -3.287696

H -0.549465 -2.303833 -3.996944

H -1.808663 -1.121052 -3.593207

H -2.111611 -2.854438 -3.369793

H -2.516863 -0.811020 -1.167404

H -0.094289 0.068874 -2.135173

Gibbs Energy: -1252.200781 au

1 imaginary frequency found: -166 cm-1

Phosphine Oxide (34) GS

P -0.587676 0.000000 -1.412991

C -0.572517 1.174558 0.009018

C -0.096236 0.000000 0.913645

C -0.572517 -1.174558 0.009018

C 1.098710 0.000000 -2.113964

H 1.218413 -0.887488 -2.742172

H 1.872106 0.000000 -1.339836

H 1.218413 0.887488 -2.742172

C 0.244565 2.456146 -0.002570

H -0.153258 3.174997 -0.726622

H 1.292068 2.260221 -0.259607

H 0.229086 2.933336 0.984499

O -1.659128 0.000000 -2.457838

C 0.244565 -2.456146 -0.002570

H -0.153258 -3.174997 -0.726622

H 0.229086 -2.933336 0.984499

H 1.292068 -2.260221 -0.259607

C -0.621672 0.000000 2.342929

H -0.278826 -0.885761 2.890105

H -1.718122 0.000000 2.350961

H -0.278826 0.885761 2.890105

H 1.003337 0.000000 0.938457

H -1.625190 1.392770 0.236667

H -1.625190 -1.392770 0.236667

Gibbs Energy: -692.087788 au

No imaginary frequencies found.

Phosphine Oxide (34) TS

P -0.495044 -0.663974 0.097471

H 1.074698 0.483106 0.505026

O -1.107460 0.640483 0.710893

Si 0.273527 1.747805 1.193174

C 0.205290 -1.849207 1.286289

C 0.209085 -0.837634 -1.592189

C -1.843739 -1.579987 -0.764823

O -0.918928 2.938641 1.337673

O 1.381836 2.761842 0.393265

C 0.788811 1.341744 2.961739

H 1.796821 0.911474 3.009495

H 0.088637 0.627190 3.413399

H 0.774264 2.245782 3.582764

C 2.734461 2.462182 0.195361

H 3.101589 3.035196 -0.665224

H 2.896733 1.389726 -0.000644

H 3.332371 2.737421 1.077375

C -0.625710 4.270588 1.667803

H 0.014639 4.346413 2.561876

H -1.571916 4.781049 1.883637

H -0.118148 4.788055 0.844077

C -0.819294 -1.973763 -1.864665

H -0.356468 -2.933744 -1.590544

H 0.420954 -2.796595 0.781578

H -0.544223 -2.028762 2.064049

H 1.114560 -1.458133 1.742024

C 1.684189 -1.122442 -1.806122

H 2.296980 -0.265099 -1.514341

H 1.876491 -1.337652 -2.863940

H 2.010144 -1.991146 -1.221200

C -2.650752 -2.680250 -0.095257

H -2.002715 -3.458193 0.324820

H -3.319409 -3.162056 -0.818358

H -3.269799 -2.279234 0.713738

C -1.351586 -2.069358 -3.287696

H -0.549465 -2.303833 -3.996944

H -1.808663 -1.121052 -3.593207

H -2.111611 -2.854438 -3.369793

H -2.516863 -0.811020 -1.167404

H -0.094289 0.068874 -2.135173

Gibbs Energy: -1252.195882

1 imaginary frequency found: -158 cm-1

Phosphine Oxide (35) GS

P -1.327393 0.002730 0.083109

C 0.072192 -1.207492 -0.037507

C 1.018308 -0.002210 -0.436589

C 0.078260 1.207228 -0.035026

C -2.129994 0.002745 1.722200

H -2.768104 0.889061 1.793251

H -1.417248 0.003363 2.550466

H -2.767306 -0.884022 1.793993

C 0.498884 -1.849374 1.286885

H -0.259710 -2.551489 1.652761

H 0.685722 -1.114504 2.077160

H 1.430750 -2.410449 1.138444

C -0.146722 -2.292096 -1.091336

H -0.876400 -3.024875 -0.729099

H 0.789821 -2.825669 -1.296619

H -0.533893 -1.887905 -2.029827

O -2.323386 0.006700 -1.040545

C -0.137392 2.294539 -1.086606

H -0.853243 3.037227 -0.716478

H -0.540430 1.896033 -2.020917

H 0.803834 2.815153 -1.301773

C 0.508248 1.845447 1.289729

H -0.247583 2.549319 1.657759

H 1.441164 2.404001 1.141078

H 0.693854 1.108508 2.078144

C 1.500344 -0.001574 -1.884392

H 2.127938 0.874350 -2.079043

H 0.672759 0.014071 -2.599626

H 2.101608 -0.893170 -2.090062

H 1.905117 -0.005646 0.210468

Gibbs Energy: -770.642083 au

No imaginary frequencies found.

Phosphine Oxide (35) TS

P -0.287634 -0.704166 0.368053

H 1.286954 0.414306 0.809850

O -0.893703 0.620292 0.959520

Si 0.459198 1.715180 1.453960

C 0.342402 -1.880670 1.605156

C 0.479972 -0.870994 -1.307967

C -1.670767 -1.578655 -0.527133

O -0.734098 2.897735 1.663873

O 1.483355 2.706536 0.534877

C 1.059062 1.352888 3.205933

H 2.087874 0.974746 3.217048

H 0.415441 0.598903 3.676531

H 1.014214 2.250626 3.833340

C 2.827095 2.441010 0.252152

H 3.116897 3.007917 -0.639486

H 3.006744 1.371256 0.063278

H 3.474068 2.749772 1.084606

C -0.438225 4.225641 1.999935

H 0.150680 4.296790 2.929678

H -1.384996 4.755274 2.159610

H 0.123334 4.728609 1.202489

C -0.645516 -1.902826 -1.669887

H -0.239242 -2.904359 -1.469596

H 0.560722 -2.842690 1.133030

H -0.438966 -2.030272 2.356715

H 1.241088 -1.494011 2.084227

C 0.427946 0.452615 -2.076577

H 1.126754 1.170352 -1.637555

H -0.559046 0.920253 -2.075057

H 0.719102 0.280635 -3.119106

C 1.894694 -1.437424 -1.349033

H 2.613659 -0.722293 -0.938266

H 2.175345 -1.644064 -2.389496

H 1.985923 -2.374333 -0.788768

C -2.790435 -0.611122 -0.930986

H -2.427331 0.310685 -1.389001

H -3.367107 -0.318100 -0.049002

H -3.467672 -1.101374 -1.641266

C -2.294696 -2.816984 0.115756

H -1.548021 -3.556999 0.421439

H -2.967224 -3.306528 -0.600156

H -2.890202 -2.549915 0.996334

C -1.158831 -1.894042 -3.103760

H -0.350496 -2.132281 -3.804264

H -1.573128 -0.922008 -3.386292

H -1.945184 -2.645913 -3.234737

Gibbs Energy: -1330.756542 au

1 imaginary frequency found: -165 cm-1

Phosphine Oxide (36) GS

C -0.208061 0.789459 -0.266472

C 0.074238 -0.782065 -0.344891

P -0.980981 -0.227761 1.015740

C -0.155580 -0.160792 2.633821

H -0.631558 0.622284 3.230198

H 0.913881 0.043683 2.556084

H -0.304560 -1.120049 3.137538

O -2.454935 -0.497290 1.075585

C -1.134586 1.374033 -1.324962

H -0.641379 1.382216 -2.305292

H -1.383572 2.408063 -1.064006

H -2.077078 0.829484 -1.414607

C -0.612354 -1.545521 -1.470722

H -0.169909 -1.281207 -2.439696

H -1.687697 -1.359866 -1.517234

H -0.477304 -2.621988 -1.319926

C 1.503714 -1.258378 -0.135316

H 2.104321 -1.053638 -1.030987

H 1.516110 -2.340304 0.033954

H 2.010230 -0.789781 0.711918

C 0.971560 1.708075 0.014655

H 1.600256 1.799173 -0.881491

H 1.613858 1.371642 0.832354

H 0.611386 2.710528 0.273754

Gibbs Energy: -692.061530 au

No imaginary frequencies found.

Phosphine Oxide (36) TS

P -0.344194 -1.080442 0.261171

H 1.555789 -0.233468 0.716482

O -0.610438 0.208668 1.087618

Si 1.045062 1.067328 1.474698

C 0.126079 -2.534708 1.228054

C -0.088104 -1.040046 -1.515655

C -1.561533 -1.390557 -1.046307

O 0.102134 2.340644 2.130570

O 1.863882 1.936829 0.268667

C 1.913662 0.631487 3.090341

H 1.343623 -0.149135 3.614380

H 1.982409 1.492016 3.763192

H 2.917232 0.234724 2.895325

C 2.251670 3.288745 0.381563

H 2.402369 3.691232 -0.627449

H 3.200942 3.367468 0.929601

H 1.504677 3.898131 0.902493

C -0.941936 2.975138 1.444965

H -1.153154 3.932220 1.938142

H -1.856979 2.366096 1.457791

H -0.687819 3.184677 0.391308

H 0.170125 -3.427452 0.599433

H -0.626401 -2.680512 2.009783

H 1.101286 -2.355834 1.686361

C 0.167922 0.326602 -2.134629

H 1.232687 0.566815 -2.064126

H -0.367255 1.137382 -1.636870

H -0.130076 0.312677 -3.190422

C 0.754947 -2.122090 -2.172937

H 1.809112 -1.827301 -2.146936

H 0.457576 -2.236722 -3.222682

H 0.674110 -3.103106 -1.697264

C -2.634610 -0.331003 -1.267746

H -2.851341 -0.228282 -2.338713

H -2.357477 0.648857 -0.874098

H -3.557352 -0.632990 -0.760991

C -2.087097 -2.789736 -1.332619

H -1.362906 -3.586334 -1.144039

H -2.390707 -2.864939 -2.384498

H -2.967919 -2.993081 -0.713955

Gibbs Energy: -1252.171988 au

1 imaginary frequency found: -96 cm-1

5. References

1 P. Ertl and T. Schuhmann, *J Nat Prod*, 2019, **82**, 1258–1263.

2 N. J. Lawrence, *Preparation of alkenes: a practical approach*, Oxford University Press, 1996.

3 J. Magano and J. R. Dunetz, *Chem Rev*, 2011, **111**, 2177–2250.

4 J. T. Edwards, R. R. Merchant, K. S. McClymont, K. W. Knouse, T. Qin, L. R. Malins, B. Vokits, S. A. Shaw, D.-H. Bao, F.-L. Wei, T. Zhou, M. D. Eastgate and P. S. Baran, *Nature*, 2017, **545**, 213–218.

5 A. H. Hoveyda and A. R. Zhugralin, *Nature*, 2007, **450**, 243–251.

6 C. J. O'Brien, J. L. Tellez, Z. S. Nixon, L. J. Kang, A. L. Carter, S. R. Kunkel, K. C. Przeworski and G. A. Chass, *Angew Chem Int Ed*, 2009, **48**, 6836–6839.

7 G. Wittig and G. Geissler, *Justus Liebigs Ann Chem*, 1953, **580**, 44–57.

8 D. G. Gilheany, *Chem Rev*, 1994, **94**, 1339–1374.

9 A. El-Batta, C. Jiang, W. Zhao, R. Anness, A. L. Cooksy and M. Bergdahl, *J Org Chem*, 2007, **72**, 5244–5259.

10 P. A. Byrne and D. G. Gilheany, *Chem Soc Rev*, 2013, **42**, 6670.

11 M. Schlosser and B. Schaub, *J Am Chem Soc*, 1982, **104**, 5821–5823.

12 V. K. Aggarwal, J. R. Fulton, C. G. Sheldon and J. de Vicente, *J Am Chem Soc*, 2003, **125**, 6034–6035.

13 V. Patil and M. Schlosser, *Synlett*, 1993, **1993**, 125–126.

14 S. Jeganathan, M. Tsukarmoto and M. Schlosser, *Synthesis (Stuttg)*, 1990, **1990**, 109–111.

15 Q. Wang, M. el Khoury and M. Schlosser, *Chem Eur J*, 2000, **6**, 420–426.

16 E. Vedejs and C. F. Marth, *J Am Chem Soc*, 1988, **110**, 3948–3958.

17 B. E. Maryanoff and A. B. Reitz, *Chem Rev*, 1989, **89**, 863–927.

18 R. Robiette, J. Richardson, V. K. Aggarwal and J. N. Harvey, *J Am Chem Soc*, 2006, **128**, 2394–2409.

19 M. Schlosser and K. F. Christmann, *Angew Chem Int Ed*, 1966, **5**, 126–126.

20 M. Schlosser and K.-F. Christmann, *Synthesis (Stuttg)*, 2002, **1969**, 38–39.

21 D. M. Hodgson and T. Arif, *J Am Chem Soc*, 2008, **130**, 16500–16501.

22 D. M. Hodgson and T. Arif, *Org Lett*, 2010, **12**, 4204–4207.

23 L. Horner, H. Hoffmann and H. G. Wippel, *Chem Ber*, 1958, **91**, 61–63.

24 W. S. Wadsworth and W. D. Emmons, *J Am Chem Soc*, 1961, **83**, 1733–1738.

25 A. Arbuzov, *J. Russ. Phys. Chem. Soc.*, 1906, **38**, 687.

26 A. Michaelis and T. Becker, *Berichte der deutschen chemischen Gesellschaft*, 1897, **30**, 1003–1009.

27 R. O. Larsen and G. Aksnes, *Phosphorus Sulfur Silicon Relat Elem*, 1983, **15**, 219–228.

28 R. O. Larsen and G. Aksnes, *Phosphorus Sulfur Silicon Relat Elem*, 1983, **15**, 229–237.

29 W. C. Still and C. Gennari, *Tetrahedron Lett*, 1983, **24**, 4405–4408.

30 K. Ando, *Tetrahedron Lett*, 1995, **36**, 4105–4108.

31 K. C. Nicolaou, M. W. Härter, J. L. Gunzner and A. Nadin, *Liebigs Annalen*, 1997, **1997**, 1283–1301.

32 H. Pommer and P. C. Thieme, in *Wittig Chemistry*, Springer-Verlag, Berlin/Heidelberg, pp. 165–188.

33 H. Pommer, *Angew Chem Int Ed*, 1977, **16**, 423–429.

34 M. Eggersdorfer, D. Laudert, U. Létinois, T. McClymont, J. Medlock, T. Netscher and W. Bonrath, *Angew Chem Int Ed*, 2012, **51**, 12960–12990.

35 M. Baumann and I. R. Baxendale, *Beilstein J Org Chem*, 2013, **9**, 2265–2319.

36 United States Patent Office, US 2005/0222415A1, 2005, 1–11.

37 M. Watanabe, H. Koike, T. Ishiba, T. Okada, S. Seo and K. Hirai, *Bioorg Med Chem*, 1997, **5**, 437–444.

38 United States Patent Office, US 5466861, 1995, 1–22.

39 D. L. Hughes, *Org Process Res Dev*, 2017, **21**, 800–815.

40 United States Patent Office, US 9,139,597 B2, 2015, 1–11.

41 M. A. Maestro, F. Molnár and C. Carlberg, *J Med Chem*, 2019, **62**, 6854–6875.

42 United States Patent Office, US 4866048, 1989, 1–24.

43 D. C. Batesky, M. J. Goldfogel and D. J. Weix, *J Org Chem*, 2017, **82**, 9931–9936.

44 A. R. Hergueta, *Org Process Res Dev*, 2022, **26**, 1845–1853.

45 D. Hérault, D. H. Nguyen, D. Nuel and G. Buono, *Chem Soc Rev*, 2015, **44**, 2508–2528.

46 J.-L. Montchamp, *Acc Chem Res*, 2014, **47**, 77–87.

47 C. J. O'Brien, Z. S. Nixon, A. J. Holohan, S. R. Kunkel, J. L. Tellez, B. J. Doonan, E. E. Coyle, F. Lavigne, L. J. Kang and K. C. Przeworski, *Chem Eur J*, 2013, **19**, 15281–15289.

48 C. J. O'Brien, F. Lavigne, E. E. Coyle, A. J. Holohan and B. J. Doonan, *Chem Eur J*, 2013, **19**, 5854–5858.

49 T. Werner, M. Hoffmann and S. Deshmukh, *European J Org Chem*, 2014, **2014**, 6873–6876.

50 E. E. Coyle, B. J. Doonan, A. J. Holohan, K. A. Walsh, F. Lavigne, E. H. Krenske and C. J. O'Brien, *Angew Chem Int Ed*, 2014, **53**, 12907–12911.

51 E. Vedejs and M. J. Peterson, *J Org Chem*, 1993, **58**, 1985–1986.

52 T. Werner, M. Hoffmann and S. Deshmukh, *Eur J Org Chem*, 2014, **2014**, 6630–6633.

53 T. Werner, M. Hoffmann and S. Deshmukh, *Eur J Org Chem*, 2015, **2015**, 3286–3295.

54 M.-L. Schirmer, S. Adomeit and T. Werner, *Org Lett*, 2015, **17**, 3078–3081.

55 M.-L. Schirmer, S. Adomeit, A. Spannenberg and T. Werner, *Chem Eur J*, 2016, **22**, 2458–2465.

56 Y.-L. Tsai and W. Lin, *Asian J Org Chem*, 2015, **4**, 1040–1043.

57 N. Saleh and A. Voituriez, *J Org Chem*, 2016, **81**, 4371–4377.

58 N. Saleh, F. Blanchard and A. Voituriez, *Adv Synth Catal*, 2017, **359**, 2304–2315.

59 C. Lorton, T. Castanheiro and A. Voituriez, *J Am Chem Soc*, 2019, **141**, 10142–10147.

60 K. Zhang, L. Cai, Z. Yang, K. N. Houk and O. Kwon, *Chem Sci*, 2018, **9**, 1867–1872.

61 C.-J. Lee, T.-H. Chang, J.-K. Yu, G. Madhusudhan Reddy, M.-Y. Hsiao and W. Lin, *Org Lett*, 2016, **18**, 3758–3761.

62 L. Longwitz, A. Spannenberg and T. Werner, *ACS Catal*, 2019, **9**, 9237–9244.

63 G. Li, Z. Qin and A. T. Radosevich, *J Am Chem Soc*, 2020, **142**, 16205–16210.

64 J. M. Lipshultz and A. T. Radosevich, *J Am Chem Soc*, 2021, **143**, 14487–14494.

65 H. A. van Kalkeren, A. L. Blom, F. P. J. T. Rutjes and M. A. J. Huijbregts, *Green Chem*, 2013, **15**, 1255.

66 J. Tönjes, L. Longwitz and T. Werner, *Green Chem*, 2021, **23**, 4852–4857.

67 In *Comprehensive Organic Name Reactions and Reagents*, John Wiley & Sons, Inc., Hoboken, NJ, USA, 2010.

68 J.-L. Montchamp, F. Tian and J. W. Frost, *J Org Chem*, 1995, **60**, 6076–6081.

69 E. A. Boyd, M. E. K. Boyd and F. Kerrigan, *Tetrahedron Lett*, 1996, **37**, 5425–5426.

70 R. P. Polniaszek and A. L. Foster, *J Org Chem*, 1991, **56**, 3137–3146.

71 A. M. Gregson, S. M. Wales, S. J. Bailey, A. C. Willis and P. A. Keller, *J Org Chem*, 2015, **80**, 9774–9780.

72 A. Briot, M. Bujard, V. Gouverneur, S. P. Nolan and C. Mioskowski, *Org Lett*, 2000, **2**, 1517–1519.

73 P. Wheeler, J. H. Phillips and R. L. Pederson, *Org Process Res Dev*, 2016, **20**, 1182–1190.

74 S. Ortial, H. C. Fisher and J.-L. Montchamp, *J Org Chem*, 2013, **78**, 6599–6608.

75 Y. Ben-Tal, P. J. Boaler, H. J. A. Dale, R. E. Dooley, N. A. Fohn, Y. Gao, A. García-Domínguez, K. M. Grant, A. M. R. Hall, H. L. D. Hayes, M. M. Kucharski, R. Wei and G. C. Lloyd-Jones, *Prog Nucl Magn Reson Spectrosc*, 2022, **129**, 28–106.

76 J. Burés, *Angew Chem Int Ed*, 2016, **55**, 16084–16087.

77 E. L. Stoll, T. Barber, D. J. Hirst and R. M. Denton, *Chem Comm*, 2022, **58**, 3509– 3512.

78 A. M. Kirk, C. J. O'Brien and E. H. Krenske, *Chem Comm*, 2020, **56**, 1227–1230.

79 H. A. van Kalkeren, S. H. A. M. Leenders, C. R. A. Hommersom, F. P. J. T. Rutjes and F. L. van Delft, *Chem Eur J,* 2011, **17**, 11290–11295.

80 A. Ficks, I. Martinez-Botella, B. Stewart, R. W. Harrington, W. Clegg and L. J. Higham, *Chem Comm*, 2011, **47**, 8274.

81 Y. Li, L.-Q. Lu, S. Das, S. Pisiewicz, K. Junge and M. Beller, *J Am Chem Soc*, 2012, **134**, 18325– 18329.

82 J. Long, W. Zhao, Y. Xu, W. Wu, C. Fang, H. Li and S. Yang, *RSC Adv*, 2019, **9**, 3063–3071.

83 N. J. Lawrence, M. D. Drew and S. M. Bushell, *J Chem Soc Perkin 1*, 1999, 3381–3391.

84 B. Verbelen, W. Dehaen and K. Binnemans*, Synthesis (Stuttg)*, 2018, **50**, 2019–2026.

85 S. C. Watson and J. F. Eastham, *J Organomet Chem*, 1967, **9**, 165–168.